Doctoral Dissertation

Development of chromosomal FISH markers and molecular cytogenetic analysis for scleractinian corals

（有藻性サンゴの FISH マーカーの開発およびそれを活用した分子細胞遺伝学的解析）

by

JOSHUA VACARIZAS

Graduate School of Integrated Arts and Sciences

Kuroshio Science Program

Kochi University

March 2023

Acknowledgments

I dedicate this work to myself and to the people important to me, especially to Grace and my family for their unwavering love and support which made this difficult endeavor possible.

My gratitude to Professor Satoshi Kubota and Professor Takahiro Taguchi for their technical guidance and support to finish this work.

To God be the glory.

ジョシュア　バカリザス

J. Vacarizas

Table of Contents

List of Tables

List of Figures

List of Main Papers

Main papers used in creating the dissertation

Peer-reviewed papers

1. **Vacarizas, J**., Taguchi, T., Mezaki, T., Okumura, M., Kawakami, R., Ito, M., & Kubota, S. (2021). Cytogenetic markers using single-sequence probes reveal chromosomal locations of tandemly repetitive genes in scleractinian coral *Acropora pruinosa*. Scientific Reports, 11(1), 11326. https://doi.org/10.1038/s41598-021-90580-1

Additional papers

1. **Vacarizas, J**., Manalili SE., Mezaki, T., Taguchi, T., & Kubota, S. (2022). Studies on Coral Diversity and Biology Using Emerging Cytogenetic and Molecular Approaches. In T. Shinbo, S. Akama, & S. Kubota (Eds.), Interdisciplinary Studies for Integrated Coastal Zone Management in the Region along the Kuroshio: Problem-based approach by Kuroshio Science (pp. 151-162). Livre Publishing. ISBN978-4-86338-339-5

2. Kawakami, R., Taguchi, T., **Vacarizas, J.**, Ito, M., Mezaki, T., Tominaga, A., & Kubota, S. (2022). Karyotypic analysis and isolation of four DNA markers of the scleractinian coral *Favites pentagona* (Esper, 1795) (Scleractinia, Anthozoa, Cnidaria). Comparative Cytogenetics, 16(1), 77–92. https://doi.org/10.3897/COMPCYTOGEN.V16.I1.79953

3. Kubota, S., Manalili, SE., **Vacarizas, J.**, Avila, TN., Canon, KL., and Nieves, PM. (2022). Trial for Setting-up of Biotechnology Laboratory in SUCs in the Philippines for Kuroshio Science Research Network. In T. Shinbo, S. Akama, & S. Kubota (Eds.), Interdisciplinary Studies for Integrated Coastal Zone Management in the Region along the Kuroshio: Problem-based approach by Kuroshio Science (pp. 200-211). Livre Publishing. ISBN978-4-86338-339-5

4. Taguchi, T., Tagami, E., Mezaki, T., **Vacarizas, J. M.**, Canon, K. L., Avila, T. N., Bataan, D. A. U., Tominaga, A., & Kubota, S. (2020). Karyotypic mosaicism and molecular cytogenetic markers in the scleractinian coral *Acropora pruinosa* Brook, 1982 (Hexacorallia, Anthozoa, Cnidaria). Coral Reefs, 39(5), 1415–1425. https://doi.org/10.1007/s00338-020-01975-x

List of Conference Presentations

1. **Joshua Vacarizas**, Takahiro Taguchi, Takuma Mezaki, Masatoshi Okumura, Rei Kawakami, Masumi Ito, & Satoshi Kubota. Karyotyping and cytogenetic analysis of scleractinian coral *Acropora tumida* using fluorescence in situ hybridization (FISH). 23rd Annual Meeting of the Japanese Coral Reef Society /Online, Nov 21-23, 2020

2. **Joshua Vacarizas**, Takahiro Taguchi & Satoshi Kubota. FISHing corals: the potential role of fluorescence in situ hybridization in coral karyotyping and polyploidy determination. 16th Symposium on Marine Science (PAMS 16) /Online, Jul 22-24, 2021

3. **Joshua Vacarizas**, Takahiro Taguchi, Takuma Mezaki, Rei Kawakami, & Satoshi Kubota. Coral chromosome variations and their potential sexual characteristics using molecular cytogenetic analysis. 14th Kuroshio Science International Symposium/ Online, Nov 13-14, 2021

4. **Joshua Vacarizas**, Takahiro Taguchi, Takuma Mezaki, Sam Edward Manalili, & Satoshi Kubota. Molecular cytogenetic analysis of seven *Acropora* species reveals chromosome number variations and polyploidy formation. 24th Annual Meeting of the Japanese Coral Reef Society /Online, Nov 27-29, 2021

5. **Joshua Vacarizas**, Takahiro Taguchi, Takuma Mezaki, Sam Edward Manalili, Rei Kawakami, & Satoshi Kubota. Karyotypic analysis reveals the presence of Y chromosome in gonochoric stony coral *Goniopora djiboutiensis*. 25th Annual Meeting of the Japanese Coral Reef Society/ Ishigaki, Okinawa, Japan, Nov 10-13, 2022.

Chapter 1 General Introduction

1.1. Importance of scleractinian corals

Scleractinian corals are among the most diverse organisms in the world. They possess high genetic and morphological variation with nearly 1300 described extant species (Cairns, 1999). Hard skeletons of scleractinian corals form the reefs after long periods of skeletons piling up on top of another. Coral reefs provide important ecological goods and services estimated to be 375 billion USD/yr mainly comes from recreation, sea defense services, and food production (Costanza et al., 1997). However, studies have shown that the world's coral reefs cover has been declining for the past several decades. About 20% of the world's coral reefs have been destroyed with no prospects of recovery, and 24% are under imminent risk of collapse (Wilkinson, 2012). The Great Barrier Reef, the world's most extensive coral reef system, has lost 40% of its cover since 1986 (Bellwood et al., 2004). This decline is mainly attributed to coral bleaching brought by increase of the sea surface temperature, exacerbated by the climate change. This threat to scleractinian corals can be understood more by studying their biology, physiology, and ecology. Molecular sequence data of corals become increasingly available as sequencing cost has decreased over the years. These sequence data have become useful to understand more the molecular mechanism of coral responses to environmental stresses. Although genome data of several stony coral species have become available, their cytogenetic information, which shows how genome is organized in the nucleus, is not widely explored.

1.2. Molecular Cytogenetics

Cytogenetics is the branch of genetics that studies the condensed form of the DNA (chromatin, chromosome) within the cell nucleus. The early foundation of cytogenetics is characterization of the organism's chromosome structure and organization through karyotyping, which is the process of pairing and ordering all the chromosomes of an organism. G-banding after trypsin treatment is an early method of staining the chromosomes which provides distinct banding patterns, called G-band, to the chromosomes. The exact mechanism how the G-banding creates the banding patterns is still unknown. Researchers suggested that the heterochromatic regions which are regions of the chromosomes that are more condensed, contains few genes, and AT-rich are stained more darkly with the Giemsa stain. In human chromosomes, Giemsa staining produces between 400 and 800 bands distributed among the 23 chromosome pairs. Banding patterns produced by trypsin-Giemsa have being used until today as markers to give unique location identifier to each known genes of many model organisms. The banding patterns, which are identical for each chromosome pair, are also used to effectively generate the karyotype for an organism. Standard procedures involve pairing the homologous chromosomes and arranged them according to decreasing size except for the sex chromosomes. Chromosomes are then numbered by assigning the starting number 1 to the longest chromosome followed by the rest. This presentation of this arrangement of the chromosome is called the karyogram.

Cytogenetic techniques have become advanced that geared away from conventional staining techniques. With the advent of fluorescence microscopy, standard staining techniques can be combined with fluorescent stains and labels which gives better image quality and resolution for karyotyping. Specific genes can be labeled using fluorescent probes and hybridized to chromosomes to identify their locus. This technique is called fluorescence in situ

hybridization (FISH). This advancement in molecular cytogenetics allows scientists to detect aneuploidy accurately and understand more how changes in gene loci affect the biology of not only humans but also in a wide range of organisms.

With the advent of whole genome sequencing, gene mapping for each chromosome can be done *in silico*. A great number of genes from model organisms have been mapped on their chromosomes and this has become very useful to understand more of the organism's genetics and physiology. However, identifying the changes in the chromosome structure and organization using the genome data alone is still a challenge, especially among non-model organisms. Molecular cytogenetics thus still offers versatile approach for non-model organisms in studying their chromosomes.

1.3. Molecular cytogenetic studies on stony corals

There is limited information on the chromosomes of scleractinian corals. The scarcity of cytogenetic data from stony corals can be attributed to several factors. The first one is the relatively slow growth rate of corals compared with most animals. This means that they contain few actively dividing cells, which are often used in chromosome preparation. The second one is their short chromosomes. Short chromosomes cannot produce enough G-banding patterns to be used to distinguish and identify chromosome pairs. Aside from their size, there is a high degree of similarity among chromosome lengths. This also causes difficulty if a researcher tries karyotyping based solely on chromosome size.

To circumvent the problems of obtaining high number of mitotic cells for microscopic observations, chromosomes can be prepared from early embryonic cells (1-day old) which contains high number of actively dividing cells. Professor Takihiro Taguchi and Professor Satoshi Kubota of Kochi Gakuen University, Japan have been collecting artificially fertilized

coral embryos from a coral community in Otsuki, Kochi, Japan. Using chromosomes from coral embryos, molecular cytogenetic study of corals can be conducted.

Although new stains and technique modifications have been introduced to enhance the visualization of chromosomes under the light microscope, coral chromosomes were best observed using fluorescence microscopy using fluorophores and DAPI as counterstain. Professor Taguchi has been detecting the chromosomal location of ribosomal RNA, Alu repeats, telomeres in the chromosomes of stony corals from the embryonic cells using FISH. To date, cytogenetic information of six stony coral species from three different families of stony corals has been characterized. These are *Acropora solitaryensis* and *Acropora pruinosa* (Acroporidae); *Coelastrea aspera*, *Platygyra contorta*, and *Favites pentagons* (Merulinidae), and *Echinophyllia aspera* (Lobophylliidae) (Kawakami et al., 2022; Taguchi et al., 2013, 2014, 2016, 2017, 2020). In those studies, new cytogenetic evidence was presented, including information regarding chromosome numbers, ribosomal RNA (rRNA) gene loci, the presence of a homogenously staining region (HSR), and some repeated sequences shared with human satellite DNA.

However, FISH probes from these studies were prepared from mixture of amplicons that were amplified using one or two primers for a specific gene. Thus, which amplicon resulted to the observed hybridization signals cannot be identified and subsequent characterization of the gene through sequencing was mostly not done. In this study, FISH probes were prepared from single amplicons which enable us to characterize the observed loci through sequencing.

Chapter 2 Development of single-sequence probe to characterize loci of tandemly repetitive genes in *Acropora pruinosa*

2.1. Abstract

The short and similar sized chromosomes of *Acropora* pose a challenge for karyotyping. Conventional methods, such as staining of heterochromatic regions, provide unclear banding patterns that hamper identification of such chromosomes. In this study, we used short single-sequence probes from tandemly repetitive 5S ribosomal RNA (rRNA) and core histone coding sequences to identify specific chromosomes of *Acropora pruinosa*. Both the probes produced intense signals in fluorescence in situ hybridization, which distinguished chromosome pairs. The locus of the 5S rDNA probe was on chromosome 5, whereas that of core histone probe was on chromosome 8. The sequence of the 5S rDNA probe was composed largely of U1 and U2 spliceosomal small nuclear RNA (snRNA) genes and their interspacers, flanked by short sequences of the 5S rDNA. This is the first report of a tandemly repetitive linkage of snRNA and 5S rDNA sequences in Cnidaria. Based on the constructed tentative karyogram and whole genome hybridization, the longest chromosome pair (chromosome 1) was heteromorphic. The probes also hybridized effectively with chromosomes of other Acropora species and population, revealing an additional core histone gene locus. We demonstrated the applicability of short-sequence probes as chromosomal markers with potential for use across populations and species of *Acropora*.

2.2. Introduction

Karyotyping is the process of pairing homologous chromosomes and arranging them in order of decreasing lengths. Karyotype, the systematic presentation of chromosomes, reveals the chromosome number, aneuploidy, ploidy variation, structural rearrangements, and the sexual form of an organism through the sex chromosomes. A karyotype, with its distinct markers, also provides the physical structure for cytogenetic and gene mapping. Aside from model organisms, karyotypes of most important crops and farmed animals are well documented, considering the important role of karyological data in genotyping and breeding . However, karyotypes of other propagated animals, such as scleractinian corals, are poorly documented despite the increasing popularity of coral breeding as a strategy to rehabilitate degraded reefs (Barton et al., 2017; Bellwood et al., 2004; Hughes et al., 2003). Among 800 species of scleractinian corals, karyotypes of only 29 species have been reported, representing less than 4% of the total number of species (Flot et al., 2006; Kenyon, 1997). For the karyotyped species, (Brown & Blackman, 1988; Mohanty et al., 2004) chromosome numbers are highly variable; for example in *Acropora*, the number ranges from 2n = 24 to 2n = 54 (Kenyon, 1997). This limited and varying karyological data for scleractinian corals can be attributed to the difficulty in constructing their karyotype due to their short (1–5 µm) and equally sized chromosomes (Flot et al., 2006; Kenyon, 1997). Observations of unique banding patterns based on heterochromatic regions (G- and C-bandings) were shown difficult for short chromosomes of some scleractinian corals (Taguchi et al., 2016, 2020). These banding patterns and chromosomal lengths are features that are conventionally used in pairing homologous chromosomes to construct the karyotype. Karyotyping of corals has recently been improved with the use of fluorescence *in situ* hybridization (FISH), which provides a higher resolution that aids the observation of chromosomes by targeting gene loci as chromosomal markers .

(Kawakami et al., 2022; Taguchi et al., 2013, 2017, 2020; Vacarizas et al., 2021). This improvement revealed a chromosome number (2n) of 28 for most of the species of scleractinian corals and suggested slight variations in the number even within the species. However, to gain a better understanding of these karyotypic variations, effective FISH probes that can be used across *Acropora* populations and species must be developed.

In cytogenetic analysis using FISH, large BAC probes (>100 kbp) are commonly used because they target long regions of the chromosomes, creating bright and broad hybridization signals. However, due to the size of BAC probes, they may partly or largely contain simple tandem repeats (e.g., microsatellites), the lengths and composition of which vary between individuals and populations (Li et al., 2006; D. J. Miller et al., 1993; Reddy et al., 2017a). This necessitates cross validation when applying BAC probes outside the tested individual. In contrast, short probes that target only the conserved regions are potentially useful across populations and related taxa. However, to produce a bright FISH signal, the target gene needs to be either immensely long (>6 kbp) or tandemly repeated. Fortunately, the nuclear ribosomal RNA (rRNA) genes and the core histone genes have highly conserved and repetitive properties, and their loci can therefore be detected using FISH employing only short probes containing the sequence of a single array that compose the tandem repeats. In contrast to large BAC probes, short probes (<2 kbp) are also easier to develop with standard PCR and cloning procedures.

In this study, the loci of sequences associated to tandemly repetitive genes (5S rRNA and core histone genes) were detected in the chromosomes of *Acropora pruinosa* using suitable short single-sequence FISH probes. We propose that the loci detected using only short probes can produce bright hybridization signals that can be used as chromosomal markers for the identification of chromosome pairs. To identify the chromosome number on which the loci were observed, a tentative karyotype was constructed based on average chromosomal lengths. The developed FISH probes were then applied to the chromosomes of other population of

Acropora pruinosa and species (*Acropora muricata*) to test the range of its applicability. These results reveal the potential of short single-sequence probes as tools for identification and pairing of homologous pairs within *Acropora*.

2.3. Results

2.3.1. Karyological features and whole genome hybridization

The majority (55%) of the observed metaphase spreads (n = 100) of *A. pruinosa* had a chromosome number (2n) of 28 (Fig. 2.1a), followed by 27 (26%). Neither of the two conventional staining techniques (G- and C-banding) provided a unique and clear banding pattern that could distinguish the homologous chromosomes (Fig. 2.1b and 2.1c). In C-banding, not all chromosomes showed a darkly stained centromeric region (Fig. 2.1c). On the contrary, 4',6-diamidino-2-phenylindole (DAPI) staining revealed constricted regions of the centromeres (Fig. 2.1d). Using the DAPI-stained chromosomes, their average centromere locations and individual lengths were measured, and chromosomes were arranged in order of decreasing lengths (Fig. 2.1d, Table 2.1). The centromere indices (0.54–0.57) indicated a centromeric characteristic for all the chromosomes (Table 2.1). Differences in chromosome lengths were not readily noticeable, in which the shortest chromosome was more than half (64.7% ± 4.3%) the size of the longest chromosome. To determine a heteromorphic pair, the size difference between each putative homologous chromosome was statistically compared (Supplementary Table S1). The size difference of the first homologous pair (chromosome 1) was found to be significantly larger than that of the other homologs (Table 2.1). This indicates that the first chromosome pair is heteromorphic in *A. pruinosa*.

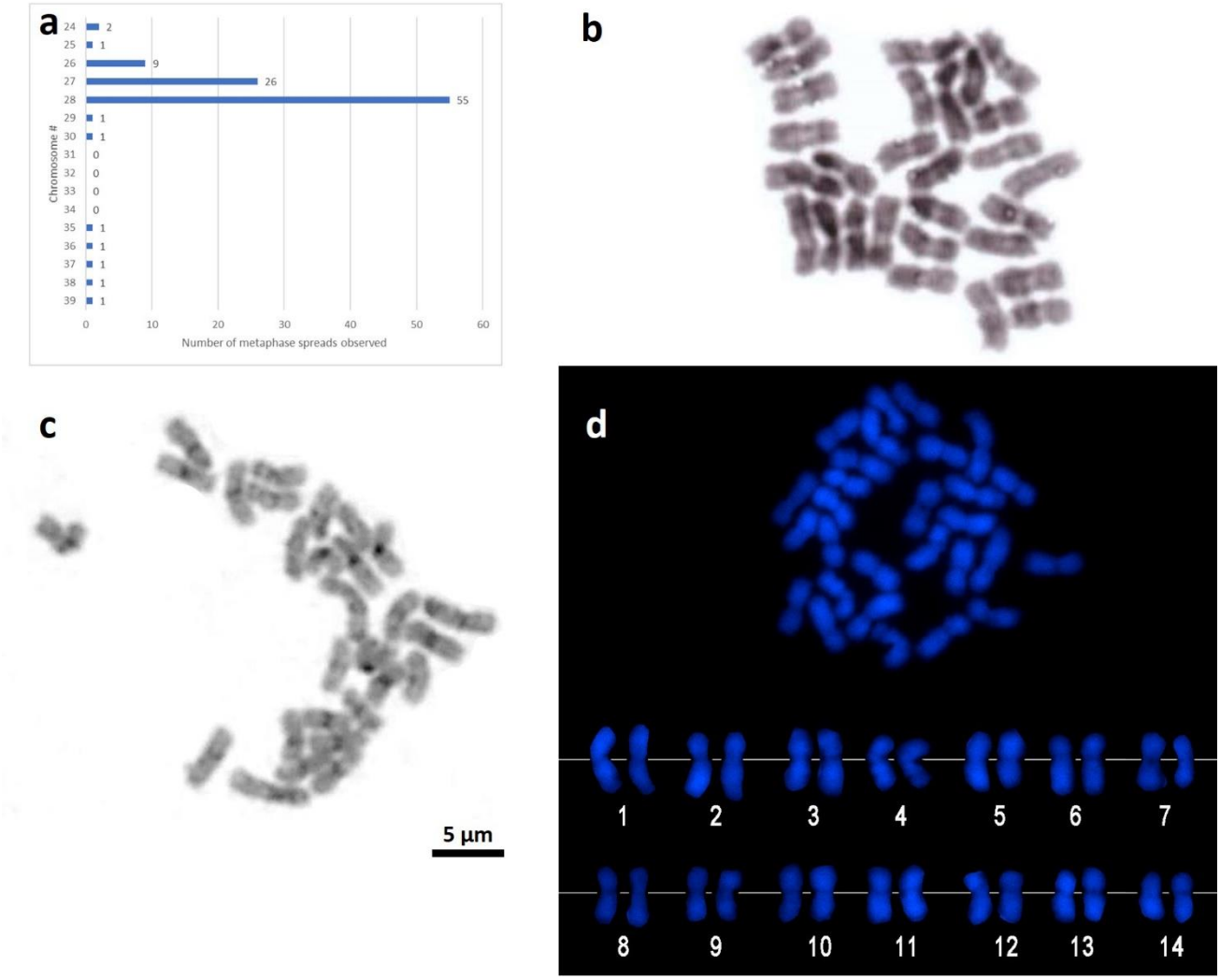

Figure 2.1. Chromosome numbers observed from 100 metaphase spreads (a). *Acropora pruinosa* chromosomes visualized by G- staining (b) and C-banding (c). DAPI staining showing distinct centromeres (d).

Table 2.1. Morphometric characteristics of the chromosomes of *Acropora pruinosa* (n = 20 metaphase spreads).

Rank according to length	Long arm length (µm)	Chromosome length (µm)	Centromere index (long arm/total length)	Relative size (%)	Assigned chromosome #	Size difference between homologs (µm)*
1	1.89 ± 0.4	3.37 ± 0.7	0.56 ± 0.04	100	1	0.17 ± 0.11[a]
2	1.82 ± 0.4	3.2 ± 0.6	0.57 ± 0.04	95.18 ± 2.5		
3	1.77 ± 0.3	3.11 ± 0.6	0.57 ± 0.04	92.41 ± 3.2	2	0.08 ± 0.07[b]
4	1.69 ± 0.3	3.03 ± 0.6	0.56 ± 0.04	90.13 ± 3.7		
5	1.7 ± 0.3	2.98 ± 0.6	0.57 ± 0.03	88.45 ± 3.2	3	0.06 ± 0.07[bc]
6	1.62 ± 0.4	2.92 ± 0.5	0.55 ± 0.04	86.73 ± 3.4		
7	1.59 ± 0.3	2.87 ± 0.5	0.55 ± 0.04	85.48 ± 3.7	4	0.04 ± 0.03[bc]
8	1.6 ± 0.3	2.83 ± 0.5	0.56 ± 0.04	84.3 ± 3.4		
9	1.56 ± 0.3	2.8 ± 0.5	0.56 ± 0.04	83.19 ± 3.4	5	0.03 ± 0.05[bc]
10	1.55 ± 0.3	2.76 ± 0.5	0.56 ± 0.03	82.22 ± 3.9		
11	1.51 ± 0.3	2.73 ± 0.5	0.55 ± 0.04	81.33 ± 3.9	6	0.03 ± 0.02[bc]
12	1.52 ± 0.3	2.71 ± 0.5	0.56 ± 0.04	80.56 ± 4.1		
13	1.49 ± 0.3	2.67 ± 0.5	0.56 ± 0.04	79.52 ± 4.1	7	0.03 ± 0.04[bc]
14	1.43 ± 0.2	2.64 ± 0.5	0.54 ± 0.03	78.63 ± 3.9		
15	1.45 ± 0.3	2.61 ± 0.5	0.55 ± 0.04	77.82 ± 3.8	8	0.02 ± 0.02[bc]
16	1.41 ± 0.3	2.59 ± 0.5	0.54 ± 0.03	77.15 ± 3.9		
17	1.38 ± 0.3	2.56 ± 0.5	0.54 ± 0.03	76.13 ± 3.5	9	0.01 ± 0.01[c]
18	1.41 ± 0.3	2.54 ± 0.4	0.55 ± 0.03	75.71 ± 3.5		
19	1.41 ± 0.3	2.52 ± 0.5	0.56 ± 0.04	75.06 ± 3.5	10	0.03 ± 0.02[bc]
20	1.34 ± 0.2	2.5 ± 0.4	0.54 ± 0.03	74.31 ± 3.5		

21	1.35 ± 0.3	2.47 ± 0.44	0.55 ± 0.04	73.42 ± 3.3	11	0.02 ± 0.03^{bc}
22	1.33 ± 0.3	2.44 ± 0.44	0.55 ± 0.04	72.72 ± 3.5		
23	1.3 ± 0.2	2.41 ± 0.43	0.54 ± 0.03	71.81 ± 3.3	12	0.04 ± 0.03^{bc}
24	1.33 ± 0.3	2.38 ± 0.42	0.56 ± 0.04	70.8 ± 3.5		
25	1.3 ± 0.2	2.34 ± 0.42	0.56 ± 0.05	69.71 ± 3.3	13	0.06 ± 0.06^{bc}
26	1.27 ± 0.3	2.29 ± 0.43	0.55 ± 0.03	67.97 ± 3.7		
27	1.23 ± 0.3	2.24 ± 0.41	0.55 ± 0.03	66.56 ± 3.9	14	0.06 ± 0.06^{bc}
28	1.17 ± 0.3	2.18 ± 0.42	0.54 ± 0.03	64.71 ± 4.3		

*Different letters indicate significant differences ($p < 0.05$). Details of the analysis are shown in Supplementary Table S1.

To assess the locations of all repetitive loci that are readily detected by FISH, whole genome hybridization (WGH) was conducted using a probe prepared from the whole genome of *A. pruinosa* sperm. Results showed several faint hybridization signals on some chromosomes, but a broad and intense signal was detected at the telomeric region of the q-arm of a single chromosome (Fig. 2.2a). The arrangement of chromosomes according to size revealed that the intense hybridization signal was on the longer chromosome of the heteromorphic chromosome 1 (Fig. 2.2b). This indicates that a long and unique array of sequences was present only on this single chromosome and was absent from other chromosomes, as well as on its homologous pair. Because this hybridization pattern was observed on all metaphase spreads and across different embryos, we eliminated the possibility of allelic variation between the heteromorphic pair of chromosome 1. In addition, the location of the hybridization signal is the portion of the chromosome that is missing in its homologous pair (Fig. 2.2b), thus suggesting a region that may not have the function and characteristics of a locus.

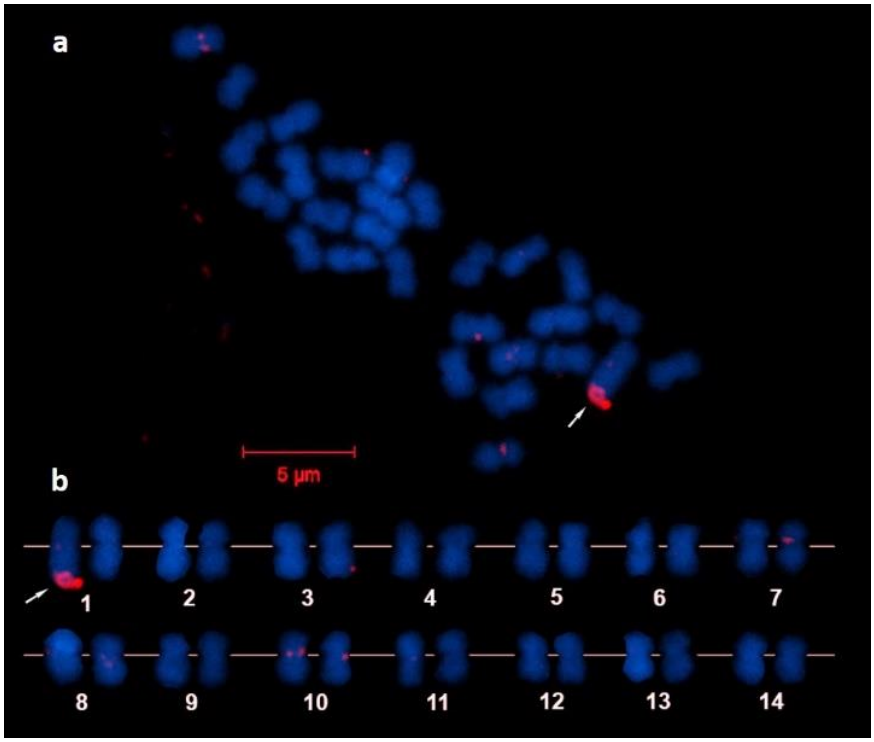

Figure 2.2. Whole genome hybridization of sperm DNA on chromosomes of *Acropora pruinosa* (a). Chromosomes arranged in order of decreasing length (b).

2.3.2. Probe hybridization and sequence characterization

Hybridization of the At-p5S and At-pH2AB probes revealed readily detected single loci in separate homologous pairs (Fig. 2.3). The hybridization with At-p5S and At-pH2AB probes manifested as band-like and dot-like signals, respectively. This indicates that the location of At-pH2AB is clustered but may include a relatively long interspersed region between arrays, whereas that of At-p5S is broader and more contiguous. Based on the average relative sizes of the chromosomes where the hybridization signals were detected, the At-p5S loci were located on chromosome 5 and the At-pH2AB loci were on chromosome 8 (Table 2.2).

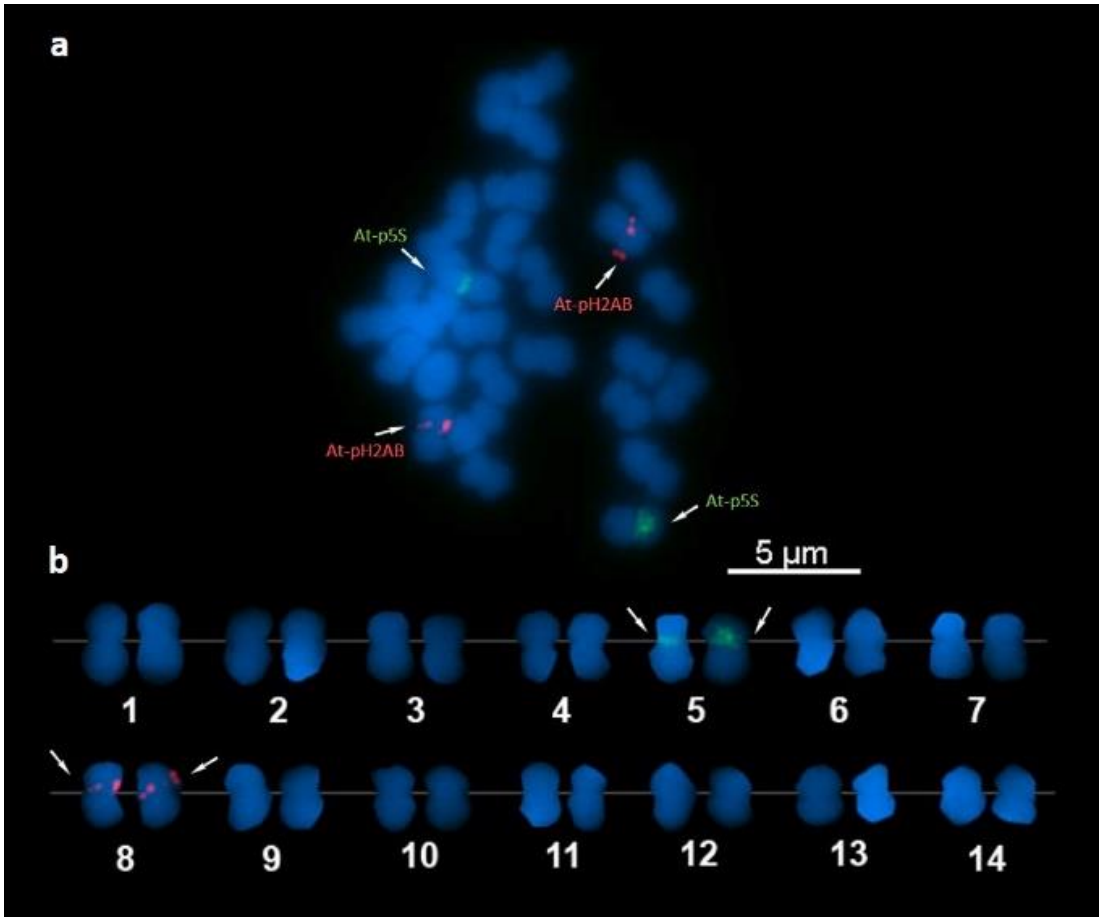

Figure 2.3. Fluorescence in situ hybridization image showing hybridization signals of the At-p5S probe labeled with Cy3-dUTP (red) and At-pH2AB probe labeled with digoxigenin-dUTP (green) in *Acropora pruinosa* chromosomes (a). corresponding karyogram (b).

Table 2.2. Characterization of the fluorescence in situ hybridization probes and their hybridization signals on the chromosomes of *Acropora pruinosa*.

FISH probe	**Length**	**Sequence (GenBank accession)**	**Loci position in the chromosome**	**Fluorescence signal length (µm)**	**Relative length of chromosomal location (%)**	**Assigned chromosome number**
At-WGH	-	-	Telomeric region of the q arm (one chromosome only)	0.62 ± 0.17	98.27 ± 5.05	1*
At-p5S	1731 bp	LC557013.1	p arm, near the centromere	0.40 ± 0.10	83.12 ± 6.03	5
At-pH2AB	813 bp	LC557014.1	q arm, near the centromere	dot signal	77.42 ± 5.92	8

*Only the longer chromosome of the homologous pair

Characterization of the probe sequence revealed that At-p5S is composed of small nuclear spliceosomal RNA genes (U1 and U2 snRNAs) and contains three interspacer regions (Fig. 2.4a). These regions were flanked by short sequences of the 5S rDNA, arranged in a head-to-tail fashion. The At-pH2AB probe is composed of two histone domains (H2A and H2B), separated by a spacer region (Fig. 2.4b). The two genes are arranged in a tail-to-tail fashion, which is typical among invertebrates (Pratlong et al., 2017).

To confirm whether the short 5S rDNA sequence of the At-p5S probe is involved in the hybridization, we blasted the probe sequence (divided into identified regions) against the whole

genome of *Acropora digitifera* (supplementary Table S2). Result of the analysis showed that the entire probe's length including the short 5S rDNA sequences on both ends was present and tandemly repeated. The arrangement of 5S-ITS1-U2-ITS2-U1-ITS3-5S was also highly consistent within estimated length of 423,641 bp (supplementary Table S2, highlighted in yellow).

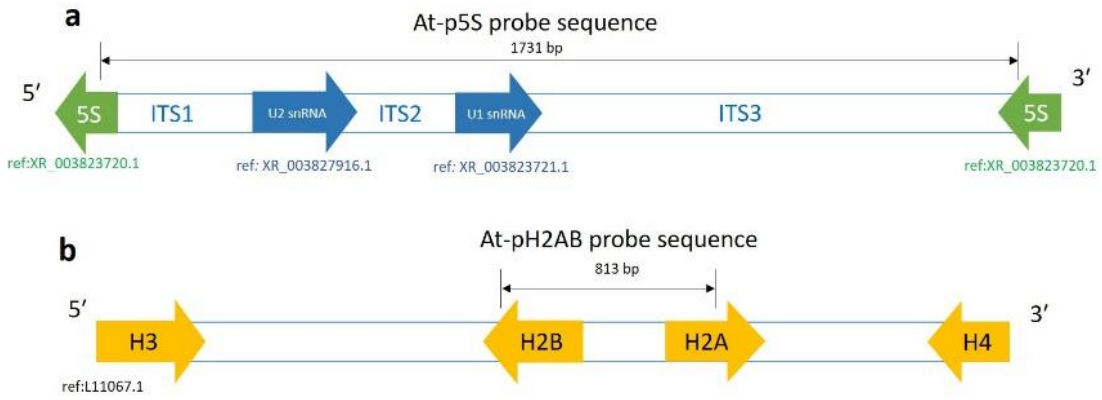

Figure 2.4. Characterization of the At-p5S (a) and At-pH2AB (b) probe sequences based on sequence alignment with their most homologous sequences from the GenBank.

The probes prepared from *A. pruinosa* were tested for the chromosomes of *A. muricata* and *A. pruinosa* Kochi. Hybridization signals were effectively detected in these two *Acropora* chromosomes (Fig. 2.5). In *A. muricata*, the hybridization pattern was the same as observed in *A. pruinosa* (one homologous pair for each probe). In addition, the loci were also observed at roughly the same chromosomal position, near the centromere of the p-arm (Fig. 2.5a). Conversely, in *A. pruinosa* Kochi, the hybridization signal for At-pH2AB was detected on two homologous pairs, with additional signal that was less intense than the other (Fig. 2.5b). This indicates that this locus contains fewer copies of core histone gene repeats than the other. Aside

from the differences in signal intensity, the chromosomal positions of the additional At-pH2AB loci slightly departed from the centromere compared with those for the other At-pH2AB loci.

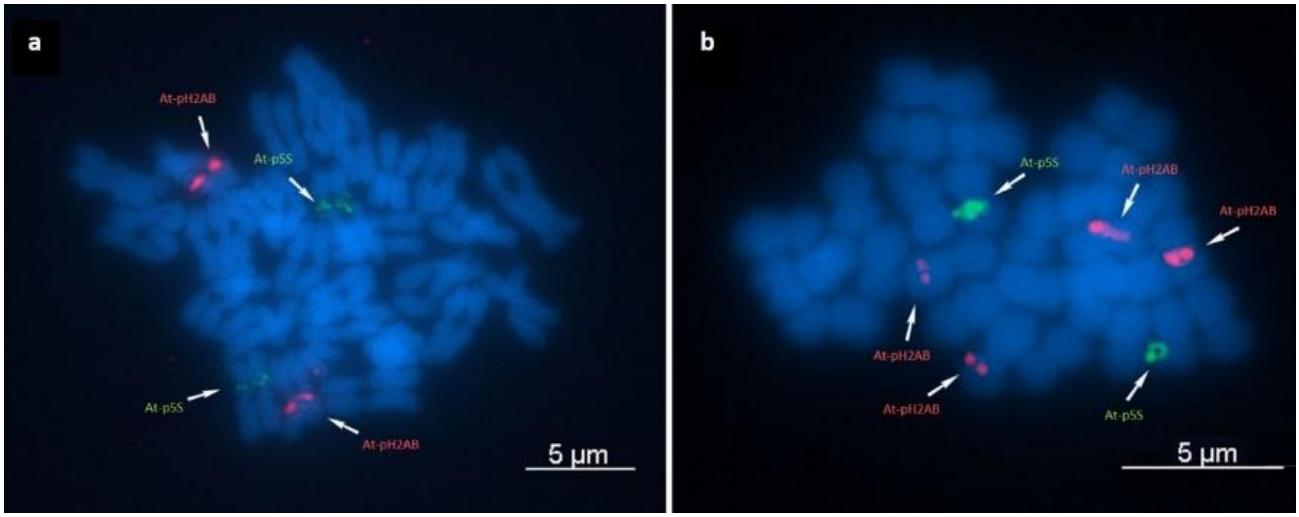

Figure 2.5. Fluorescence in situ hybridization image showing hybridization signals of the At-p5S (green) and At-pH2AB (red) probes on the chromosomes of *Acropora muricata* (a) and *Acropora pruinosa* Kochi (b).

2.4. Discussion

The chromosome number (2n = 28) of *A. pruinosa* agrees with those of other 18 species of *Acropora* and five other species from other coral genera (*Montipora* and *Fungia*) (Kenyon, 1997). It is unclear whether the chromosome number 2n = 27 observed in this study was a result of missing one chromosome during mitotic preparations or it is another karyological characteristics in this coral species. Having two chromosome numbers (karyotypic mosaicism) is not uncommon in *Acropora* (Kenyon, 1997; Taguchi et al., 2020). *Acropora pruinosa* Kochi was reported with chromosome numbers, 2n = 28 and 2n = 29, which was confirmed by the

presence of an additional and unpaired chromosome in the case of 2n = 29 (Taguchi et al., 2020).

Large-scale hybridization signals on a single chromosome were observed using WGH in this study on *A. pruinosa* (2n = 28) as well as in a previous study on *A. pruinosa* Kochi (2n = 29) (Taguchi et al., 2020) . However, for *A. pruinosa* with even number of chromosomes, the presence of a unique chromosome with no apparent pair based on length and hybridization pattern might indicate the presence of heteromorphic pairs. In most animals, these heteromorphic pairs are often associated with sex chromosomes. Although the sex-linked loci and genes have been identified in the gonochoric coral *Corallium rubrum* (Pratlong et al., 2017), the role of heteromorphic chromosomes in the sexual characteristics of scleractinians has not been explored. This investigation is particularly important in *Acropora* because colonies of some coral species may contain male or female polyps, aside from the well-known co-sexual polyps (Guest et al., 2012). The heteromorphic pairs observed in this study were present in all mitotic cells, and we propose two mechanisms how these cells maintained to carry this unusually long chromosome: (1) After meiotic segregation in the hermaphroditic gonads, either the eggs or the sperms exclusively receive this chromosome, (2) a cycle that involves translocation of the portion of chromosome from the autosomes, causing the chromosome that receives it the longest one. The second mechanism has been demonstrated in other organisms, which involves translocation of the nucleolar organizer region (NOR) containing repetitive tandem arrays of 18S and 28S rRNA genes from autosomes to the telomeric end of sex chromosomes (Gallagher et al., 1998; Hsu et al., 1975; Pardue & Hsu, 1975). This NOR in the sex chromosomes functions in the pairing of X-Y chromosomes during meiosis21. This is also supported by the presence of 18/28S rDNA loci at the telomere of one of the longest chromosome pairs in *A. pruinosa* Kochi (Taguchi et al., 2020). Further work must be conducted to characterize the sequence arrays that constitute this hybridization signal

on the longest chromosome and to confirm whether this chromosome is associated with functioning as a sex chromosome.

The loci of the U1/U2 snRNA and core histone gene clusters showed intense hybridization signals on separate chromosome pairs. However, because the minimum sequence length of hybridization that can be readily detected in FISH is 6 kbp (Lamb et al., 2007), which is greater than the length of our probes (Table 2), it is possible that other loci composed of fewer or shorter arrays of the target genes exist. This is supported by the results of the experiment on the presence of several rDNA arrays obtained from subcloning, with shorter size of the target gene (LC557012, LC557015) that showed no hybridization signal. A sequence of similar length, but composed of indels (LC557016), compared with the identified repetitive histone array also showed no hybridization in FISH. Because these sequences were confirmed in the genome of *A. pruinosa*, we speculate that these arrays were either not repetitive (single-copy locus) or were short enough to be detected by FISH. Nonetheless, this study confirms the existence and chromosomal locations of highly clustered arrays of these genes. Studies have reported that this clustering of highly conserved genes is related to pseudogenes, which are acquired through hybridization of ancestral genes and have lost their coding potential (Caburet et al., 2005; Robicheau et al., 2017). Pseudogenes are implicated in the diversity of the nuclear ribosomal genes in *Acropora*, but only one rDNA sequence has been implicated to present across several species that are associated with pseudogenes (Marquez, 2003). It has also been reported previously that large clusters of pseudogenes consist of tRNAs and snRNAs on mammalian chromosomes (Shibuya et al., 1982; van der Drift et al., 1999). Other identified pseudogenes that have repetitive gene copies in humans are the ribosome biogenesis protein gene (RLP24) and E3 ubiquitin-protein ligase gene (MDM2) (Browning et al., 2020). Clustering of pseudogenes was also implicated in a mechanism to disable its function as a result of acquired mutations (Jacq et al., 1977; Vanin, 1985). The arrangement of these genes in these

clusters is tandemly repeated and lacks introns, and thus presumably arose from reverse transcription of mRNA, followed by multiple integration to specific regions in the chromosome (Nishioka et al., 1980; Vanin, 1985; Vanin et al., 1980).

The linkage of snRNA genes and 5S rDNA sequence and their tandemly repetitive characteristics observed in this study was first reported for mollusks (Cross & Rebordinos, 2005). The same linkage involving U1, U2, and U5 snRNA genes was also found in fish (Manchado et al., 2006) and crustaceans involving only U1 snRNA (Pelliccia et al., 2001). Here, we report for the first time a tandemly repetitive linkage of 5S rDNA sequence and snRNA genes in the phylum Cnidaria. Although many FISH studies of single or multiple loci of repetitive 5S rRNA genes (Insua et al., 2001; Morescalchi et al., 2011; Pérez-García, Cambeiro, et al., 2010) and snRNA genes (Araya-Jaime et al., 2017; Úbeda-Manzanaro et al., 2010) have been reported, it is uncertain whether the loci observed in these studies may involve linkage to one another or to any other gene. We showed that repetitive linkage of snRNA and putative 5S rRNA genes produced a single locus on the chromosomes. Conversely, in fish, the loci of these two repetitive genes were not linked and were located on different chromosomes (Utsunomia et al., 2014).

Only the H2A and H2B genes arranged in a typical manner were confirmed to constitute the observed loci. However, in cnidarians, various arrangements of repetitive core histone genes, including H1, H3, and H4, have been documented (Reddy et al., 2017b). In *Mytilus edulis*, aside from the core histone genes, the sequence of the solitary linker H1 gene is also tandemly repeated (Albig et al., 2003; Drabent et al., 1999). The loci of these solitary H1 gene clusters were found to be located on chromosome pairs different from core histone genes (Eirín-López et al., 2002). This suggests the possible presence of other repetitive histone loci that can be observed in scleractinian chromosomes. Surprisingly, a unique arrangement of

repetitive arrays involving linkage between histone and 5S rRNA genes was observed among crustaceans (Barzotti et al., 2000) and fish (Piscor et al., 2016, 2020).

The varying hybridization patterns of core histone probes in other *Acropora* population might suggest chromosomal rearrangements during the evolutionary processes within *Acropora*. In the genus *Mus*, locations of clusters of conserved genes are shifted across different chromosomes, providing evidence of genome reshuffling that occurred during its evolution (Cazaux et al., 2011). Variations in the number of histone loci within closely related taxonomic groups have also been observed in other taxa. In bivalves, loci of histone genes are in two chromosome pairs in the mussel, *Mytilus galloprovinciali* (Eirín-López et al., 2004), and in the scallop, *Patinopecten yessoensis* (L. Zhang et al., 2007), but there is only one locus in the mussel species, *Perumytilus purpuratus* (Pérez-García, Guerra-Varela, et al., 2010) and in three other species of scallops (*Argopecten irradians*, *Chlamys farreri*, and *C. nobilis*) (L. Zhang et al., 2007).

We demonstrated that single-sequence probes containing conserved genes produced a readily detectable hybridization signal on the chromosomes of *A. pruinosa*. These probes also hybridized on chromosomes of other *Acropora* population and species and thus have a potential for use as chromosomal markers within the taxa. In addition, the single-sequence probes revealed the presence of other loci in other species, which revealed the differences in chromosome organization. This study may provide a foundation for discovering the loci of other tandemly repetitive genes, such as 18 and 28S rDNA that can be used as additional chromosomal markers for improved karyotyping of *Acropora*.

2.5. Methods

2.5.1. Sample collection and chromosome preparation

Embryos of *A. pruinosa* were obtained from artificial fertilization of egg-sperm bundles collected from spawning colonies in Kaiyo-Cho, Tokushima, Japan (33.545 °N, 134.315 °E) (Fig. 2.6a) on the night of July 20, 2019. The coral is characterized by indeterminate colony outline (Fig. 2.6b), with appressed and tubular radial corallites (Fig. 2.6c) (Wallace et al., 2012). Embryos were grown in 0.2 µm filtered seawater for 10–14 h and treated with 0.01 % (v/v) colchicine followed by the addition of hypotonic solution (seawater: dH_20 = 1:1). Other coral embryos used in this study were preserved ones such as *Acropora* muri*cata* and another *Acropora pruinosa* collected in Otsuki, Kochi, Japan [32.777, 132.731]. To distinguish *A. pruinosa* collected in Otsuki, Kochi, Japan, the name *A. pruinosa* Kochi was used throughout this study. Chromosomes were prepared from the embryos based on the previous method (Taguchi et al., 2016), with slight modifications. About 30–50 embryos were collected by centrifugation and 0.5 mL of Carnoy's fixative (absolute methanol:glacial acetic acid = 3:1) was added. Lipids were removed by soaking the embryos in diethyl ether for 4–6 h. Cells were centrifuged at 2000 × *g* for 2 min and then resuspended in 0.5 mL of Carnoy's fixative. A drop of cell suspension was placed on a slide and then flame-dried.

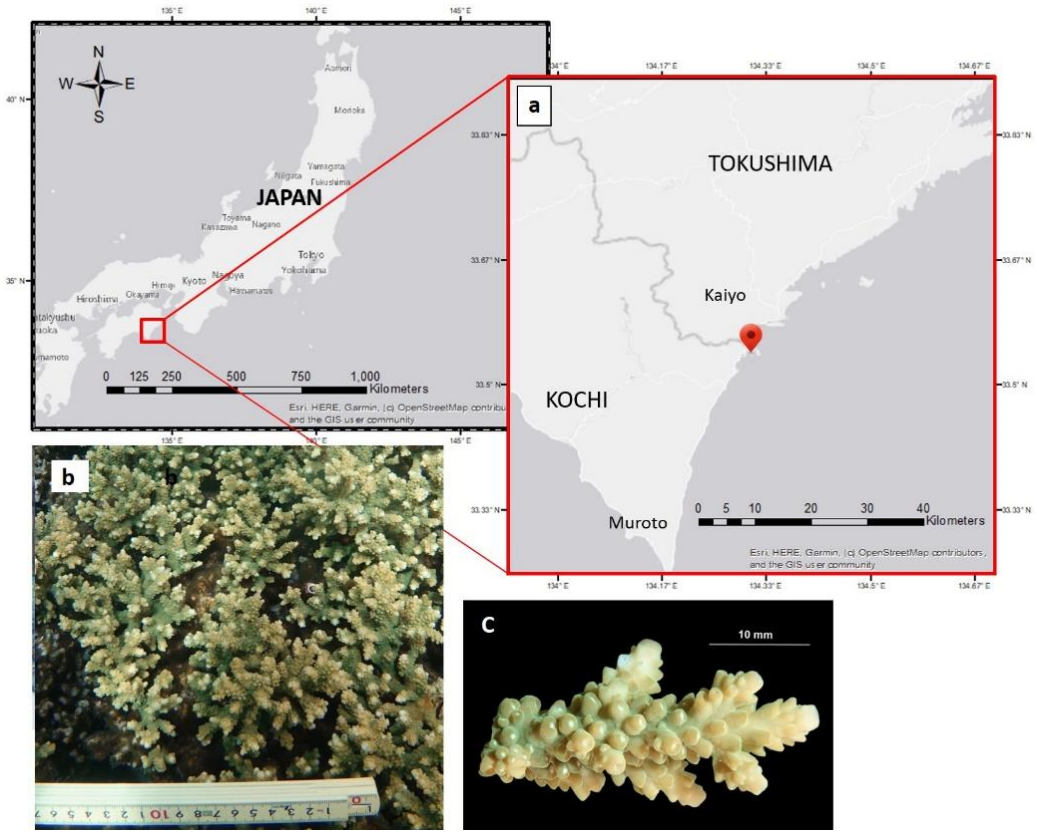

Figure 2.6. Map showing the location from where *Acropora pruinosa* gametes were obtained and used for artificial fertilization (a). The coral colony which released the egg-sperm bundles (b). A branch from the colony (c).

For G-banding, slides were treated with 0.025 % trypsin solution for 1 min, and then stained with Giemsa solution diluted with 5% 0.06 M phosphate buffer (pH 6.8). To examine the chromosomal distribution of constitutive heterochromatin, C-banding was performed using the standard barium hydroxide/saline/Giemsa method (Sumner, 1972) with slight modifications. Chromosome slides were treated with 0.2 N HCl at 25 °C for 30 min and then with 5% $Ba(OH)_2$ at 50 °C for 1 min. The slides were then soaked in 2X SSC (saline sodium citrate) at 60 °C for 30 min. Experimental research, including the collection of the coral bundles, complied with the relevant institutional, national, and international guidelines and legislation.

2.5.2. PCR and DNA cloning

A. pruinosa genomic DNA was extracted from sperms using the Wizard Genomic DNA Purification kit (Promega, USA). The 5S rRNA genes were amplified using the forward primer described by Stover & Steel (2001) and the reverse primer (R: 5′-GGGCCAGGGTAGTACTTGGA-3′) designed by us. Histone genes were amplified using the primers (F: 5′-TTGCAAGTTCACCGGGAAGC-3′, R: 5′-TTCCAGCCAACTCGAGAATC-3′) designed by us based on the partial histone gene sequences of *Acropora* species retrieved from the GenBank. The PCR conditions for all amplifications were as follows: 30 cycles of 98 °C for 20 s, 60 °C for 30 s, and 72 °C for 1 min 30 s.Gel electrophoresis showed the expected size for both genes (Supplementary Figure S1). The PCR products were ligated into a bacterial plasmid using the pGEM-T Easy Vector Systems (Promega, USA) and transformed into JM109 competent cells (Promega, USA). The cells were then spread plated onto Luria broth (LB) plates containing 100 mg/mL of ampicillin, 40 mg/mL of 5-bromo-4-chloro-3-indolyl-β-D-galactoside (X-Gal), and 0.05 mmol/L isopropyl-β-D-thio-galacto-pyranoside (IPTG). The plates were incubated for 15 h, and bacterial colonies were screened for positive inserts using colony PCR followed by gel electrophoresis. Positive colonies were grown in LB medium for 15 h and plasmids were extracted thereafter using Mini *Plus* Plasmid DNA (Viogene, USA). The inserts that were positive in FISH screening were sequenced with M13 universal primers using the ABI Prism BigDye Terminator Cycle Sequencing Ready Reaction Kit ver.2.0 (PE Biosystems, Japan). Primer walking was conducted for insert sizes greater than 1 kbp. The sequence reads were checked, assembled, and vector sequences were removed manually using MEGA X55. DNA sequences were submitted to the DNA Data Bank of Japan (DDBJ) with accession numbers LC557012-LC557016.

2.5.3. Probe preparation and FISH

FISH probes were prepared from the plasmid DNA using the Random Primed DNA Labeling Kit (Roche, USA) according to the manufacturer's protocol. The DNA was fluorescently labeled directly using cyanine-3-dUTP (Cy3-dUTP) (PerkinElmer, USA) or indirectly using digoxigenin-dUTP (DIG-dUTP)/anti-Digoxigenin-FITC (Roche, USA) at 37 °C for 15–18 h. The probe obtained using 5S rDNA sequence as the target was named At-p5S, whereas that obtained from histone was named At-pH2AB. FISH was performed according to the method described by Taguchi et al (2020), with slight modifications. Slides of *A. pruinosa* chromosomes were denatured in 70% formamide solution at 70 °C for 2 min and then serially submerged in ice-cold 70%, 90%, and 99% EtOH for a total of 6 min. About 1 µL of DNA probes were mixed with 10 µL hybridization solution (H7782, Sigma, Japan) and then denatured at 80 °C for 1 h. For whole genome hybridization experiment, probes were then incubated at 37 °C for 1 h to allow pre-annealing of simple tandem repeats (i.e. G-C repeats). This is to minimize the hybridization signals and reveal clusters composed of high-complexity sequences. The slides with denatured chromosomes were incubated with the probe solution at 37 °C for 12–15 h to allow hybridization. Post hybridization washing was performed with 50% formamide at 43 °C for 20 min and subsequently with 2X SSC at 37 °C for 8 min. The slides were incubated twice in 1X phosphate-buffered detergent (PBD) at 25 °C for 5 min. The chromosomes were then counterstained with DAPI-Vectashield (Vector Laboratories, USA) and viewed under an AxioImager A2 fluorescence microscope equipped with an Axiocam MRm CCD camera (Zeiss, Germany). Images of suitable metaphase spreads from different embryos were captured using the AxioVision software (Zeiss). The FISH images were analyzed by measuring the chromosome lengths and hybridization signal locations using the DRAWID software (Kirov et al., 2017). Centromere indices (long arm/total length) was computed based on the formula of Lucas and Gray (1987).

Chapter 3 Investigation of polyploidy in *Acropora* based on FISH-detected loci

3.1. Abstract

Polyploidy is an important driver of evolution not only among plants but also animals. Studies on polyploidy in animals were limited among several species of fish. Aside from fish, polyploidy has been also suggested to occur among scleractinian corals based on the wide-range of chromosome numbers observed in cells of many *Acropora* species. In this study, we confirmed the polyploidy formation in 7 *Acropora* species by investigating genome duplications through counting the number of loci of conserved genes (core histone and spliceosomal snRNA genes) using fluorescence in situ hybridization. Results revealed two loci for chromosome numbers 28 and 29, indicating diploid cells for 6 *Acropora* species. Three loci were observed for *A. muricata* with 42 chromosomes, suggesting possession of triploid cells. For *A. digitifera* with 56 cells, 4 loci were observed, indicating tetraploidy. Temporal comparisons in chromosome numbers suggest that diploid and tetraploid's chromosome numbers did not change, while triploid chromosome number changed from 42-44. Phylogenetic analysis showed that the ancestral chromosome number is diploid which splits into two clades, one of which arises to triploids and tetraploids. Our findings add information into the polyploidy formation in animals by providing basal invertebrate representatives.

3.2. Introduction

Polyploidy is the possession of more than two chromosome sets in cells of organisms. The two common forms of polyploidy are autoploidy and alloploidy. Autopolyploids arise from the union of unreduced (2n) gametes caused by abnormal meiotic segregations. Allopolyploids, on the other hand, are formed as a result of hybridization of gametes from close related species with different chromosome number but compatible chromosome sets. Polyploidy are common among plants and regarded to be the main drivers of plant evolution. Although rare in animals, recent genome evidence showed that polyploidy is also a significant driver in the animal evolution (Mable et al., 2011; Yang et al., 2022). Study showed that several diploid land animals were derived from polyploid ancestors ray-finned fishes (Meyer & van de Peer, 2005). This evolutionary insight is also supported by high degree of polyploidy in basal animals such as with scleractinian corals (Kenyon, 1997). Polyploidy in scleractinian corals has been suggested to reflect reticulate evolution, which is frequent and repeated hybridization of closely related lineages, the same evolutionary process that give rise to diversification of plants (Kenyon, 1997). However, previous investigations on the chromosome numbers of scleractinian corals relied only on the counting the chromosomes in each cell under the light microscope showing high diversity of chromosome numbers ranging from 24 to 54 (Kenyon, 1997). The previous study proposed triploidy and tetraploidy events resulting to higher chromosome numbers. However, to date, there is no empirical evidence supporting whether these variations of chromosome sets is a function of polyloidy as a result of genome duplications or the inherent genome organization of the species.

In this study, we verified whether the highly varied chromosome numbers observed among stony corals from genus *Acropora* is a result of polyploidy and genome duplication. We detected the locus of the conserved repetitive genes such as core histone and spliceosomal

snRNA genes using Fluorescence in situ hybridization (FISH) to identify the number of chromosome sets (ploidy level) of each coral species. We then relate their chromosome structure and polyploidy level to their phylogeny using molecular sequences to observe patterns of evolution relating to these chromosome number changes.

3.3. Results

3.3.1. Chromosome number composition

Results showed that most of the *Acropora* species (*A. hyacinthus, A. japonica, A. valida, A. solitaryensis*) and *Goniopora djiboutiensis* has 28 chromosomes as the highest proportion of all the cells observed (Fig. 3.1). Lower number of chromosomes than 28 in some cells may infer loss of chromosomes during preparations. However, in the case of *A. valida*, more than 25 % of all its cells contained 27 chromosomes. Chromosome numbers of higher than 28 that are highest in proportion were observed in *A. pruinosa* (29), *A. muricata* (42), and *A. digitifera* (56). The distribution of the chromosomes numbers on these species are more spread compare with coral species with 29 chromosomes except for *A. pruinosa*

These findings on the chromosome numbers of the investigated coral species reveals high variations not only on the dominant chromosome numbers between species but also on the highly varied chromosome numbers within cells of a coral species. To determine temporal variations in dominant chromosome numbers, counts for two different sampling seasons were compared (Fig. 3.2). Data showed that for *A. pruinosa*, there is no change in the dominant chromosome number (29) between Jul 2014 and Aug 2015. Likewise, in A. digitifera, there is no change in the dominant chromosome number (56) between its two sampling dates. In contrast, for *A. muricata*, dominant chromosome differs between two sampling dates (Jun 2014 and Jul 2018) which were 42 and 44, respectively.

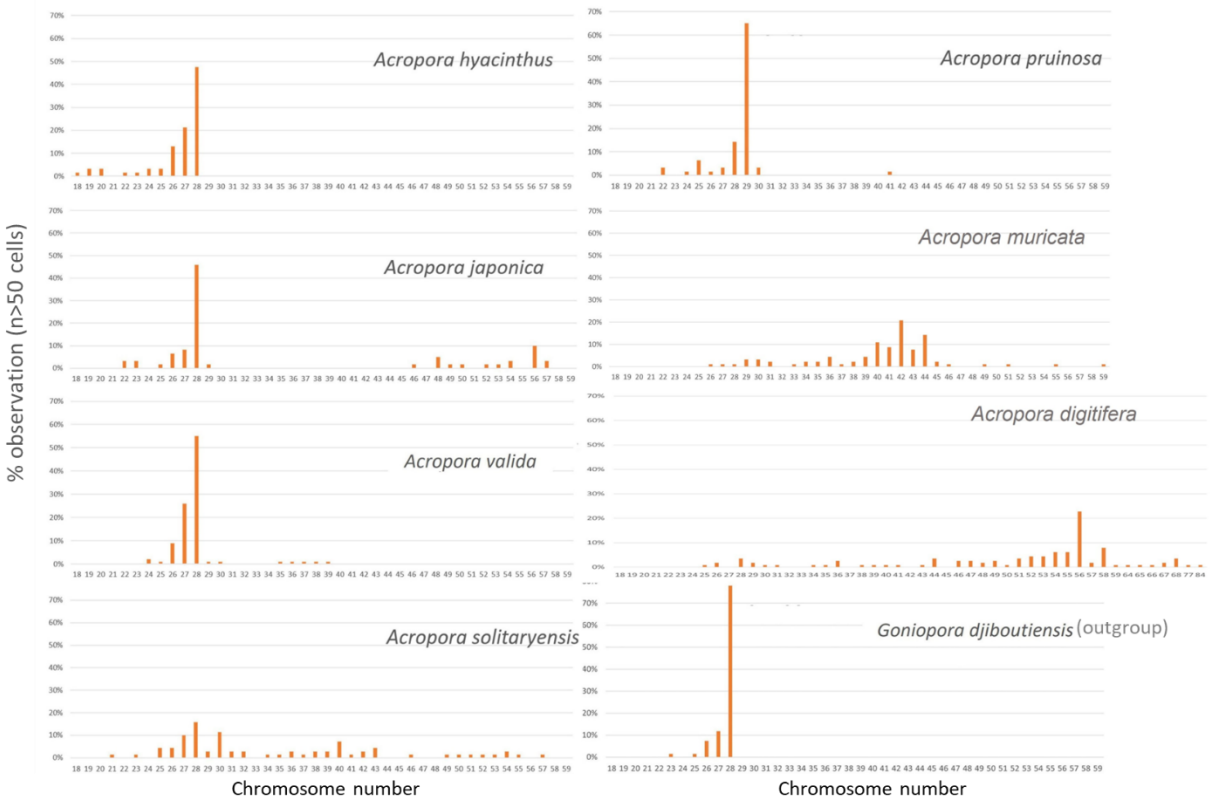

Figure 3.1. Chromosome number composition of 7 *Acropora* species and *Goniopora djiboutiensis*.

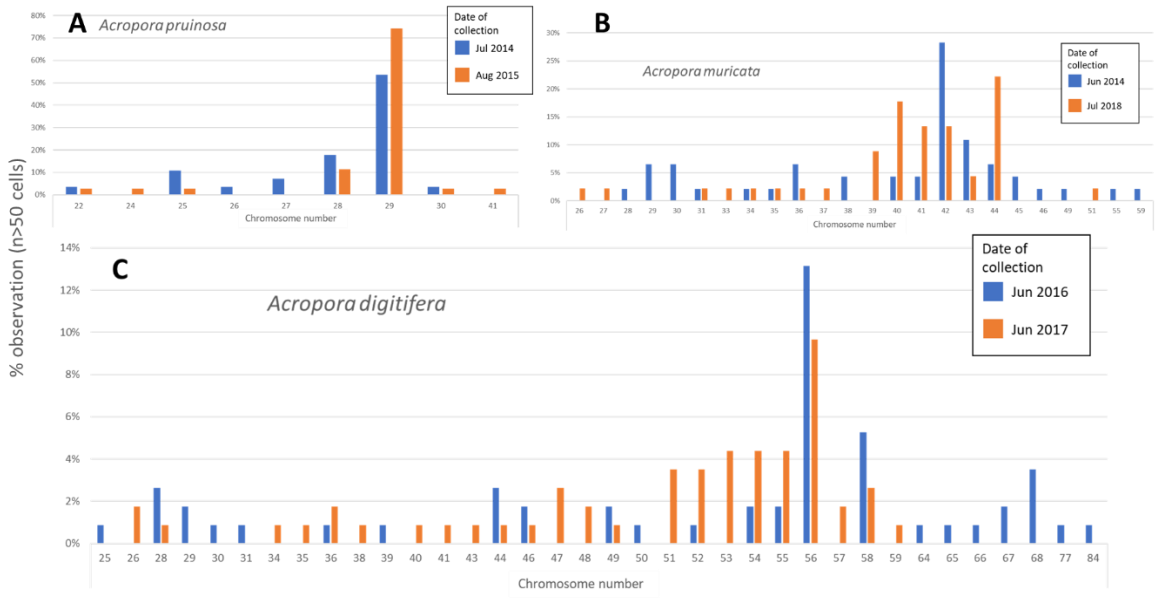

Figure 3.2. Comparison of chromosome number composition between two different sampling dates of (A) *A. pruinosa*, (B) *A. muricata*, and (C) *A. digitifera*.

3.3.2. Ploidy level determination

FISH results showed that coral species with predominant chromosome numbers of 28 and 29 (*Acropora japonica*, *A. pruinosa*, *A. valida*, *A. solitaryensis*, *A. hyacinthus*, *Goniopora djiboutiensis*) have two loci of target gene loci (Fig. 3.3), which infer diploid chromosomes (2n). The *A. muricata*, which has predominant chromosome numbers of 42, has 3 loci, indicating triploid chromosomes (3n). Karyotyping of the triploid cells showed that the loci of core histone gene is on chromosome 11 (Fig. 3.4A). The *A. digitifera*, which has 56 chromosomes, has 4 loci, indicating tetraploid chromosomes (4n). Karyotyping showed the duplicated chromosome pairs in a tetraploid cell of *A. digitifera* (Fig. 3.4B). These ploidy levels revealed that the haploid number of these stony coral species, except for *A. pruinosa* (2n=29) is n=14.

Karyotyping of the odd chromosome numbers (29) reveals that the longest chromosome is unpaired (Fig. 3.5). We speculate that this chromosome is related to functioning as the sex chromosome. To test this, we used FISH probe from the sperm genome and it showed hybridization signal on that longest chromosome, signifying as the putative Y chromosome (Fig. 3.5B).

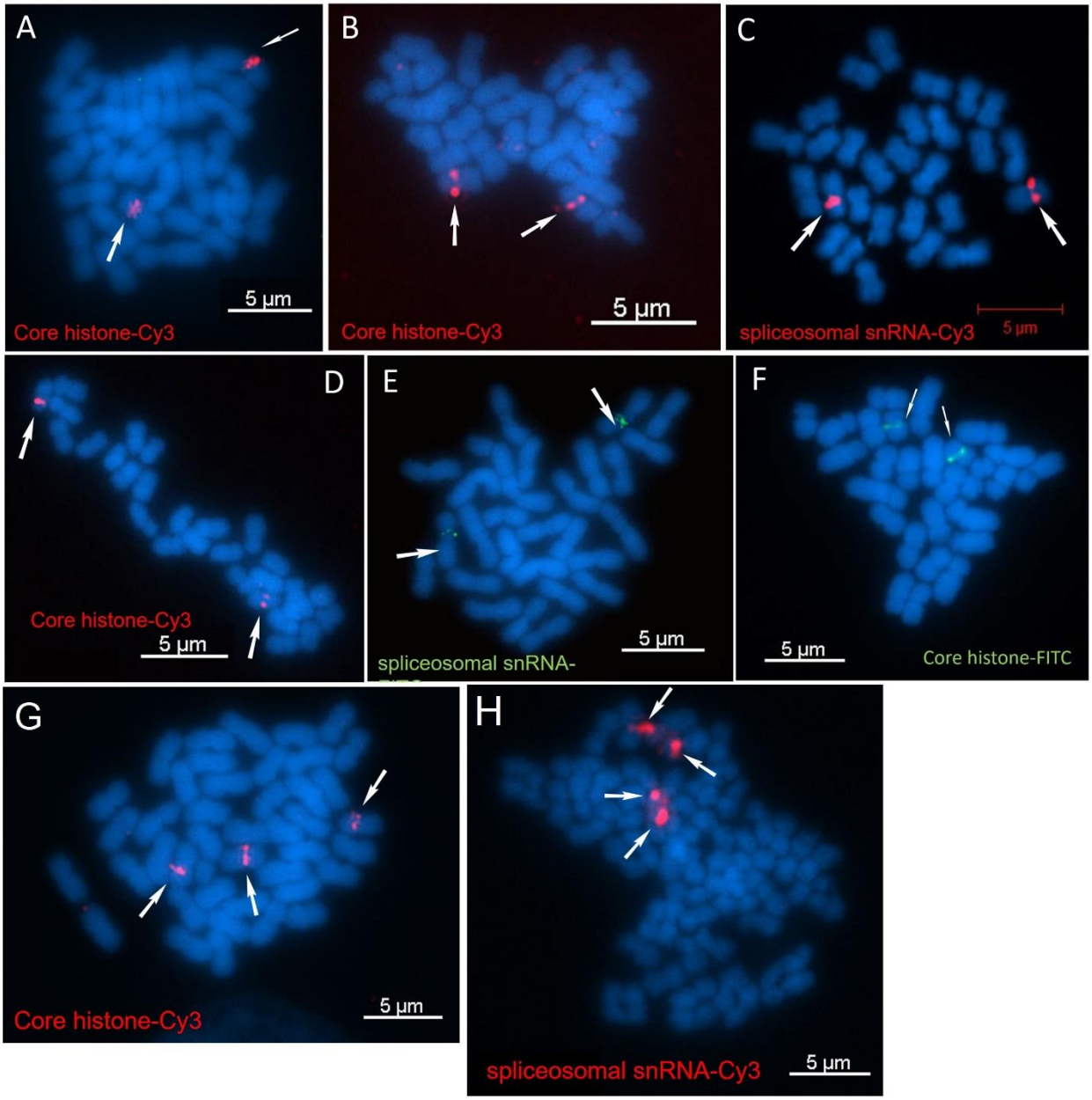

Figure 3.3. Ploidy level based on the number of conserved gene loci. (A) *Acropora japonica* (2n=28), (B) *A. pruinosa* (2n=29), (C) *A. valida* (2n=28), (D) *A. solitaryensis* (2n=28), (E) *A. hyacinthus* (2n=28), (F) *Goniopora djiboutiensis* (2n=28), (G) *Acropora muricata* (3n=42), (H) *A. digitifera* (4n=56)

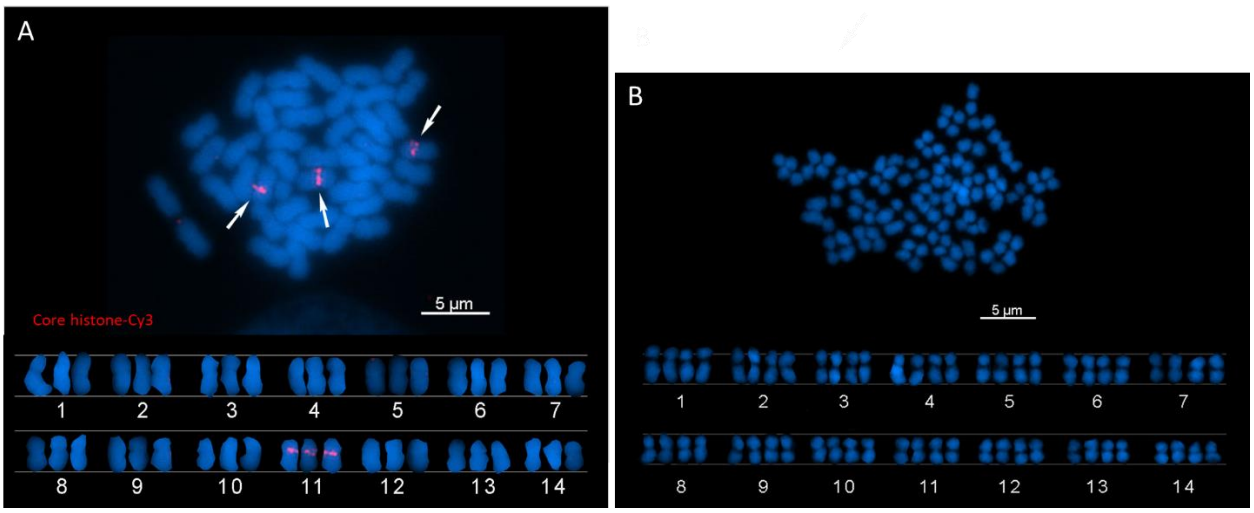

Figure 3.4. Karyotypes of triploid cell of (A) *Acropora muricata* and tetraploid cell of (B) *A. digitifera*.

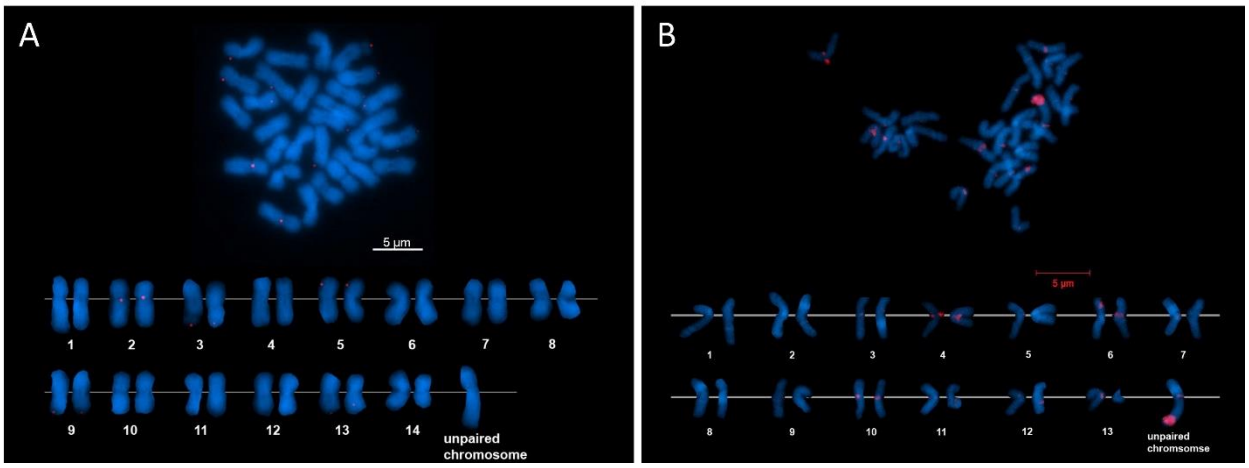

Figure 3.5. Karyotypes of odd chromosomes showing unpairing of the longest chromosome. (A) *Acropora pruinosa* (2n=29), (B) *Acropora valida* (2n=27).

3.3.3. Phylogenetic relationships

Sequence analysis using mitochondrial control region and cytochrome c oxidase subunit III (COX3) gene showed the phylogenetic relationships of the 7 *Acropora* species and *Goniopora djiboutiensis* as outgroup (Fig 3.6). The tree separates into two major clades: The first clade was composed of *A. solitaryensis*, *A. valida*, and *A. pruinosa*, *A. digitifera* and *A.*

muricata and *A. digitifera*. The other major clade is composed of only *A. japonica* and *A. hyacinthus*. The diploid species formed a polyphyletic group.

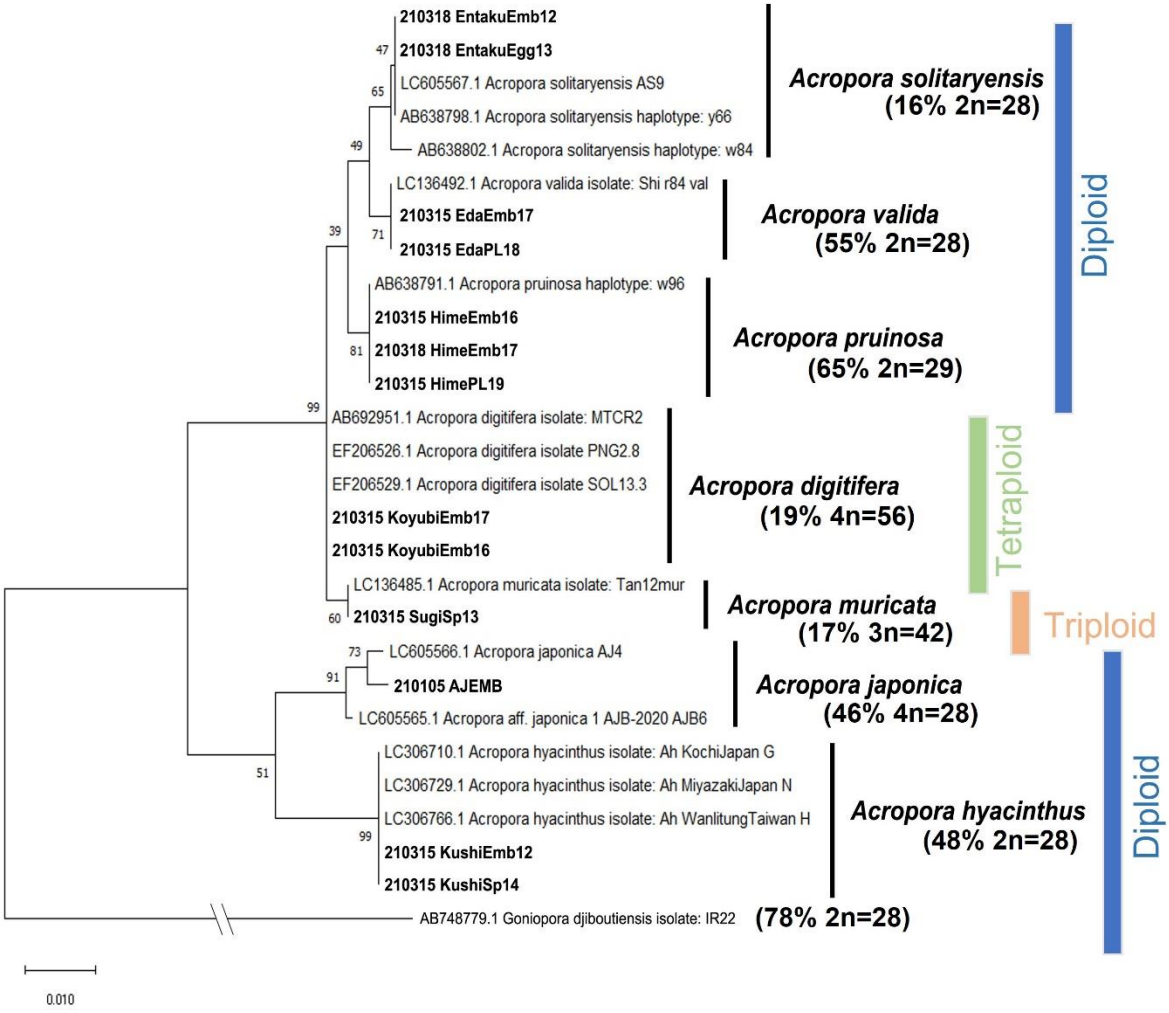

Figure 3.6. Phylogenetic tree showing the evolutionary relationship of the 7 Acropora species with *Goniopora djiboutiensis* as the outgroup.

3.4. Discussion

Previous reports have shown that genus *Acropora* has chromosome numbers ranging from 24-54 (Kenyon, 1997). Our result revealed that chromosome numbers can reach up to 56

as observed in *A. digitifera*. The 24 chromosomes in cells were observed very rarely. Most of the investigated *Acropora* species have diploid number of 28 (2n=28) in high percentage of cells. The 2n=28 has been already demonstrated from the karyotype of several stony species (Kawakami et al., 2022; Taguchi et al., 2013, 2014, 2016, 2017, 2020; Takaoka et al., 2012) but ploidy levels of higher chromosome numbers (>40) have been investigated only now. In this study, we demonstrated that cells with 42 are triploids and 56, are tetraploids based on the number of conserved gene loci. Although common knowledge indicates that 42 and 56 are triploid and tetraploid of 2n=28, respectively, our FISH results provided evidence of this occurrence for the first time.

There is limited information on the biology of triploid stony corals. Triploids are known sterile individuals because it leads to errors in chromosome segregation during meiotic division resulting to aneuploid gametes (Tiwary et al., 2005). Although sterile, triploids grow better than diploid counterparts since energy expenditure is diverted more to somatic growth than to sexual maturation and gametogenesis. Behavior was also observed to change for triploid individuals. Triploid Atlantic salmon tend to be less aggressive than diploids (Carter et al., 2011). A study also showed lesser response to sound and light stimuli in triploid ayu than diploids (Aliah et al. 1990). Most of the triploid studies are from fish because of its usefulness for aquaculture. In scleractinian corals, the role of triploidy to their growth, reproduction, and behavior remains unexplored. It is important to note that scleractinian corals can reproduce asexually which produces clones through vegetative fragmentation, thus triploids can still propagate. However, in this experiment, cells were prepared from artificially fertilized gametes. This signifies that to arrive for triploid cells (3n=42), either the diploid egg is fertilized by the haploid sperm or the haploid egg is fertilized by the diploid sperm. Diploid gametes might be a result of meiotic errors of diploid individuals. Preliminary investigations on chromosomes of *A. muricata* revealed a high number of diploid cells suggesting that seasonal

variations also include diploid individuals. In addition, triploid numbers changed between seasons suggesting that triploidy formation is labile but tolerated by the organism without compromising reproductive success.

Our study observed dominance of tetraploid cells in two sampling seasons of *Acropora digitifera*. Karyotyping of the tetraploid cells showed that most of the duplicated homologous pairs are positioned beside each other. This indicates the possibility that the chromosomes undergo multivalent pairing type of meiotic segregation, in which all similar chromosomes align together (Otto, 2007). Multivalent pairing is more common among autopolyploids than allopolyploids, in the case of plants (Ramsey & Schemske, 2003). Although diploid chromosomes (2n= 28) were previously reported for this species (Shinzato et al., 2011), the proportion of the diploid cells from the population of sampled cells were not reported, thus it remained unclear whether diploid is the dominant chromosome number. Nonetheless, diploid cells of *Acropora digitifera* were also observed in this study but in a very low percentage (4%). Moreover, preliminary investigation on chromosomes of *A. digitifera* also revealed a high number of diploid cells, suggesting that seasonal variations also include diploid individuals. Since diploid *A. digitifera* is more common than triploid counterparts, the more likely event that led to the tetraploid formation is a result of fertilization of unreduced gametes (2n), rather than fertilization of unreduced triploids gametes (3n) and the normal reduced gametes (n). Unlike triploids, tetraploids have the ability to produce viable gametes such as in tetraploid goldfish and tetraploid common carp (Liu et al., 2016).

Our findings showed that polyploidy occurs in several *Acropora* species. Further studies must identify whether this polyploidy occurred spontaneously due to meiotic/mitotic errors that is tolerated by the organism (autopolyploidy) or a result of hybridization of unreduced but compatible gametes from different but closely related species (allopolyploids). Previous studies support more of allopolyploidy than autopolyploidy in *Acropora* because of

their unique reproductive characteristics in which new hybrids can be formed through hybridization, driving sympatric speciation. In relation, hybridization between certain *Acropora* species has been widely reported. Example of this are *Acropora palmata* x *A. cervicornis* (Vollmer & Palumbi, 2002), *A. florida* x *A. intermedia* (Kitanobo et al., 2016), and *A. donei* x *A. tenuis* (Morita et al., 2019). However, how this hybridization influences the chromosome numbers of the resulting hybrids, especially among parents with different chromosome numbers (e.g., 2n=28 and 2n=29), has not been investigated. In addition, it is also important to explore intraspecific variations or variations among cells of an individual and how polyploidy influences the morphological and reproductive characteristics of *Acropora*.

In this study, we highlight the application of cytogenetics through FISH techniques in investigating polyploidy. Recent studies on plant and animal polyploidy and genome duplication are based on comparative genomics of organisms with available genome data (Christoffels et al., 2004; Conant, 2014; Hermansen et al., 2016; Town et al., 2006). However, for cnidarians such as stony corals, reference genomes are limited only to few species. In *Acropora*, there were only 2 reference genomes available to date and one of them is not genome-level assembly, thus tracing genome duplication within lineages may be challenging. Here, we demonstrated that investigation of polyploidy and genome duplication using detection of loci through FISH can be done, which more suitable for taxa with few genomic data available.

3.5. Methods

3.5.1. Sample collection and chromosome preparation

Egg-sperm bundles of 7 *Acropora* species were collected from spawning colonies in 3 different locations in Japan (Fig 3.6). For *Goniopora djiboutiensis*, which is a gonochoric coral, eggs and sperms were collected from female and male colony, respectively. Spawning events occurred during the summer season in Japan (Jun, July, Aug) (Table 3.1). Collected gametes were artificially fertilized in the laboratory in 0.2 μm filtered local seawater and fertilized eggs were grown for 10–14 h. Embryos were then treated with 0.01 % (v/v) colchicine followed by the addition of hypotonic solution (seawater: dH_20 = 1:1). Chromosomes were prepared from the embryos based on the method described by Taguchi et al. (2016), with slight modifications. About 30–50 embryos were collected by centrifugation and 0.5 mL of Carnoy's fixative (absolute methanol:glacial acetic acid = 3:1) was added. Lipids were removed by soaking the embryos in diethyl ether for 4–6 h. Cells were centrifuged at 2000 × *g* for 2 min and then resuspended in 0.5 mL of Carnoy's fixative. A drop of cell suspension was placed on a slide and then flame-dried.

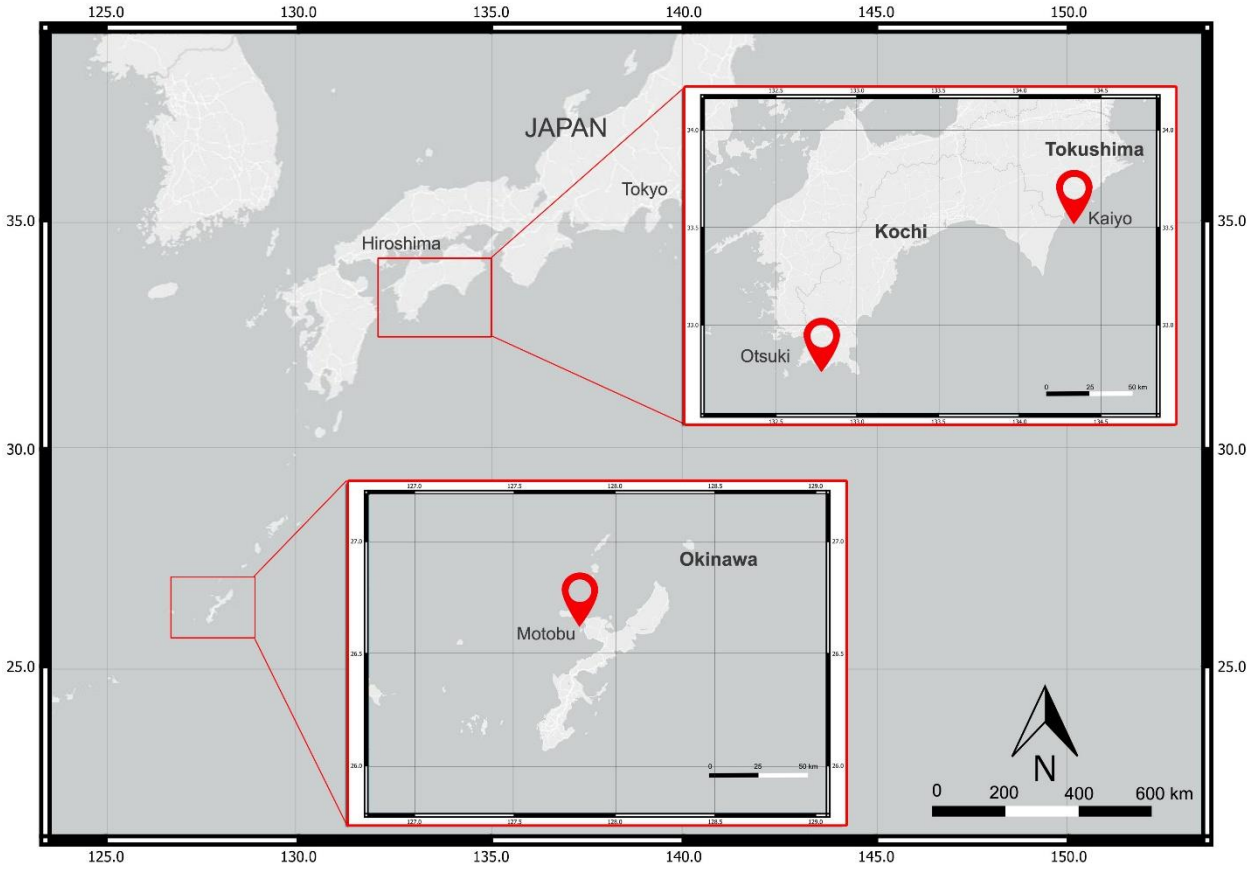

Figure 3.7. Map showing the sampling locations of the gametes from 7 *Acropora* species and 1 outgroup stony coral (*Goniopora djiboutiensis*)

Table 3.1. Date of collections and specific location where the 8 coral samples were collected.

Species	**Date coral bundle collected**	**Location**
1. *Acropora solitaryensis*	8.15.2015	Nishidomari Bay, Otsuki, Kochi
2. *Acropora valida*	7.31.2019	Kaiyo, Tokushima
3. Acropora pruinosa	7.28.2014/8.16.2015	Nishidomari Bay, Otsuki, Kochi
4. Acropora muricata	6.27.2014/7.12.2018	Nishidomari Bay, Otsuki, Kochi
5. Acropora digitifera	6.22.2016/6.7.2017	Sesoko Island, Motobu, Okinawa
6. Acropora japonica	7.29.2014	Nishidomari Bay, Otsuki, Kochi
7. Acropora hyacinthus	7.11.2019	Nishidomari Bay, Otsuki, Kochi
8. Goniopora djiboutiensis(outgroup)*	8.24.2019	Nishidomari Bay, Otsuki, Kochi

3.5.2. DNA extraction and PCR

Genomic DNA was extracted from sperms of each *Acropora* species using the Wizard Genomic DNA Purification kit (Promega, USA). The core histone genes were amplified using the primers F: 5′-TTGCAAGTTCACCGGGAAGC-3′, R: 5′-TTCCAGCCAACTCGAGAATC-3′ based on the consensus sequence of *Acropora* histone genes retrieved from the GenBank. The spliceosomal snRNA genes were amplified using the forward primer described by Stover & Steele (2001) and the reverse primer (R: 5′-GGGCCAGGGTAGTACTTGGA-3′) designed by us. The PCR conditions for all amplifications were as follows: 30 cycles of 98 °C for 20 s, 60 °C for 30 s, and 72 °C for 1 min

30 s. Amplicons were verified in gel electrophoresis and purified using AMPure XP beads (Pacific Biosciences, USA) before sequencing. The sequence reads were checked, assembled, and vector sequences were removed manually using MEGA X (Kumar et al., 2018).

3.5.3. Probe preparation and FISH

FISH probes were prepared from the plasmid DNA using the Random Primed DNA Labeling Kit (Roche, USA) according to the manufacturer's protocol. The DNA was fluorescently labeled directly using cyanine-3-dUTP (Cy3-dUTP) (PerkinElmer, USA) or indirectly using digoxigenin-dUTP (DIG-dUTP)/anti-Digoxigenin-FITC (Roche, USA) at 37 °C for 15–18 h. FISH was performed according to the method described by Taguchi et al. (2017), with slight modifications. Chromosome slides were denatured in 70% formamide solution at 70 °C for 2 min and then serially submerged in ice-cold 70%, 90%, and 99% EtOH for a total of 6 min. About 1 µL of DNA probes were mixed with 10 µL hybridization solution (H7782, Sigma, Japan) and then denatured at 80 °C for 10 min. The denatured chromosomes were incubated with the probe solution at 37 °C for 12–15 h to allow hybridization. Post hybridization washing was performed with 50% formamide at 43 °C for 20 min and subsequently with 2X SSC at 37 °C for 8 min. The slides were incubated twice in 1X phosphate-buffered detergent (PBD) at 25 °C for 5 min. The chromosomes were then counterstained with DAPI-Vectashield (Vector Laboratories, USA) and viewed under an AxioImager A2 fluorescence microscope equipped with an Axiocam MRm CCD camera (Zeiss, Germany). Images of suitable metaphase spreads from different embryos were captured using the AxioVision software (Zeiss).

Chapter 4 Identification of putative Y-sex chromosome using locus of dmrt gene

4.1. Abstract

The diversity of sex determination systems in animals suggests that sex chromosomes evolve independently across different lineages. However, the present data on these systems is largely limited and represented mainly by bilaterian animals. Sex chromosomes and sex determination system based on cytogenetic evidence remain a mystery among non-bilaterians, the most basal animals. Here, we investigated the sex determination system of a non-bilaterian (*Goniopora djiboutiensis*) based on karyotypic analysis and identification of locus of *dmrt1*, a known master sex-determining gene in many animals. Results showed that among the three isolated *dmrt* genes, *GddmrtC* was sperm-linked. Fluorescence in situ hybridization revealed that 47 % of the observed metaphase cells contained the *GddmrtC* locus on the shorter chromosome of the heteromorphic pair, whereas the other 53 % contained no *GddmrtC* locus and pairing of the longer chromosome of the heteromorphic pair was observed. These findings provided the cytogenetic evidence for the existence of the Y sex chromosome in a non-bilaterian animal and supports male heterogamety as previously reported in other non-bilaterian species using RAD sequencing. The Y chromosome-specific *GddmrtC* sequence was most homologous to the vertebrate *dmrt1*, which is known for its role in male sex determination and differentiation. Our result on identification of putative sex chromosomes for *G. djiboutiensis* may contribute into understanding of the possible genetic sex determination systems in non-bilaterian animals.

4.2. Introduction

Sex of animals is determined by either environmental sex determination (ESD), genetic sex determination (GSD), or both. ESD is exhibited primarily by some reptiles, fish, and certain species of invertebrates (crustaceans, worms, hydrozoans), in which the sex of the animal is dictated by temperature or other environmental cues. GSD, on the other hand, is the most widely recognized sex determination mechanism in animals. In GSD, sex is generally determined by the presence of a sex chromosome that carries the key genes responsible for the development of male or female-specific characteristics. Various GSD systems based on different sex chromosome configurations have been reported in animals. These are male heterogamety (XX/XY) in mammals and many insects; female heterogamety (ZZ/ZW) in birds, reptiles, and Lepidoptera insects; homomorphic sex chromosomes in some reptiles; and haplodiploidy in some arthropods (Bachtrog et al., 2014; Kaiser & Bachtrog, 2010; Reinhold & Engqvist, 2013). The diversity and complexity of these sex determination systems appear to have no clear evolutionary patterns, which formed the consensus understanding that sex chromosomes evolve independently across different lineages (Ellegren, 2011; Fridolfsson et al., 1998). However, current empirical data on sex determination systems of animals are still highly limited and underrepresented, as previous investigations are limited among the bilaterians. The GSD system from a non-bilaterian animal might provide important insight into the sex determination mechanisms of basal animals, which may contribute to the overall understanding of the evolution of sex determination systems and sex chromosomes in animals.

The conventional approach to identify the GSD system of an organism is based on cytogenetic methods. Using cytogenetic data, chromosome structures and organization are revealed in karyotypes, from which sex chromosomes can be identified. This method serves as the foundation for the discovery of various sex determination systems among many important organisms (Bridges, 1914; Ford et al., 1959; Koller & Darlington, 1934). Recent advancements in cytogenetic techniques include fluorescence in situ hybridization (FISH) which can identify sex chromosomes through detection of sex-specific genes or loci using fluorescent DNA probes. The most popular gene used for this FISH analysis is the *dsx* and mab-3 related transcription factor 1 (*dmrt1*), a known master sex-determining gene in some animals. This FISH technique has led to the identification of sex determination systems of several animals such as the male heterogamety (XX/XY) for medaka fish *Oryzias latipes* (Matsuda et al., 2002) and female heterogamety (ZZ/ZW) for both African clawed frog *Xenopus laevis* (Yoshimoto et al., 2008) and domestic chicken *Gallus gallus domesticus* (Smith et al., 2009). Recent approaches in identifying sex determination systems have taken advantage of the applications of high-throughput sequencing to identify the sex-linked markers. This approach has been applied to many animal species even without any prior robust cytogenetic information (Cui et al., 2015; Shi et al., 2018; Zhou et al., 2019). In fact, the XX/XY sex determination system in non-bilaterian animals was first inferred based on this method with the use of RAD-sequencing and SNP markers (Pratlong et al., 2017). However, this approach requires genetic data from a high number of male and female individuals to differentiate sex-linked loci from the polymorphic loci in the autosomes (Darolti et al., 2019). In addition, due to its infancy, bioinformatic and statistical tools are still being validated to accurately infer sex determination systems using these data (Palmer et al., 2019). A karyotypic analysis which offers direct observation of the chromosome structures and organization, as well as the loci of specific genes, might serve as important in-situ

reference to explore its sex determination system. Although several cytogenetic data from non-bilaterians have been reported, all the species investigated are hermaphroditic, in which their karyotypes may provide no information on their sex chromosomes and thus to their GSD system (Anokhin & Kuznetsova, 2018; Taguchi et al., 2013, 2016, 2017). Chromosome information from gonochoric non-bilaterian species would provide the evidence for identifying the GSD system for these animals.

Hence, in this study, we provide the GSD system for a gonochoric non-bilaterian *Goniopora djiboutiensis* based on cytogenetic data and FISH analysis. First, we karyotyped several metaphase cells to identify the presence of heteromorphic chromosome pairs, an indication of sex chromosomes. We then isolated the sperm-specific *dmrt* and identified its locus in their chromosomes. Here, we hypothesized that the *dmrt* locus is on one member of the heteromorphic chromosome pair, providing the evidence for the presence of the male chromosome and validate male heterogamety (XY) for *G. djiboutiensis*. We used *G. djiboutiensis* because of its commonality in many shallow coral reef ecosystems and established gonochorism (Fellegara et al., 2013; Suzuki, 2012).

4.3. Results

4.3.1. Karyotyping and chromosome structure

Chromosome lengths from 10 representative karyotypes with similar mitotic stages (composed of intermediately condensed chromosomes) showed the existence of two types of karyotypes (Fig 4.1A). The first karyotype (Fig 4.1A, blue trendline) has unpaired longest

chromosome (tentatively named chromosome 0) based on its conspicuous length and its lower centromeric index compared to the next longest chromosome (Table 4.1). In addition, chromosome lengths alone indicate that this karyotype has three copies of chromosome 3 (Fig 4.1B). However, a careful inspection showed that one of the three chromosome 3 has a slightly different centromere position (Fig 4.1B and C) based on its lower centromeric index (Table 4.1). Further investigation using Giemsa staining also revealed that one of those 3 chromosomes has a different banding pattern by having 1 heterochromatic region in the short arm and 3 heterochromatic regions in the long arm (Fig 4.1C, 3* arrow). In contrast, the other two chromosome 3 have indistinguishable and lighter heterochromatin regions in the entire length of the chromosome. These observations suggest the presence of another unpaired chromosome (tentatively named chromosome 3*). These two unpaired chromosomes (chromosome 0 and 3*) in several cells are considered as the heteromorphic chromosome pairs, an indication of sex chromosomes. Although the other 23 non-representative karyotypes, which composed of long (less condensed) and short (highly condensed) chromosomes, showed inconspicuous size differences between each chromosome, identification of these heteromorphic pairs was still possible due to their distinct centromere locations and other chromosome features (i.e, stain intensity, secondary constriction).

The other karyotype (Fig 4.1A, red trendline) revealed that the chromosome 0 is paired (Fig 4.1D). This observation is supported by the conspicuous longer sizes of their first 3 chromosome pairs (chromosomes 0-2) than the rest of the chromosomes (Figs 4.1D and E), as compared with the karyotype with heteromorphic chromosome pairs in which one of those long chromosomes was missing (Fig 4.1B). In addition, these karyotypes are characterized by the absence of the unique chromosome 3*, as revealed in Giemsa staining (Fig 4.1E). The proportion of the two karyotypes observed in mitotic cells of *G. djiboutiensis* is 52 % (17/33) for karyotypes with heteromorphic pair and 48 % (16/33) for karyotypes with paired

chromosome 0. The ratio of the two identified karyotypes is approximately 1:1, indicating the presence of a sex-specific karyotype. The average morphometrics of each identified chromosome pair from the 33 analysed metaphase cells showed that the chromosomes 0-5 including the chromosome 3* are all submedian types of chromosomes, while the chromosomes 6-13 are all median types (Table 4.1).

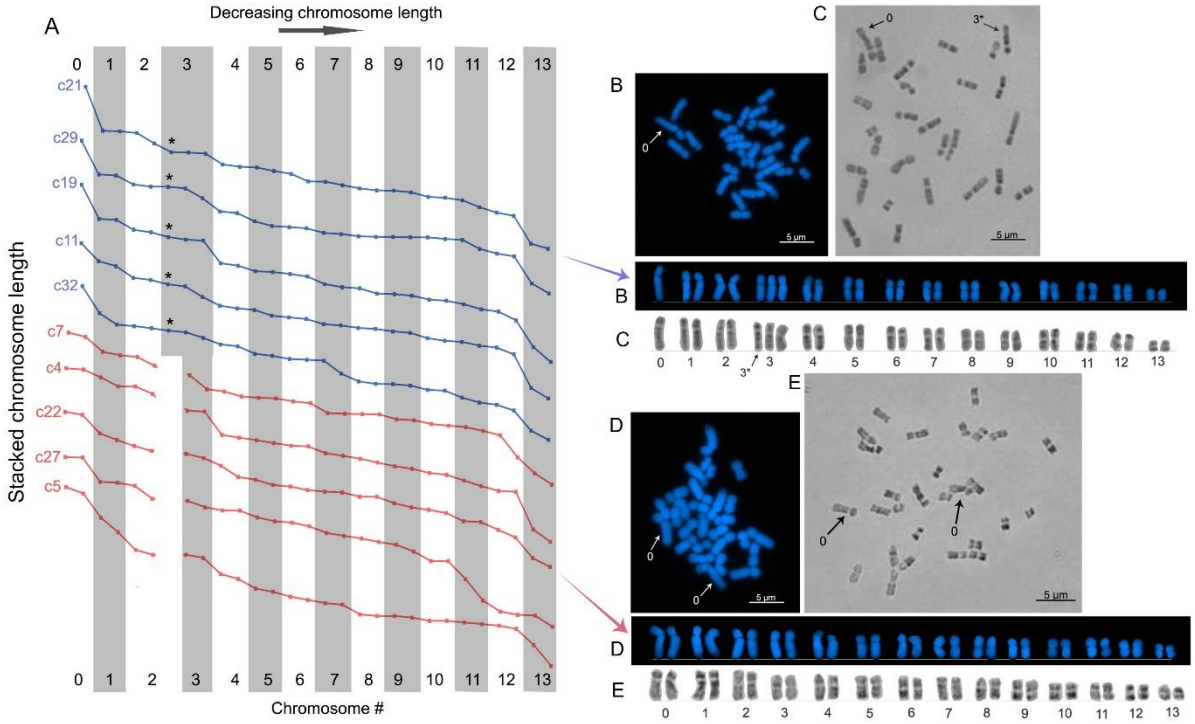

Figure 4.1. Chromosome length profile from 10 representative metaphase cells showing two types of karyotypes (blue and red trendline) for *G. djiboutiensis*. (B) Karyotype c21 stained with DAPI showing the presence of heteromorphic pair composed of unpaired longest chromosome (chromosome 0) and additional chromosome 3 (3*). (C) Giemsa-stained metaphase cell of same karyotype showing the unique G-banding patterns of chromosome 3*. (D) Karyotype c22 stained with DAPI showing the pairing of the chromosome 0. (E) A metaphase cell of the same karyotype stained with Giemsa showing the absence of chromosome 3* with its distinctive G-banding patterns.

Table 4.1. Average morphometrics of each chromosome pair from 33 metaphase spreads. Data are represented as mean ± SEM. Centromeric index is the ratio of short arm to chromosome length. The formula and classification are based on (Levan et al., 1964).

Chromosome #	**Short arm length (µm)**	**Chromosome length (µm)**	**Relative length**	**Centromeric index X 100**	**Classification**
0	1.83±0.53	5.96±1.53	0.99±0.02	30.78±3.88	Submedian
1	1.73±0.44	5.48±1.35	0.92±0.05	31.74±3.53	Submedian
2	1.75±0.47	5.13±1.18	0.86±0.07	34.24±4.63	Submedian
3*	1.73±0.4	4.92±1.15	0.84±0.07	35.3±2.96	Submedian
3	1.7±0.39	4.81±1.08	0.8±0.07	35.71±5.11	Submedian
4	1.49±0.55	4.44±1.03	0.74±0.05	33.67±9.15	Submedian
5	1.62±0.53	4.24±0.98	0.71±0.05	38.06±8.5	Submedian
6	1.62±0.48	4.11±0.97	0.69±0.04	39.94±8.5	Median
7	1.62±0.49	3.96±0.93	0.66±0.04	40.91±7.07	Median
8	1.61±0.41	3.83±0.9	0.64±0.05	42.29±7.02	Median
9	1.57±0.41	3.68±0.85	0.62±0.05	42.54±5.72	Median
10	1.57±0.39	3.53±0.77	0.59±0.05	44.3±4.77	Median
11	1.49±0.3	3.35±0.67	0.56±0.05	44.67±4.59	Median
12	1.38±0.28	3.09±0.55	0.52±0.06	44.77±4.84	Median
13	1.08±0.19	2.31±0.4	0.39±0.05	46.77±2.12	Median

*Chromosome is unpaired

4.3.2. Characterization of the *dmrt* genes

Three *dmrt* genes were successfully isolated from the *G. djiboutiensis*. The genes were named *GddmrtA* (996 bp, NCBI accession no. LC704528), *GddmrtB* (4284 bp, NCBI accession no. LC704529), and *GddmrtC* (6762 bp, NCBI accession no. LC704530). As expected, all *dmrt* sequences contained the DM and the DMA domain, a common gene architecture of the *dmrt* (Fig 4.2A). Comparisons of the translated domains against that of wide range of animal groups showed the highly conserved DM domains, while DMA domains are less conserved (Fig 4.2B). Further inspection of the DM domains showed that among the three identified *G. djiboutiensis dmrt*, *GddmrtC* is most homologous to the *dmrt* of these model organisms.

PCR amplification with sperm and egg genomes showed that *GddmrtA* and *GddmrtB* are present in both gametes, while *GddmrtC* are present only in the sperm genome (Fig 4.2C, lane 8 and 9). To confirm any traces of the amplicon that may not have appeared visibly in the gel electrophoresis, we conducted nested PCR which showed persistent absence of the target *GddmrtC* band size (6.3 kbp) (Fig 3C, most right lane).

To determine the splicing sites of the sperm-specific *GddmrtC* gene, the sequence was blasted against the transcriptome assembly of hermaphroditic *Goniopora lobata* (http://www.comp.hkbu.edu.hk/~db/CoralTBase/index.php) (Zhang et al. 2019). The blast result (score: 542) outputs a single isoform of mRNA transcript (1.3 kbp) which contains the highly similar DM domain sequences and less similar DMA domain sequences. The RNA-Seq reads were then aligned to that transcript to assemble the corresponding *GddmrtC*

transcript for *Goniopora djiboutiensis*. The *GddmrtC* gene map (Fig 4.2A) revealed the splicing sites in which the 5′ splicing site features the conventional GT/AG, a common splicing site for almost all eukaryotic genes [30,31]. The upstream of the 5′ splicing site, which is an important recognition site for the U2 small nuclear ribonucleoprotein, consists of the putative CCGTTAG branch point, polypyrimidine motif CCTTTTT, and the consensus AG site in the 3′ end of the intron [32]. The 6.2 kbp intron region (37 % GC content) contains no repetitive elements such as microsatellites and known transposable elements based on RepeatMasker analysis (http://www.repeatmasker.org/).

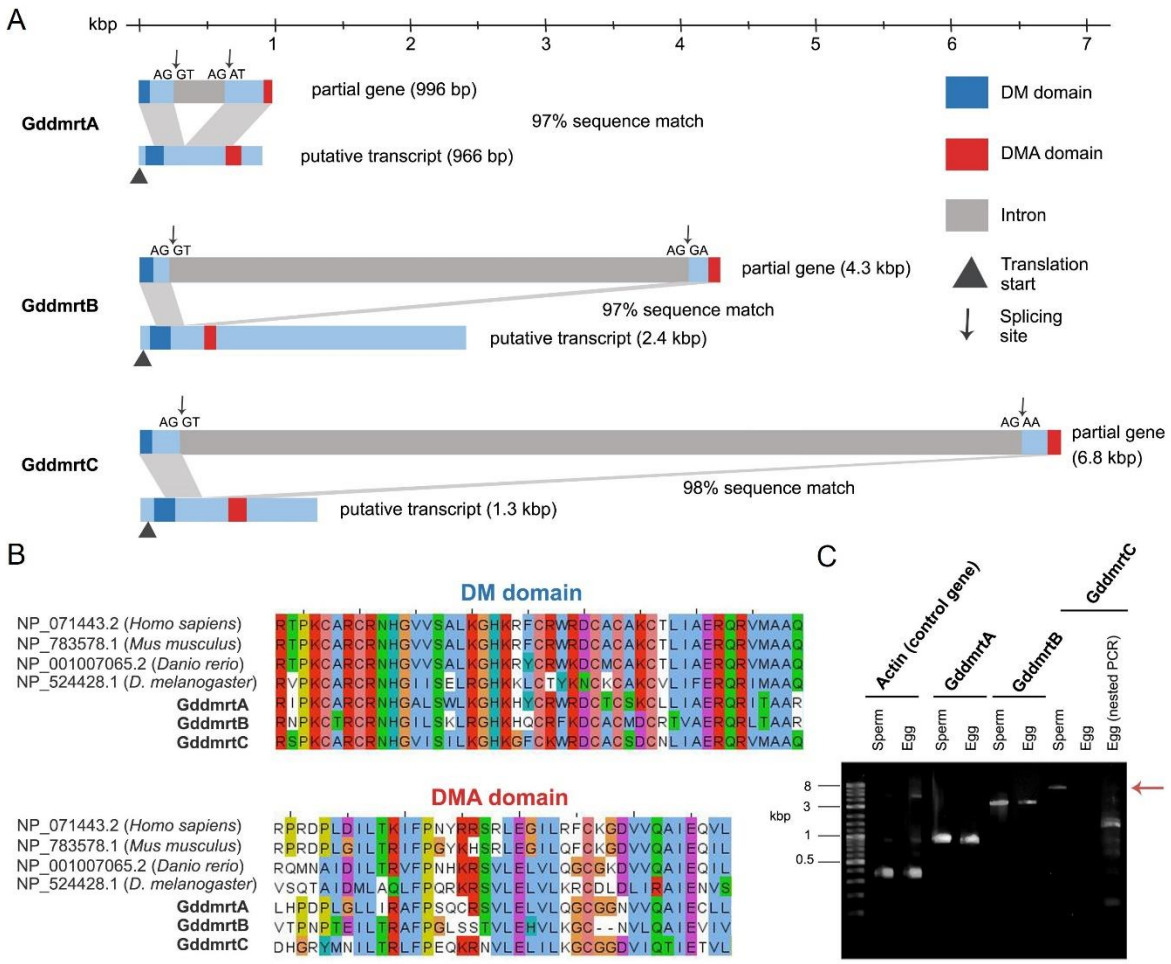

Figure 4.2. Gene map of the 3 isolated *G. djiboutiensis* dmrt (GddmrtA, GddmrtB, and GddmrtC) showing the splicing sites and the locations of the DM and DMA domains. The corresponding transcript sequences were constructed based on the assembled RNA-seq reads. (B) Protein sequence alignment of the DM and DMA domains of the 3 dmrt genes along with sequences from model organisms. (C) Gel electrophoresis image of the amplified dmrt genes and the control *actin* gene from sperm and egg genomes. Expected band size for GddmrtC (Red arrow).

Homology analysis of the translated coding regions of the three *dmrt* sequences revealed that the sperm-linked *GddmrtC* is most homologous to the doublesex- and mab-3-related transcription factor 1 (*dmrt1*) of the model organisms (Fig 4.3). Included in this cluster is the W chromosome-linked *dmrt* (DM-W) of African clawed frog *Xenopus laevis*. The protein sequence of the *GddmrtA*, on the other hand, is most homologous to *Dmrtb1* identified in mice and humans. The *GddmrtB* has the most divergent protein sequence, which appeared between most of the animal *dmrt* and *dmrt-dmd10* of *Caenorhabditis elegans*.

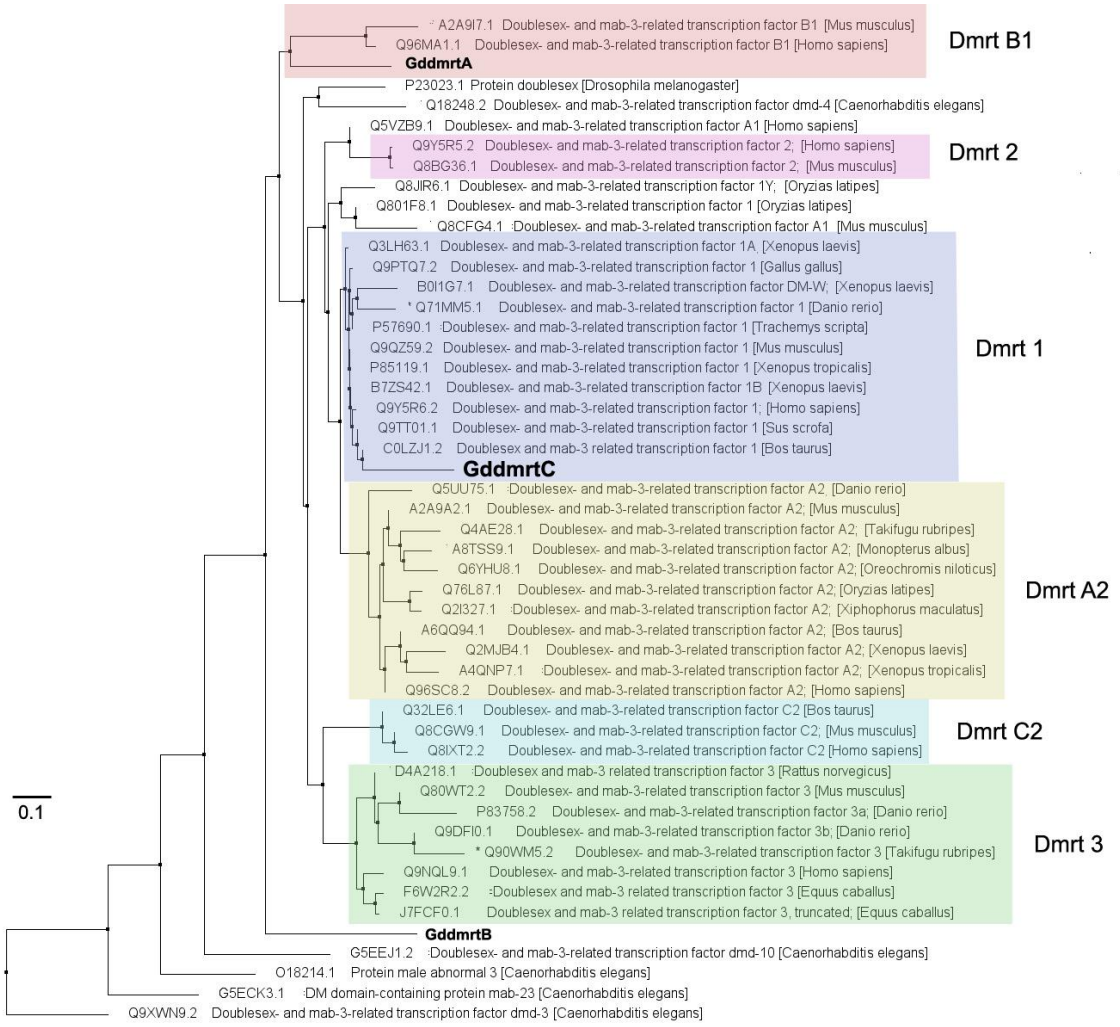

Figure 4.3. Fast minimum evolution tree of the predicted protein sequence of the GddmrtA, GddmrtB, and GddmrtC of *Goniopora djiboutiensis* against the dmrt from UniProtKB database. The tree was based on BLASTP pairwise alignments and Grishin (protein) substitution model.

4.3.3. GddmrtC gene locus

FISH analysis revealed that the locus of the sperm-specific *GddmrtC* gene (Fig 4.4A, red signal) was on the p-arm of a single chromosome. Karyotype showed that this chromosome is one of the chromosome 3 and appears to be the shorter chromosome of the heteromorphic pair (chromosome 3*) based on its unique centromere location. This revealed that the chromosome 3* contains the sperm-specific locus and possibly has the characteristics of the male chromosome Y. The locus of the control FISH probe (histone H3 gene), on the other hand, was detected on the chromosome pair of chromosome 12 (Fig 4.4A, green signal). This karyotype along with this FISH signal pattern was observed in 15 out of 32 (47 %) metaphase spreads analysed by FISH, which is comparable to the 52 % with heteromorphic chromosome pairs previously described. In addition, the unpaired longest chromosome in this FISH signal pattern resembles the karyotypes with heteromorphic chromosome pairs (Fig 4.1A, blue trendline).

The other 53 % (17/32) of FISH images showed no locus for *GddmrtC* as shown by hybridization signal only from the control H3 probe (Fig 4.4B, green signal). Interestingly, these 17 cells also revealed karyotypes with pairing of the chromosome 0, which appeared to be the karyotypes previously described (Fig 4.1A, red trendline). The unpairing of the chromosome 0 in karyotypes that contained the putative chromosome Y and the pairing of chromosome 0 in karyotypes that do not contain the chromosome Y strongly suggests chromosome 0 as the female chromosome X. The proportion of the two FISH patterns observed is 47 % and 53 % (approximately 1:1 ratio), also indicating the presence of sex-specific karyotype.

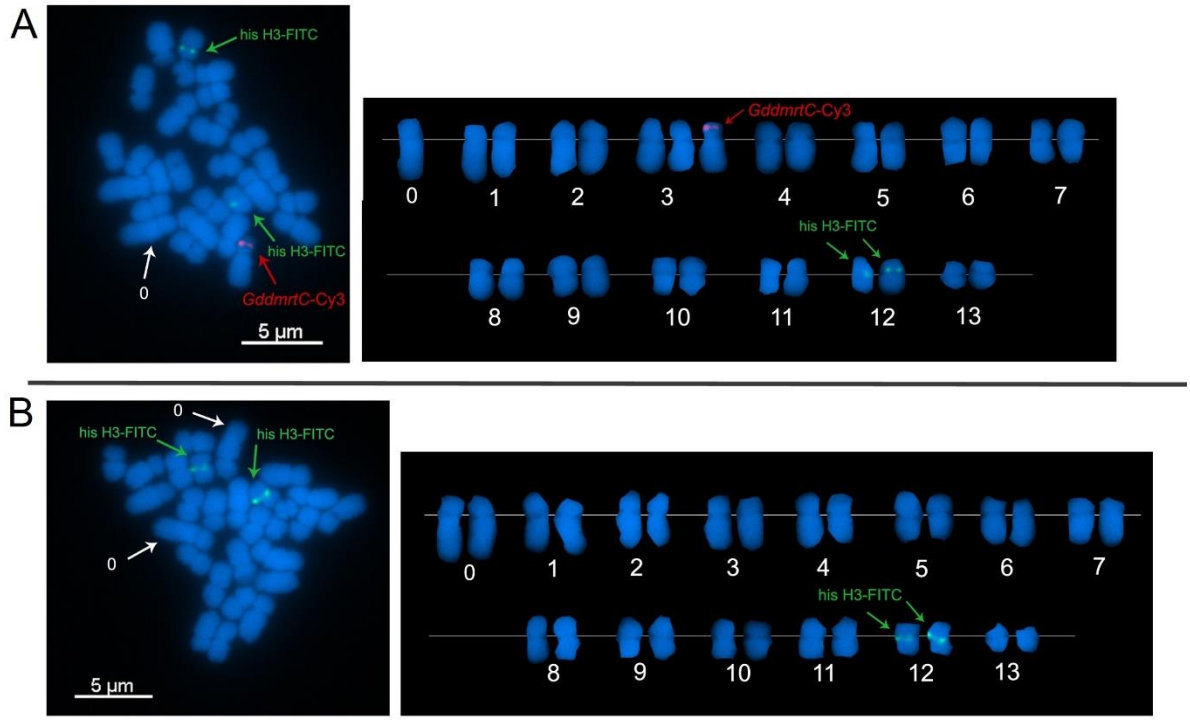

Figure 4.4. FISH images showing hybridization signal of GddmrtC probe (red) and control gene histone H3 (green) in (A) mitotic cell with heteromorphic chromosome pair and (B) mitotic cell with paired chromosome 0.

To summarize, the result on karyotyping provided the evidence on the presence of heteromorphic chromosome pairs in almost half of the metaphase cells observed. Further, FISH analysis identified the locus of sperm-specific *dmrt* gene on the shorter chromosome of the heteromorphic pair. Combining these two results implies male heterogamety and suggests XX/XY sex determination system for *G. djiboutiensis*.

4.4. Discussion

Heteromorphic chromosome pairs have already been observed in the karyotypes of non-bilaterians, particularly among stony corals (Kawakami et al., 2022; Taguchi et al., 2014, 2020; Vacarizas et al., 2021). First attempts to identify these heteromorphic chromosome pairs as sex chromosomes were conducted in the chromosomes of *Acropora solitaryensis* (Taguchi et al., 2014) and *Acropora pruinosa* (Vacarizas et al., 2021) using sperm DNA as the FISH probe. Although results showed intense hybridization signal on one member of the heteromorphic pair, this did not provide clear evidence whether the hybridized chromosomal region is composed of sperm-specific gene sequences.

In chromosomes of story coral *Favites pentagona,* a FISH probe from 18S ribosomal DNA (rDNA) sequences also showed intense hybridization signal on a single chromosome (Kawakami et al., 2022). Studies have shown that repetitive 18S rDNA sequences, along with 28S and 5.8S, are part of the Nucleolar Organizing Region (NOR), known to reside in the sex chromosomes of some animals (Born & Bertollo, 2000; Pardue & Hsu, 1975). This NOR in the sex chromosomes functions in the pairing of X and Y chromosomes during the metaphase 1 stage of meiosis (McKee & Karpen, 1990). The findings from *F. pentagona,* may infer that the 18S rDNA sequence can be used as FISH marker to identify the sex chromosomes. However, the 18S rDNA sequences are not exclusively located in the sex chromosomes, as it is also known to reside in the autosomes (Cabral-de-Mello et al., 2011; de Souza-Firmino et al., 2020; Grozeva et al., 2011). A better method is to use sex-specific genes as FISH probes to identify either the male or female sex chromosomes. Our study developed for the first time a FISH probe from sperm-specific *dmrt* gene to identify the male sex chromosomes in non-bilaterians.

Two of the isolated *dmrt* (*GddmrtA* and *GddmrtB*) are found to be non-sex specific. The *GddmrtA* is most homologous to *Dmrtb1*, which is autosomal in humans and plays a role in the entry of spermatogonia into meiosis (Hilbold et al., 2019). *GddmrtB*, on the other hand, appears to be related to *Caenorhabditis elegans dmrt-dmd10* which functions in promoting neural signal of sensory receptor activation (Mason et al., 2008), a role not related to sex determination or gamete development. The autosomal characteristics of the *Dmrtb1* and the functional role of the *dmrt-dmb10* may support the non-sex specificity of the *GddmrtA* and *GddmrtB*, although there is greater possibility that chromosomal locations of certain genes might vary across different species. In contrast, the sperm-specific *GddmrtC* was most homologous to the *dmrt1*, in which experimental evidence has shown its involvement in male sex determination and differentiation by controlling the male gonad development (Matson et al., 2010, 2011; Raymond et al., 2000). In birds, the *dmrt1* gene is also linked to male Z-chromosome and knocking down the gene in males leads to transformation of the developing male gonads to female gonads (Smith et al., 2009). The nucleotide sequence of the *GddmrtC* showed its highest similarity to the *dmrt* of *Acropora millepora* (*AmDM1*). Expression study of *AmDM1* showed that it undergoes alternative splicing that produces a transcript having both the *dmrt* domains (DM and DMA) and an alternative transcript having the DMA domain only (S. W. Miller et al., 2003). The alternative transcript with the DMA domain only seems more involved in sex determination based on its higher expression during late embryonic stages when sex-specific gonad germ cells start to develop (S. W. Miller et al., 2003). These studies on male-specificity and homology of the *GddmrtC* to *dmrt1* highly suggest its role as the master-sex determining gene in *G. djiboutiensis* and verify its potential use as chromosomal marker to identify the male sex chromosomes. It is important to note the possibility of existence of other sex-linked *dmrt* genes and their alternative spliced transcripts

in *G. djiboutiensis* because the reference genomes and transcripts used in this study are from other species.

We found a single locus for the sperm-specific *GddmrtC* and that locus is located on the shorter chromosome of the heteromorphic chromosome pairs. These observations led to identification of the putative Y chromosome on *G. djiboutiensis*. *Dmrt* has also been reported to be sex chromosome-linked in other higher animals. For instance, DM-containing gene DMY is Y chromosome-linked in medaka fish *Oryzias latipes* (XX/XY system) (Matsuda et al., 2002), female-specific DM-W linked to W chromosomes of african clawed frog *Xenopus laevis* (ZZ/ZW system) (Yoshimoto et al., 2008), linkage of *dmrt1* in Z chromosome of domestic chicken *Gallus gallus domesticus* (ZZ/ZW system) (Smith et al., 2009), and linkage of *iDMY* in Y chromosome of Eastern spiny lobster *Sagmariasus verreauxi* (Chandler et al., 2017). Among the non-bilaterians, a study showed that in *Hydra*, the *dmrt* locus is on their homomorphic chromosome pair (Anokhin et al., 2010), but whether the pair is an autosome or sex chromosomes remains unknown. In case that this chromosome pair functions as their sex chromosome implies that its mechanism of sex determination may not be influenced by the single *dmrt* gene in the sex chromosome but rather mediated by dosage compensation or locus inactivation. There is limited information on the role of the number and action of the *dmrt* locus on the sex determination of non-bilaterians. The most recognized study on mechanism on sex determination among non-bilaterians is on *Hydra*, showing that its sex was determined by the presence of specific germline stem cells (Nishimiya-Fujisawa & Kobayashi, 2012). In that study, male polyps were found to originate from sperm-restricted stem cells, while female polyps originate from egg-restricted stem cells. Despite this discovery, the role of sex-determining genes and sex chromosomes in the formation of these sex-specific germ line cells has not been investigated yet in non-bilaterians. Our discovery of the Y chromosome-linked *dmrt* gene in *G. djiboutienesis* requires further investigation of its

potential role as the master sex-determining gene in non-bilaterians. Likewise, future studies must also consider the possible influence of ESD on the role of these sex chromosomes and its associated *dmrt* genes.

The locus of the sperm-specific *dmrt* on the shorter chromosome of heteromorphic pair in the half of the population of cells analysed indicates male heterogamety and suggests XX/XY sex determination system for *G. djiboutiensis*. This is the first report on the cytogenetic identification of sex determination system using the locus of sex-specific gene in non-bilaterians. This method circumvents the problems associated with identifying the sex chromosomes based on traditional chromosome staining such as G-banding. Our findings therefore support the XX/XY sex determination system for gonochoric cnidarian, initially proposed based on genomic markers from the population of *Corallium rubrum* (Order Anthozoa) (Pratlong et al., 2017). However, in *C. rubrum*, none of its *dmrt* analogs was found to be sex-specific or sex chromosome-specific. This is in contrast with our findings showing the linkage of one *dmrt* gene in the Y chromosome of *G. djiboutiensis*. Considering no *dmrt* is sex-linked in gonochoric *C. rubrum*, we speculate that the key genes involved in sex determination vary across different taxa of non-bilaterians.

The possible XX/XY sex determination system of cnidarian, as represented by precious coral *C. rubrum* and stony coral *G. djiboutiensis*, is similar with that of the mammals. However, cytogenetic study of other non-bilaterians such as in *Hydra* (Hydrozoan) showed no heteromorphic pairs, and its sex chromosomes might be homomorphic (Anokhin et al., 2010; Anokhin & Kuznetsova, 2018). Between the non-bilaterians and mammals are other various modes of sex determination system. These are male heterogamety (XX/XY) also in many insects; female heterogamety (ZZ/ZW) in birds, reptiles and Lepidoptera insects; homomorphic sex chromosomes in some reptiles; and haplodiploidy in some arthropods [1]. These convoluted patterns of sex determination system support the consensus understanding

that sex chromosomes evolve independently across different lineages of animals. The evolutionary convergence of male heterogamety between highly distant animals is not surprising, as the XX/XY sex determination system is also manifested by many dioecious plants. It is widely proposed that the evolutionary process that results in this diversification of the sex determination systems involves the degeneration of the chromosome that acquired a sex-determining function. This degeneration is caused by the suppression of the non-recombining parts of the sex chromosome, which ensures that the advantageous alleles for a particular sex are linked and always coinherited (Bergero & Charlesworth, 2009; Charlesworth, 1978). These chromosome events appeared to be continuous and reoccur frequently across different taxa, creating sex chromosome divergence and heteromorphy (Bachtrog et al., 2014). However, the time and the evolutionary pressure that drives sex chromosome evolution in animals is poorly understood. Estimates based on genomic data of the avian and gecko sex chromosomes revealed that the Z and W sex chromosomes started to differentiate at least 140 million-120 million years ago, before the split of most basal extant lineages (Nam & Ellegren, 2008). In the case of male heterogamety, the time when the X and Y started to differentiate in any animal taxa has not been investigated, probably due to rare synapomorphy between large animal lineages. Within non-bilaterians, differentiated sex chromosomes was observed for anthozoans (Pratlong et al., 2017; Taguchi et al., 2014; Vacarizas et al., 2021) and homomorphic sex chromosomes for hydrozoans (Anokhin et al., 2010; Anokhin & Kuznetsova, 2018). Because the phylogeny of the two taxa has not been established yet, it is difficult to confirm whether heteromorphic chromosomes evolved from homomorphic chromosomes in non-bilaterians. The other closely related invertebrate to non-bilaterians with known sex determination system is the *Caenorhabditis elegans* (X0), in which sex determination is not according to sex-limiting chromosomes but based on the counting mechanism of the X chromosome doses relative to the autosomes (Villeneuve &

Meyer, 1990). However, whether the sex determination in non-bilaterians depends on dosage composition of X rather than the role of the sex-determining gene in Y needs further investigation. Evaluating the sex determination systems from a wide range of animal taxa, either through cytogenetics or genomic analysis, would provide a better understanding in the patterns of lineage-specific evolution of sex chromosomes and GSD system in animals.

4.5. Methods

4.5.1. Sample collection and chromosome preparation

Eggs and sperms of the stony coral *G. djiboutiensis* were collected from separate colonies during its spawning in Otsuki, Kochi, Japan (32.777 °N, 132.731 °E). Both colonies spawned on the evening of August 29, 2021. Approximately 10 to 30 min after the male released its sperm, the female began releasing eggs. Comparisons of skeletal morphology of the two sexes from which the gametes were collected showed larger colony and wider corallite diameters in female than in male (Figs 4.5A and B). Aside from the spawned gametes, the sexes of the animal were confirmed by the presence of mature eggs and sperms in the gonads through microscopic observation (Figs 4.5C and D). A portion of the collected gametes were preserved in EtOH for DNA extraction, while the remaining gametes were combined and transferred in 0.2 μm filtered seawater to allow fertilization. The 12-hr-old embryos were then treated with 0.01 % colchicine, followed by treatment with hypotonic solution (seawater: dH_20 = 1:1). Embryo samples were preserved in Carnoy's fixative (absolute methanol: glacial acetic acid = 3:1) until further processing. Embryos were collected by centrifugation, and lipids were removed by 100 % diethyl ether for 4–6 h. Cells were centrifuged at 2000 × g for 2 min and then resuspended in 0.5 mL of Carnoy's fixative. Embryos were dissociated manually by rigorous pipetting. A cell suspension was dropped onto the slide and dried

quickly by flame. For G-banding, dried chromosome slides were treated with 0.025 % trypsin solution for 1 min, and then stained with 5 % Giemsa solution diluted with 0.06 M phosphate buffer (pH 6.8) for 2 min before washing with dH_20.

Thirty-three metaphase spreads were observed which represent both the highly condensed and less-condensed chromosomes. Arm lengths of each chromosome were measured using the Drawid software (Kirov et al., 2017). Karyotyping was based primarily on chromosome length, as clearly revealed in DAPI staining. We used embryonic cells for chromosome analysis because they contain a substantial number of actively dividing cells, suitable to obtain high-quality metaphase spreads. In addition, adult tissues of corals are known to harbor endosymbiotic microalgae in which cells can contaminate with the target coral cells during the chromosome preparation. Collection of the samples was granted by permit no. 745 issued by Kochi prefectural government office.

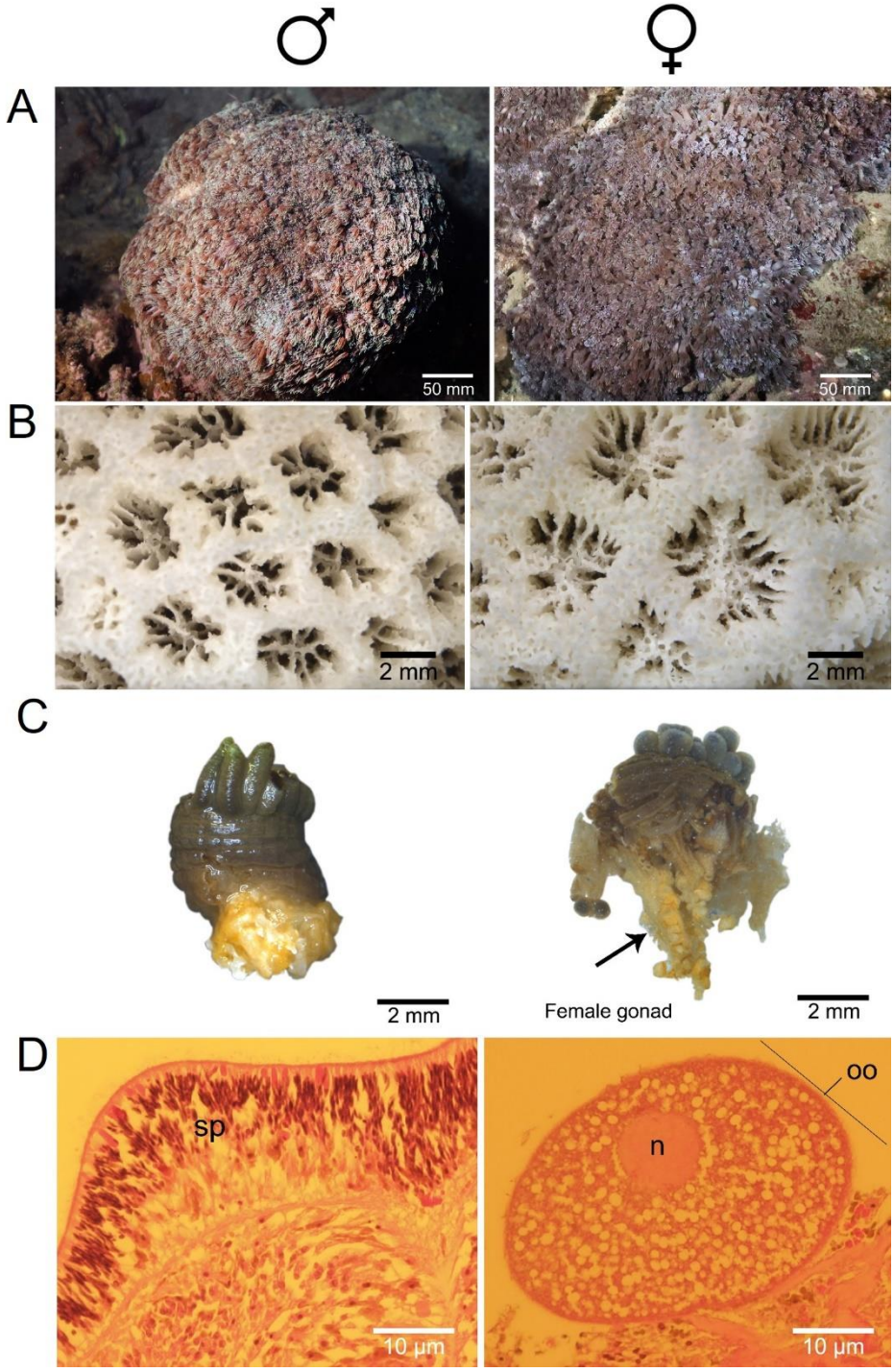

Figure 4.5. Morphological characteristics of male (left) and female (right) *G. djiboutiensis*. (A) colony (B) corallites (C) polyps and (D) portion of their gonads. sp: spermaries, n: nucleus, oo: oocyte.

4.5.2. *Dmrt* amplicon preparation and RNA-seq

Genomic DNA from *G. djiboutiensis* sperm and eggs were extracted using Wizard Genomic DNA Purification Kit (Promega, USA) according to manufacturer's protocol. Since no reference genome for *G. djiboutiensis* is available during the time of the experiment, we amplified the *dmrt* genes using its DM and DMA domain sequences, the known most conserved regions in protein structure of the cnidarian *dmrt* gene (Bellefroid et al., 2013). The conserved amino acid sequences for DM and DMA domains were obtained from http://pfam.xfam.org/, represented by a wide range of animal taxa. Sequences were then blasted (tblastn) against the NCBI database of transcriptome sequence assemblies from several cnidarian species. The mRNA transcripts were aligned and transformed to protein sequences, from which degenerate primers were designed. Forward degenerate primers were placed in DM domain, while reverse degenerate primers were placed in DMA domain. PCR were performed using Emerald PCR master mix (Takara, Japan) and sperm genomic DNA as a template. The PCR conditions were as follows: 30 cycles of 98 °C for 20 s, 60 °C for 30 s, and 72 °C for 4 min. Target amplicon sizes based on the genome analysis of *Porites rus*, the closest related species to *G. djiboutiensis* with genome data, were excised from the gel and sequenced using the degenerate primers. From the sequence data, specific primers were then designed and used to re-amplify the gel-extracted DNA. Primer walking was conducted for amplicon sizes greater than 1 kbp. PCR products containing target amplicons were purified using AMPure XP beads (Pacific Biosciences, USA) before sequencing and probe preparation. We used the nearby internal primers for nested PCR to further assess the gene presence in the egg genome. S1 Table shows all the degenerate and specific primers used for each *dmrt* gene. Eight adult samples (4 males and 4 females) were collected for RNA extraction. The two males and two females were collected 3 months before spawning, during the gametogenesis stage as confirmed from the histological analysis. The other 2 males and 2

females were collected a day before spawning. Total RNA was extracted from following the method described by the manufacturer's protocol for the Trizol reagent (Ambion, USA). Tissues from 0.5 g of coral fragments were solubilized with 2 ml of Trizol reagent and RNA was subsequently extracted using 250 µl isopropanol. A 10 µg extracted RNA was treated with 5 units of Recombinant DNase I (Takara, Japan). The crude total RNA was then purified using the standard ethanol precipitation. About 1 µg of total RNA were then sent for sequencing library preparation using the MGIEasy Library Prep Set (MGI, China) and the 150 bp paired-end reads were generated using the DNBSEQ-G400RS platform (MGI, China). Since no reference genome for *G. djiboutiensis* is available during the time of this study and de-novo transcriptome assembly was not possible due to low sequence coverage, the three *G. djiboutiensis dmrt* gene sequences were blasted against the *G. lobata* transcriptome assembly (Zhang et al. 2019) to obtain the corresponding transcript sequences. Trimmed and quality filtered RNA-Seq reads were aligned to those reference transcripts using hisat2 (Kim et al., 2015) from which transcripts corresponding to the isolated *G. djiboutiensis dmrt* genes were assembled. Using the generated SAM files, consensus sequences of aligned reads were extracted using the Integrative Genomics Viewer (IGV) software (Robinson et al., 2011). Putative transcripts were then blasted using blastx against the UniProtKB/Swiss-Prot(swissprot) database. Protein alignment was based on the result of online BLASTP algorithm (https://blast.ncbi.nlm.nih.gov/) which gives an implicit alignment between the query and search database. The tree was then constructed using Grishin (protein) substitution model and FAST Minimum Evolution using the same online platform.

4.5.3. Probe preparation and FISH

FISH probes were prepared from purified amplicons using the Random Primed DNA Labeling Kit (Roche, USA) according to the manufacturer's protocol. The DNA was fluorescently labeled directly using cyanine-3-dUTP (Cy3-dUTP) (Enzo, USA) or indirectly using digoxigenin-dUTP (DIG-dUTP)/anti-Digoxigenin-FITC (Roche, USA) at 37 °C for 15–18 h. Chromosome slides of *G. djiboutiensis* were denatured in 70 % formamide in 2x Standard Saline Citrate (SSC) solution at 70 °C for 2 min, and then serially submerged in ice-cold 70 %, 90 %, and 99 % EtOH for 2 min each. About 1 µL each of the DNA probes of different labels were mixed with 20 µL hybridization solution and then probe mixtures were denatured at 80 °C for 10 min. The probes were then gently placed onto the chromosomes denatured at 70 °C, 2 min in 2x SSC, and slides were incubated at 37 °C overnight with constant moisture to allow hybridization. Post hybridization washing was performed with 50 % formamide in 2x SSC solution at 43 °C for 20 min and slides were subsequently submerged twice in 2x SSC at 37 °C for a total of 8 min. The slides were then incubated twice in 1X phosphate-buffered detergent (PBD) at 25 °C for 5 min. Hybridized chromosome slides were then counterstained with DAPI-Vectashield (Vector Laboratories, USA) and viewed under an AxioImager A2 fluorescence microscope (Zeiss, Germany) equipped with an Axiocam MRm CCD camera (Zeiss, Germany). Primers for the preparation of the control histone H3 probe were based on related coral species *Favites pentagona* [28]. Images of suitable metaphase spreads from different embryos were captured using the AxioVision software (Zeiss, Germany). Chromosome lengths were measured, and karyotypes were constructed using the DRAWID software [24].

Chapter 5 General Conclusion

We explored the applicability of FISH technique in investigating the chromosomes of scleractinian corals. We first developed FISH probe from sequence of tandemly repetitive genes such as core histone and spliceosomal snRNA (chapter 2). Both probes provide bright hybridization signals resulting in the identification of two chromosome pairs in *Acropora pruinosa*. We then used the sequence of these probes to investigate the polyploidy in several *Acropora* species (chapter 3). FISH results based on the number of loci revealed the existence of triploidy and tetraploidy in cells of some *Acropora* species. Finally, we developed FISH probe that can identify the Y-chromosome from chromosomes of gonochoric stony coral (chapter 4). Results showed hybridization signal on one chromosome on almost 50% of the population of cells, indicating XX/XY sex determination system.

In this study, we provided evidence for the first time the existence of polyploidy and Y-chromosome in scleractinian corals using FISH. Our result highlighted the relevance of molecular cytogenetics in investigating the chromosome structure and organization in the world of advanced research where molecular analysis through next generation sequencing has becoming the trend in the field of biology. Visualizing the condensed forms of DNA under the microscope can still bring more discoveries in which sequence data cannot. This is also particularly useful especially for organisms in which genome has not been sequenced (or sequenced but not chromosome-level assembly) such as scleractinian corals. Molecular cytogenetics also allows to investigate chromosomes from individual cells which allows studying characteristics of tissue-specific chromosome formations.

Future studies may include the development of additional probes that can identify the other chromosome pairs. Popular of which is chromosome painting which produces unique patterns of colors for each of the chromosomes. Subsequently, chromosome aberrations such as aneuploidies and chromosome defects (e.g. translocation, deletion, insertion) can be identified and how these aberrations affects the morphology and health of the scleractinian corals can be studied.

Literature cited

Albig, W., Warthorst, U., Drabent, B., Prats, E., Cornudella, L., & Doenecke, D. (2003). *Mytilus edulis* core histone genes are organized in two clusters devoid of linker histone genes. *Journal of Molecular Evolution*, *56*(5), 597–606. https://doi.org/10.1007/s00239-002-2428-8

Anokhin, B. A., Hemmrich-Stanisak, G., & Bosch, T. C. G. (2010). Karyotyping and single-gene detection using fluorescence in situ hybridization on chromosomes of *Hydra magnipapillata* (Cnidaria: Hydrozoa). *Comparative Cytogenetics*, *4*(2), 97–110. https://doi.org/10.3897/compcytogen.v4i2.41

Anokhin, B. A., & Kuznetsova, V. G. (2018). FISH-based karyotyping of *Pelmatohydra oligactis* (Pallas, 1766), *Hydra oxycnida* Schulze, 1914, and *H. magnipapillata* Itô, 1947 (Cnidaria, Hydrozoa). *Comparative Cytogenetics*, *12*(4), 539–548. https://doi.org/10.3897/COMPCYTOGEN.V12I4.32120

Araya-Jaime, C., Lam, N., Pinto, I. V., Méndez, M. A., & Iturra, P. (2017). Chromosomal organization of four classes of repetitive DNA sequences in killifish *Orestias ascotanensis* Parenti, 1984 (Cyprinodontiformes, Cyprinodontidae). *Comparative Cytogenetics*, *11*(3), 463–475. https://doi.org/10.3897/compcytogen.v11i3.11729

Bachtrog, D., Mank, J. E., Peichel, C. L., Kirkpatrick, M., Otto, S. P., Ashman, T. L., Hahn, M. W., Kitano, J., Mayrose, I., Ming, R., Perrin, N., Ross, L., Valenzuela, N., & Vamosi, J. C. (2014). Sex Determination: Why So Many Ways of Doing It? *PLoS Biology*, *12*(7), 1–13. https://doi.org/10.1371/journal.pbio.1001899

Barton, J. A., Willis, B. L., & Hutson, K. S. (2017). Coral propagation: a review of techniques for ornamental trade and reef restoration. *Reviews in Aquaculture*, *9*(3), 238–256. https://doi.org/10.1111/raq.12135

Barzotti, R., Pelliccia, F., Bucciarelli, E., & Rocchi, A. (2000). Organization, nucleotide sequence, and chromosomal mapping of a tandemly repeated unit containing the four core histone genes and a 5S rRNA gene in an isopod crustacean species. *Genome*, *43*(2), 341–345. https://doi.org/10.1139/g99-142

Bellefroid, E. J., Leclère, L., Saulnier, A., Keruzore, M., Sirakov, M., Vervoort, M., & de Clercq, S. (2013). Expanding roles for the evolutionarily conserved Dmrt sex transcriptional regulators during embryogenesis. In *Cellular and Molecular Life Sciences* (Vol. 70, Issue 20, pp. 3829–3845). Springer. https://doi.org/10.1007/s00018-013-1288-2

Bellwood, D. R., Hughes, T. P., Folke, C., & Nyström, M. (2004). Confronting the coral reef crisis. In *Nature* (Vol. 429, Issue 6994, pp. 827–833). Nature Publishing Group. https://doi.org/10.1038/nature02691

Bergero, R., & Charlesworth, D. (2009). The evolution of restricted recombination in sex chromosomes. *Trends in Ecology & Evolution*, *24*(2), 94–102. https://doi.org/10.1016/J.TREE.2008.09.010

Born, G. G., & Bertollo, L. A. C. (2000). An XX/XY sex chromosome system in a fish species, *Hoplias malabaricus*, with a polymorphic NOR-bearing X chromosome. *Chromosome Research*, *8*(2), 111–118. https://doi.org/10.1023/A:1009238402051

Bridges, C. B. (1914). Direct proof through non-disjunction that the sex-linked genes of *drosophila* are borne by the x-chromosome. *Science*, *40*(1020), 107–109. https://doi.org/10.1126/science.40.1020.107

Brown, P. A., & Blackman, R. L. (1988). Karyotype variation in the corn leaf aphid, *Rhopalosiphum maidis* (Fitch), species complex (Hemiptera: Aphididae) in relation to host-plant and morphology. *Bulletin of Entomological Research*, *78*(2), 351–363. https://doi.org/10.1017/S0007485300013110

Browning, J. W. L., Rambo, T. M. E., & McKay, B. C. (2020). Comparative genomic analysis of the 3′ UTR of human MDM2 identifies multiple transposable elements, an RLP24 pseudogene and a cluster of novel repeat sequences that arose during primate evolution. *Gene*, *741*. https://doi.org/10.1016/j.gene.2020.144557

Burset, M., Seledtsov, I. A., & Solovyev, V. v. (2001). SpliceDB: database of canonical and non-canonical mammalian splice sites. *Nucleic Acids Research*, *29*(1), 255–259. https://doi.org/10.1093/NAR/29.1.255

Cabral-de-Mello, D. C., Oliveira, S. G., de Moura, R. C., & Martins, C. (2011). Chromosomal organization of the 18S and 5S rRNAs and histone H3 genes in Scarabaeinae coleopterans: Insights into the evolutionary dynamics of multigene families and heterochromatin. *BMC Genetics*, *12*(1), 1–12. https://doi.org/10.1186/1471-2156-12-88/FIGURES/5

Caburet, S., Conti, C., Schurra, C., Lebofsky, R., Edelstein, S. J., & Bensimon, A. (2005). Human ribosomal RNA gene arrays display a broad range of palindromic structures. *Genome Research*, *15*(8), 1079–1085. https://doi.org/10.1101/gr.3970105

Cairns, S. D. (1999). Species richness of recent Scleractinia. *Atoll Research Bulletin*, *459*(459–465), 1–46. https://doi.org/10.5479/si.00775630.459.1

Carter, C. G., McCarthy, I. D., Houlihan, D. F., Johnstone, R., Walsingham, M. v., & Mitchell, A. I. (2011). Food consumption, feeding behaviour, and growth of triploid and diploid Atlantic salmon, *Salmo salar* L., parr. *Https://Doi.Org/10.1139/Z94-083*, *72*(4), 609–617. https://doi.org/10.1139/Z94-083

Cazaux, B., Catalan, J., Veyrunes, F., Douzery, E. J. P., & Britton-Davidian, J. (2011). Are ribosomal DNA clusters rearrangement hotspots? A case study in the genus *Mus* (Rodentia, Muridae). *BMC Evolutionary Biology*, *11*(1). https://doi.org/10.1186/1471-2148-11-124

Chandler, J. C., Fitzgibbon, Q. P., Smith, G., Elizur, A., & Ventura, T. (2017). Y-linked iDmrt1 paralogue (iDMY) in the Eastern spiny lobster, *Sagmariasus verreauxi*: The first invertebrate sex-linked Dmrt. *Developmental Biology*, *430*(2), 337–345. https://doi.org/10.1016/j.ydbio.2017.08.031

Charlesworth, B. (1978). Model for evolution of Y chromosomes and dosage compensation. *Proceedings of the National Academy of Sciences of the United States of America*, *75*(11), 5618–5622. https://doi.org/10.1073/PNAS.75.11.5618

Christoffels, A., Koh, E. G. L., Chia, J. M., Brenner, S., Aparicio, S., & Venkatesh, B. (2004). Fugu Genome Analysis Provides Evidence for a Whole-Genome Duplication Early During the Evolution of Ray-Finned Fishes. *Molecular Biology and Evolution*, *21*(6), 1146–1151. https://doi.org/10.1093/MOLBEV/MSH114

Conant, G. C. (2014). Comparative Genomics as a Time Machine: How Relative Gene Dosage and Metabolic Requirements Shaped the Time-dependent Resolution of Yeast Polyploidy. *Molecular Biology and Evolution*, *31*(12), 3184–3193. https://doi.org/10.1093/MOLBEV/MSU250

Costanza, R., D'Arge, R., de Groot, R., Farber, S., Grasso, M., Hannon, B., Limburg, K., Naeem, S., O'Neill, R. v., Paruelo, J., Raskin, R. G., Sutton, P., & van den Belt, M. (1997). The value of the world's ecosystem services and natural capital. *Nature*, *387*(6630), 253–260. https://doi.org/10.1038/387253a0

Cross, I., & Rebordinos, L. (2005). 5S rDNA and U2 snRNA are linked in the genome of *Crassostrea angulata* and *Crassostrea gigas* oysters: Does the (CT)n·(GA)n microsatellite stabilize this novel linkage of large tandem arrays? *Genome*, *48*(6), 1116–1119. https://doi.org/10.1139/g05-075

Cui, Z., Hui, M., Liu, Y., Song, C., Li, X., Li, Y., Liu, L., Shi, G., Wang, S., Li, F., Zhang, X., Liu, C., Xiang, J., & Chu, K. H. (2015). High-density linkage mapping aided by transcriptomics documents ZW sex determination system in the Chinese mitten crab *Eriocheir sinensis*. *Heredity 2015 115:3*, *115*(3), 206–215. https://doi.org/10.1038/hdy.2015.26

Darolti, I., Wright, A. E., Sandkam, B. A., Morris, J., Bloch, N. I., Farré, M., Fuller, R. C., Bourne, G. R., Larkin, D. M., Breden, F., & Mank, J. E. (2019). Extreme heterogeneity in sex chromosome differentiation and dosage compensation in livebearers. *Proceedings of the National Academy of Sciences of the United States of America*, *116*(38), 19031–19036. https://doi.org/10.1073/pnas.1905298116

de Souza-Firmino, T. S., Alevi, K. C. C., & Itoyama, M. M. (2020). Chromosomal divergence and evolutionary inferences in *Pentatomomorpha infraorder* (Hemiptera, Heteroptera) based on the chromosomal location of ribosomal genes. *PLOS ONE*, *15*(2), e0228631. https://doi.org/10.1371/JOURNAL.PONE.0228631

Drabent, B., Kim, J. S., Albig, W., Prats, E., Cornudella, L., & Doenecke, D. (1999). *Mytilus edulis* histone gene clusters containing only H1 genes. *Journal of Molecular Evolution*, *49*(5), 645–655. https://doi.org/10.1007/PL00006585

Eirín-López, J. M., González-Tizón, A. M., Martinez, A., & Méndez, J. (2002). Molecular and evolutionary analysis of mussel histone genes (Mytilus spp.): Possible evidence of an "orphon origin" for H1 histone genes. *Journal of Molecular Evolution*, *55*(3), 272–283. https://doi.org/10.1007/s00239-002-2325-1

Eirín-López, J. M., Ruiz, M. F., González-Tizón, A. M., Martínez, A., Sánchez, L., & Méndez, J. (2004). Molecular Evolutionary Characterization of the Mussel *Mytilus* Histone Multigene Family: First Record of a Tandemly Repeated Unit of Five Histone Genes Containing an H1 Subtype with "Orphon" Features. *Journal of Molecular Evolution*, *58*(2), 131–144. https://doi.org/10.1007/s00239-003-2531-5

Ellegren, H. (2011). Sex-chromosome evolution: Recent progress and the influence of male and female heterogamety. In *Nature Reviews Genetics* (Vol. 12, Issue 3, pp. 157–166). Nature Publishing Group. https://doi.org/10.1038/nrg2948

Fellegara, I., Baird, A. H., & Ward, S. (2013). Coral reproduction in a high-latitude, marginal reef environment (Moreton Bay, south-east Queensland, Australia). *Invertebrate Reproduction and Development*, *57*(3), 219–223. https://doi.org/10.1080/07924259.2012.752766

Flot, J.-F., Ozouf-Costaz, C., Tsuchiya, M., & van Woesik, R. (2006). Comparative coral cytogenetics. *Proceedings of 10th International Coral Reef Symposium*, *1*(April), 4–8. http://www.mnhn.fr/jfflot/publications/Flot2006ICRS1.pdf

Ford, C. E., Jones, K. W., Polani, P. E., de Almeida, J. C., & Briggs, J. H. (1959). A sex-chromosome anomaly in a case of gonadal dysgenesis (Turner's syndrome). *The Lancet*, *273*(7075), 711–713. https://doi.org/10.1016/S0140-6736(59)91893-8

Fridolfsson, A. K., Cheng, H., Copeland, N. G., Jenkins, N. A., Liu, H. C., Raudsepp, T., Woodage, T., Chowdhary, B., Halverson, J., & Ellegren, H. (1998). Evolution of the avian sex chromosomes from an ancestral pair of autosomes. *Proceedings of the National Academy of Sciences of the United States of America*, *95*(14), 8147–8152. https://doi.org/10.1073/pnas.95.14.8147

Gallagher, D. S., Davis, S. K., de Donato, M., Burzlaff, J. D., Womack, J. E., Taylor, J. F., & Kumamoto, A. T. (1998). A karyotypic analysis of nilgai, *Boselaphus tragocamelus* (Artiodactyla: Bovidae). *Chromosome Research*, *6*(7), 505–514. https://doi.org/10.1023/A:1009268917856

Grozeva, S., Kuznetsova, V. G., & Anokhin, B. A. (2011). Karyotypes, male meiosis and comparative FISH mapping of 18S ribosomal DNA and telomeric (TTAGG) n repeat in eight species of true bugs (Hemiptera, Heteroptera). *Comparative Cytogenetics*, *5*(4), 355. https://doi.org/10.3897/COMPCYTOGEN.V5I4.2307

Guest, J. R., Baird, A. H., Goh, B. P. L., & Chou, L. M. (2012). Sexual systems in scleractinian corals: An unusual pattern in the reef-building species *Diploastrea heliopora*. *Coral Reefs*, *31*(3), 705–713. https://doi.org/10.1007/s00338-012-0881-4

Hermansen, R. A., Hvidsten, T. R., Sandve, S. R., & Liberles, D. A. (2016). Extracting functional trends from whole genome duplication events using comparative genomics. *Biological Procedures Online*, *18*(1), 1–10. https://doi.org/10.1186/S12575-016-0041-2/FIGURES/3

Hilbold, E., Bergmann, M., Fietz, D., Kliesch, S., Weidner, W., Langeheine, M., Rode, K., & Brehm, R. (2019). Immunolocalization of DMRTB1 in human testis with normal and

impaired spermatogenesis. *Andrology*, *7*(4), 428–440. https://doi.org/10.1111/ANDR.12617

Hsu, T. C., Spirito, S. E., & Pardue, M. lou. (1975). Distribution of 18+28S ribosomal genes in mammalian genomes. *Chromosoma*, *53*(1), 25–36. https://doi.org/10.1007/BF00329388

Hughes, T. P., Baird, A. H., Bellwood, D. R., Card, M., Connolly, S. R., Folke, C., Grosberg, R., Hoegh-Guldberg, O., Jackson, J. B. C., Kleypas, J., Lough, J. M., Marshall, P., Nyström, M., Palumbi, S. R., Pandolfi, J. M., Rosen, B., & Roughgarden, J. (2003). Climate change, human impacts, and the resilience of coral reefs. In *Science* (Vol. 301, Issue 5635, pp. 929–933). American Association for the Advancement of Science. https://doi.org/10.1126/science.1085046

Insua, A., Freire, R., Ríos, J., & Méndez, J. (2001). The 5S rDNA of mussels *Mytilus galloprovincialis* and *M. edulis*: Sequence variation and chromosomal location. *Chromosome Research*, *9*(6), 495–505. https://doi.org/10.1023/A:1011636714052

Jacq, C., Miller, J. R., & Brownlee, G. G. (1977). A pseudogene structure in 5S DNA of *Xenopus laevis*. *Cell*, *12*(1), 109–120. https://doi.org/10.1016/0092-8674(77)90189-1

Kaiser, V. B., & Bachtrog, D. (2010). Evolution of Sex Chromosomes in Insects. *Annual Review of Genetics*, *44*, 91. https://doi.org/10.1146/ANNUREV-GENET-102209-163600

Kawakami, R., Taguchi, T., Vacarizas, J., Ito, M., Mezaki, T., Tominaga, A., & Kubota, S. (2022). Karyotypic analysis and isolation of four DNA markers of the scleractinian coral *Favites pentagona* (Esper, 1795) (Scleractinia, Anthozoa, Cnidaria). *Comparative Cytogenetics*, *16*(1), 77–92. https://doi.org/10.3897/COMPCYTOGEN.V16.I1.79953

Kenyon, J. C. (1997). Models of reticulate evolution in the coral Genus *Acropora* based on chromosome numbers: parallels with plants. *Evolution*, *51*(3), 756. https://doi.org/10.2307/2411152

Kim, D., Langmead, B., & Salzberg, S. L. (2015). HISAT: a fast spliced aligner with low memory requirements. *Nature Methods 2015 12:4*, *12*(4), 357–360. https://doi.org/10.1038/nmeth.3317

Kirov, I., Khrustaleva, L., van Laere, K., Soloviev, A., Meeus, S., Romanov, D., & Fesenko, I. (2017). DRAWID: User-friendly java software for chromosome measurements and idiogram drawing. *Comparative Cytogenetics*, *11*(4), 747–757. https://doi.org/10.3897/CompCytogen.v11i4.20830

Kitanobo, S., Isomura, N., Fukami, H., Iwao, K., & Morita, M. (2016). The reef-building coral *Acropora* conditionally hybridize under sperm limitation. *Biology Letters*, *12*(8). https://doi.org/10.1098/RSBL.2016.0511

Koller, P. C., & Darlington, C. D. (1934). The genetical and mechanical properties of the sex-chromosomes - I. *Rattus norvegicus*, ♂. *Journal of Genetics*, *29*(2), 159–173. https://doi.org/10.1007/BF02982193

Kumar, S., Stecher, G., Li, M., Knyaz, C., & Tamura, K. (2018). MEGA X: Molecular evolutionary genetics analysis across computing platforms. *Molecular Biology and Evolution*, *35*(6), 1547–1549. https://doi.org/10.1093/molbev/msy096

Lamb, J. C., Danilova, T., Bauer, M. J., Meyer, U. M., Holland, J. J., Jensen, M. D., & Birchler, J. A. (2007). Single-gene detection and karyotyping using small-target fluorescence in situ hybridization on maize somatic chromosomes. *Genetics*, *175*(3), 1047–1058. https://doi.org/10.1534/genetics.106.065573

Li, C., Song, L., Zhao, J., Zou, H., Su, J., & Zhang, H. (2006). Genomic organization, nucleotide sequence analysis of the core histone genes cluster in *Chlamys farreri* and molecular evolution assessment of the H2A and H2B. *DNA Sequence - Journal of DNA Sequencing and Mapping*, *17*(6), 440–451. https://doi.org/10.1080/10425170600752593

Liu, S., Luo, J., Chai, J., Ren, L., Zhou, Y., Huang, F., Liu, X., Chen, Y., Zhang, C., Tao, M., Lu, B., Zhou, W., Lin, G., Mai, C., Yuan, S., Wang, J., Li, T., Qin, Q., Feng, H., … Zhang, Y. P. (2016). Genomic incompatibilities in the diploid and tetraploid offspring of the goldfish × common carp cross. *Proceedings of the National Academy of Sciences of the United States of America*, *113*(5), 1327–1332. https://doi.org/10.1073/PNAS.1512955113/SUPPL_FILE/PNAS.1512955113.SD03.XLSX

Lucas, J. N., & Gray, J. W. (1987). Centromeric index versus DNA content flow karyotypes of human chromosomes measured by means of slit-scan flow cytometry. *Cytometry*, *8*(3), 273–279. https://doi.org/10.1002/cyto.990080307

Mable, B. K., Alexandrou, M. A., & Taylor, M. I. (2011). Genome duplication in amphibians and fish: An extended synthesis. *Journal of Zoology*, *284*(3), 151–182. https://doi.org/10.1111/J.1469-7998.2011.00829.X

Manchado, M., Zuasti, E., Cross, I., Merlo, A., Infante, C., & Rebordinos, L. (2006). Molecular characterization and chromosomal mapping of the 5S rRNA gene in *Solea senegalensis*: A new linkage to the U1, U2, and U5 small nuclear RNA genes. *Genome*, *49*(1), 79–86. https://doi.org/10.1139/g05-068

Maniatis, T., & Reed, R. (1987). The role of small nuclear ribonucleoprotein particles in pre-mRNA splicing. *Nature*, *325*(6106), 673–678. https://doi.org/10.1038/325673A0

Marquez, L. M. (2003). Pseudogenes Contribute to the Extreme Diversity of Nuclear Ribosomal DNA in the Hard Coral *Acropora*. *Molecular Biology and Evolution*, *20*(7), 1077–1086. https://doi.org/10.1093/molbev/msg122

Mason, D. A., Rabinowitz, J. S., & Portman, D. S. (2008). dmd-3, a doublesex-related gene regulated by tra-1, governs sex-specific morphogenesis in *C. elegans*. *Development (Cambridge, England)*, *135*(14), 2373–2382. https://doi.org/10.1242/DEV.017046

Matson, C. K., Murphy, M. W., Griswold, M. D., Yoshida, S., Bardwell, V. J., & Zarkower, D. (2010). The mammalian doublesex homolog DMRT1 is a transcriptional gatekeeper that controls the mitosis versus meiosis decision in male germ cells. *Developmental Cell*, *19*(4), 612–624. https://doi.org/10.1016/J.DEVCEL.2010.09.010

Matson, C. K., Murphy, M. W., Sarver, A. L., Griswold, M. D., Bardwell, V. J., & Zarkower, D. (2011). DMRT1 prevents female reprogramming in the postnatal mammalian testis. *Nature*, *476*(7358), 101–105. https://doi.org/10.1038/NATURE10239

Matsuda, M., Nagahama, Y., Shinomiya, A., Sato, T., Matsuda, C., Kobayashi, T., Morrey, C. E., Shibata, N., Asakawa, S., Shimizu, N., Hori, H., Hamaguchi, S., & Sakaizumi, M. (2002). DMY is a Y-specific DM-domain gene required for male development in the medaka fish. *Nature*, *417*(6888), 559–563. https://doi.org/10.1038/nature751

McKee, B. D., & Karpen, G. H. (1990). Drosophila ribosomal RNA genes function as an X-Y pairing site during male meiosis. *Cell*, *61*(1), 61–72. https://doi.org/10.1016/0092-8674(90)90215-Z

Meyer, A., & van de Peer, Y. (2005). From 2R to 3R: Evidence for a fish-specific genome duplication (FSGD). In *BioEssays* (Vol. 27, Issue 9, pp. 937–945). John Wiley & Sons, Ltd. https://doi.org/10.1002/bies.20293

Miller, D. J., Harrison, P. L., Mahony, T. J., McMillan, J. P., Miles, A., Odorico, D. M., & ten Lohuis, M. R. (1993). Nucleotide sequence of the histone gene cluster in the coral *Acropora formosa* (cnidaria; scleractinia): Features of histone gene structure and organization are common to diploblastic and triploblastic metazoans. *Journal of Molecular Evolution*, *37*(3), 245–253. https://doi.org/10.1007/BF00175501

Miller, S. W., Hayward, D. C., Bunch, T. A., Miller, D. J., Ball, E. E., Bardwell, V. J., Zarkower, D., & Brower, D. L. (2003). A DM domain protein from a coral, *Acropora millepora*, homologous to proteins important for sex determination. *Evolution and Development*, *5*(3), 251–258. https://doi.org/10.1046/j.1525-142X.2003.03032.x

Mohanty, I. C., Mahapatra, D., Mohanty, S., & Das, A. B. (2004). Karyotype analyses and studies on the nuclear DNA content in 30 genotypes of potato (*Solanum tuberosum*) L. *Cell Biology International*, *28*(8–9), 625–633. https://doi.org/10.1016/J.CELLBI.2004.05.004

Morescalchi, M. A., Stingo, V., & Capriglione, T. (2011). Cytogenetic analysis in *Polypterus ornatipinnis* (Actinopterygii, Cladistia, Polypteridae) and 5S rDNA. *Marine Genomics*, *4*(1), 25–31. https://doi.org/10.1016/j.margen.2010.12.002

Morita, M., Kitanobo, S., Nozu, R., Iwao, K., Fukami, H., & Isomura, N. (2019). Reproductive strategies in the intercrossing corals *Acropora donei* and *A. tenuis* to prevent hybridization. *Coral Reefs*, *38*(6), 1211–1223. https://doi.org/10.1007/S00338-019-01839-Z/FIGURES/7

Nam, K., & Ellegren, H. (2008). The chicken (Gallus gallus) Z chromosome contains at least three nonlinear evolutionary strata. *Genetics*, *180*(2), 1131–1136. https://doi.org/10.1534/genetics.108.090324

Nishimiya-Fujisawa, C., & Kobayashi, S. (2012). Germline stem cells and sex determination in *Hydra*. *International Journal of Developmental Biology*, *56*(6–8), 499–508. https://doi.org/10.1387/ijdb.123509cf

Nishioka, Y., Leder, A., & Leder, P. (1980). Unusual α-globin-like gene that has cleanly lost both globin intervening sequences. *Proceedings of the National Academy of Sciences of*

the United States of America, *77*(5 I), 2806–2809. https://doi.org/10.1073/pnas.77.5.2806

Otto, S. P. (2007). The Evolutionary Consequences of Polyploidy. *Cell*, *131*(3), 452–462. https://doi.org/10.1016/J.CELL.2007.10.022

Palmer, D. H., Rogers, T. F., Dean, R., & Wright, A. E. (2019). How to identify sex chromosomes and their turnover. *Molecular Ecology*, *28*(21), 4709–4724. https://doi.org/10.1111/mec.15245

Pardue, M. lou, & Hsu, T. C. (1975). Locations of 18S and 28S ribosomal genes on the chromosomes of the indian muntjac. *Journal of Cell Biology*, *64*(1), 251–254. https://doi.org/10.1083/jcb.64.1.251

Pelliccia, F., Barzotti, R., Bucciarelli, E., & Rocchi, A. (2001). 5S ribosomal and U1 small nuclear RNA genes: A new linkage type in the genome of a crustacean that has three different tandemly repeated units containing 5S ribosomal DNA sequences. *Genome*, *44*(3), 331–335. https://doi.org/10.1139/gen-44-3-331

Pérez-García, C., Cambeiro, J. M., Morán, P., & Pasantes, J. J. (2010). Chromosomal mapping of rDNAs, core histone genes and telomeric sequences in *Perumytilus purpuratus* (Bivalvia: Mytilidae). *Journal of Experimental Marine Biology and Ecology*, *395*(1–2), 199–205. https://doi.org/10.1016/j.jembe.2010.09.004

Pérez-García, C., Guerra-Varela, J., Morán, P., & Pasantes, J. J. (2010). Chromosomal mapping of rRNA genes, core histone genes and telomeric sequences *in Brachidontes puniceus* and *Brachidontes rodriguezi* (Bivalvia, Mytilidae). *BMC Genetics*, *11*. https://doi.org/10.1186/1471-2156-11-109

Piscor, D., Centofante, L., & Parise-Maltempi, P. P. (2016). Highly similar morphologies between chromosomes bearing U2 snRNA gene clusters in the group Astyanax Baird and Girard, 1854 (Characiformes, Characidae): An evolutionary approach in species with 2n = 36, 46, 48, and 50. *Zebrafish*, *13*(6), 565–570. https://doi.org/10.1089/zeb.2016.1292

Piscor, D., Paiz, L. M., Baumgärtner, L., Cerqueira, F. J., Fernandes, C. A., Lui, R. L., Parise-Maltempi, P. P., & Margarido, V. P. (2020). Chromosomal mapping of repetitive sequences in *Hyphessobrycon eques* (Characiformes, Characidae): a special case of the spreading of 5S rDNA clusters in a genome. *Genetica*, *148*(1), 25–32. https://doi.org/10.1007/s10709-020-00086-3

Pratlong, M., Haguenauer, A., Chenesseau, S., Brener, K., Mitta, G., Toulza, E., Bonabaud, M., Rialle, S., Aurelle, D., & Pontarotti, P. (2017). Evidence for a genetic sex determination in Cnidaria, the Mediterranean red coral (*Corallium rubrum*). *Royal Society Open Science*, *4*(160880), 1–9. https://doi.org/10.1098/rsos.160880

Ramsey, J., & Schemske, D. W. (2003). Neopolyploidy in Flowering Plants. *Https://Doi.Org/10.1146/Annurev.Ecolsys.33.010802.150437*, *33*, 589–639. https://doi.org/10.1146/ANNUREV.ECOLSYS.33.010802.150437

Raymond, C. S., Murphy, M. W., O'Sullivan, M. G., Bardwell, V. J., & Zarkower, D. (2000). Dmrt1, a gene related to worm and fly sexual regulators, is required for mammalian

testis differentiation. *Genes & Development*, *14*(20), 2587–2595. https://doi.org/10.1101/GAD.834100

Reddy, P. C., Ubhe, S., Sirwani, N., Lohokare, R., & Galande, S. (2017a). Rapid divergence of histones in Hydrozoa (Cnidaria) and evolution of a novel histone involved in DNA damage response in hydra. *Zoology*, *123*, 53–63. https://doi.org/10.1016/j.zool.2017.06.005

Reddy, P. C., Ubhe, S., Sirwani, N., Lohokare, R., & Galande, S. (2017b). Rapid divergence of histones in Hydrozoa (Cnidaria) and evolution of a novel histone involved in DNA damage response in hydra. *Zoology*, *123*, 53–63. https://doi.org/10.1016/j.zool.2017.06.005

Reinhold, K., & Engqvist, L. (2013). The variability is in the sex chromosomes. *Evolution*, *67*(12), 3662–3668. https://doi.org/10.1111/EVO.12224

Robicheau, B. M., Susko, E., Harrigan, A. M., & Snyder, M. (2017). Ribosomal RNA Genes Contribute to the Formation of Pseudogenes and Junk DNA in the Human Genome. *Genome Biology and Evolution*, *9*(2), 380–397. https://doi.org/10.1093/gbe/evw307

Robinson, J. T., Thorvaldsdóttir, H., Winckler, W., Guttman, M., Lander, E. S., Getz, G., & Mesirov, J. P. (2011). Integrative Genomics Viewer. *Nature Biotechnology*, *29*(1), 24. https://doi.org/10.1038/NBT.1754

Shapiro, M. B., & Senapathy, P. (1987). RNA splice junctions of different classes of eukaryotes: sequence statistics and functional implications in gene expression. *Nucleic Acids Research*, *15*(17), 7155–7174. https://doi.org/10.1093/NAR/15.17.7155

Shi, X., Waiho, K., Li, X., Ikhwanuddin, M., Miao, G., Lin, F., Zhang, Y., Li, S., Zheng, H., Liu, W., Aweya, J. J., Azmie, G., Baylon, J. C., Quinitio, E. T., & Ma, H. (2018). Female-specific SNP markers provide insights into a WZ/ZZ sex determination system for mud crabs *Scylla paramamosain*, *S. tranquebarica* and *S. serrata* with a rapid method for genetic sex identification. *BMC Genomics*, *19*(1), 1–12. https://doi.org/10.1186/S12864-018-5380-8/TABLES/5

Shibuya, K., Noguchi, S., Nishimura, S., & Sekiya, T. (1982). Characterization of a rat tRNA gene cluster containing the genes for tRNAAsp, tRNAGly and tRNAGhi, and pseudogenes. *Nucleic Acids Research*, *10*(14), 4441–4448. https://doi.org/10.1093/nar/10.14.4441

Shinzato, C., Shoguchi, E., Kawashima, T., Hamada, M., Hisata, K., Tanaka, M., Fujie, M., Fujiwara, M., Koyanagi, R., Ikuta, T., Fujiyama, A., Miller, D. J., & Satoh, N. (2011). Using the *Acropora digitifera* genome to understand coral responses to environmental change. *Nature*, *476*(7360), 320–323. https://doi.org/10.1038/nature10249

Smith, C. A., Roeszler, K. N., Ohnesorg, T., Cummins, D. M., Farlie, P. G., Doran, T. J., & Sinclair, A. H. (2009). The avian Z-linked gene DMRT1 is required for male sex determination in the chicken. *Nature*, *461*(7261), 267–271. https://doi.org/10.1038/nature08298

Stover, N. A., & Steele, R. E. (2001). Trans-spliced leader addition to mRNAs in a cnidarian. *Proceedings of the National Academy of Sciences of the United States of America*, *98*(10), 5693–5698. https://doi.org/10.1073/pnas.101049998

Sumner, A. T. (1972). A simple technique for demonstrating centromeric heterochromatin. *Experimental Cell Research*, *75*(1), 304–306. https://doi.org/10.1016/0014-4827(72)90558-7

Suzuki, G. (2012). Simultaneous spawning of *Pocillopora* and *Goniopora* corals in the morning time. *Galaxea, Journal of Coral Reef Studies*, *14*(1), 115–116. https://doi.org/10.3755/galaxea.14.115

Taguchi, T., Kubota, S., Mezaki, T., Sekida, S., Okuda, K., Nakachi, S., Shinbo, T., Iiguni, Y., & Tominaga, A. (2013). Detection of characteristic heterochromatin distribution, highly amplified rRNA genes and presence of the human satellite III DNA motif in the scleractinian coral *Echinophyllia aspera* Ellis and Solander 1788. *Chromosome Science*, *16*(3+4), 33–38. https://doi.org/10.11352/scr.16.33

Taguchi, T., Kubota, S., Mezaki, T., Tagami, E., Sekida, S., Nakachi, S., Okuda, K., & Tominaga, A. (2016). Identification of homogeneously staining regions by G-banding and chromosome microdissection, and FISH marker selection using human Alu sequence primers in a scleractinian coral *Coelastrea aspera* Verrill, 1866 (Cnidaria). *Comparative Cytogenetics*, *10*(1), 61–75. https://doi.org/10.3897/CompCytogen.v10i1.5699

Taguchi, T., Kubota, S., Tagami, E., Mezaki, T., Sekida, S., Okuda, K., & Tominaga, A. (2017). Molecular cytogenetic analysis and isolation of a 5S rRNA-related marker in the scleractinian coral *Platygyra contorta* Veron 1990 (Hexacorallia, Anthozoa, Cnidaria). *Cytologia*, *82*(2), 205–212. https://doi.org/10.1508/cytologia.82.205

Taguchi, T., Mezaki, T., Iwase, F., Sekida, S., Kubota, S., Fukami, H., Okuda, K., Shinbo, T., Oshima, S., Iiguni, Y., Testa, J. R., & Tominaga, A. (2014). Molecular cytogenetic analysis of the scleractinian coral *Acropora solitaryensis* Veron & Wallace 1984. *Zoological Science*, *31*(2), 89–94. https://doi.org/10.2108/zsj.31.89

Taguchi, T., Tagami, E., Mezaki, T., Vacarizas, J. M., Canon, K. L., Avila, T. N., Bataan, D. A. U., Tominaga, A., & Kubota, S. (2020). Karyotypic mosaicism and molecular cytogenetic markers in the scleractinian coral *Acropora pruinosa* Brook, 1982 (Hexacorallia, Anthozoa, Cnidaria). *Coral Reefs*, *39*(5), 1415–1425. https://doi.org/10.1007/s00338-020-01975-x

Takaoka, E., Sonobe, H., Akimaru, K., Sakamoto, S., Shuin, T., Daibata, M., Taguchi, T., & Tominaga, A. (2012). Multiple sites of highly amplified DNA sequences detected by molecular cytogenetic analysis in HS-RMS-2, a new pleomorphic rhabdomyosarcoma cell line. *American Journal of Cancer Research*, *2*(2), 141–152. http://www.ncbi.nlm.nih.gov/pubmed/22432055

Tiwary, B. K., Kirubagaran, R., & Ray, A. K. (2005). The biology of triploid fish. *Reviews in Fish Biology and Fisheries 2005 14:4*, *14*(4), 391–402. https://doi.org/10.1007/S11160-004-8361-8

Town, C. D., Cheung, F., Maiti, R., Crabtree, J., Haas, B. J., Wortman, J. R., Hine, E. E., Althoff, R., Arbogast, T. S., Tallon, L. J., Vigouroux, M., Trick, M., & Bancroft, I. (2006). Comparative Genomics of *Brassica oleracea* and *Arabidopsis thaliana* Reveal Gene Loss, Fragmentation, and Dispersal after Polyploidy. *The Plant Cell*, *18*(6), 1348–1359. https://doi.org/10.1105/TPC.106.041665

Úbeda-Manzanaro, M., Merlo, M. A., Palazón, J. L., Cross, I., Sarasquete, C., & Rebordinos, L. (2010). Chromosomal mapping of the major and minor ribosomal genes, (GATA)n and U2 snRNA gene by double-colour FISH in species of the Batrachoididae family. *Genetica*, *138*(7), 787–794. https://doi.org/10.1007/s10709-010-9460-1

Utsunomia, R., Scacchetti, P. C., Pansonato-Alves, J. C., Oliveira, C., & Foresti, F. (2014). Comparative chromosome mapping of U2 snRNA and 5S rRNA genes in gymnotus species (Gymnotiformes, Gymnotidae): Evolutionary dynamics and sex chromosome linkage in G. pantanal. *Cytogenetic and Genome Research*, *142*(4), 286–292. https://doi.org/10.1159/000362258

Vacarizas, J., Taguchi, T., Mezaki, T., Okumura, M., Kawakami, R., Ito, M., & Kubota, S. (2021). Cytogenetic markers using single-sequence probes reveal chromosomal locations of tandemly repetitive genes in scleractinian coral *Acropora pruinosa*. *Scientific Reports*, *11*(1), 11326. https://doi.org/10.1038/s41598-021-90580-1

van der Drift, P., Chan, A., Zehetner, G., Westerveld, A., & Versteeg, R. (1999). Multiple MSP pseudogenes in a local repeat cluster on 1p36.2: An expanding genomic graveyard? *Genomics*, *62*(1), 74–81. https://doi.org/10.1006/geno.1999.5972

Vanin, E. F. (1985). Processed pseudogenes: characteristics and evolution. In *Annual review of genetics* (Vol. 19, pp. 253–272). https://doi.org/10.1146/annurev.ge.19.120185.001345

Vanin, E. F., Goldberg, G. I., Tucker, P. W., & Smithies, O. (1980). A mouse α-globin-related pseudogene lacking intervening sequences. *Nature*, *286*(5770), 222–226. https://doi.org/10.1038/286222a0

Villeneuve, A. M., & Meyer, B. J. (1990). The regulatory hierarchy controlling sex determination and dosage compensation in: *Caenorhabditis elegans*. *Advances in Genetics*, *27*(C), 117–188. https://doi.org/10.1016/S0065-2660(08)60025-5

Vollmer, S. v., & Palumbi, S. R. (2002). Hybridization and the evolution of reef coral diversity. *Science*, *296*(5575), 2023–2025. https://doi.org/10.1126/SCIENCE.1069524/SUPPL_FILE/1069524S1_THUMB.GIF

Wallace, C. C., Done, B. J., & Muir, P. R. (2012). Revision and catalogue of worldwide staghorn corals *Acropora* and *Isopora* (scleractinia: Acroporidae) in the museum of tropical Queensland. *Memoirs of the Queensland Museum-Nature*, *57*(1), 1–257.

Wilkinson, C. (2012). Status of coral reefs of the world: summary of threats and remedial action. In *Coral Reef Conservation* (pp. 3–39). Cambridge University Press. https://doi.org/10.1017/cbo9780511804472.003

Yang, L., Naylor, G. J. P., & Mayden, R. L. (2022). Deciphering reticulate evolution of the largest group of polyploid vertebrates, the subfamily cyprininae (Teleostei:

Cypriniformes). *Molecular Phylogenetics and Evolution*, *166*, 107323. https://doi.org/10.1016/J.YMPEV.2021.107323

Yoshimoto, S., Okada, E., Umemoto, H., Tamura, K., Uno, Y., Nishida-Umehara, C., Matsuda, Y., Takamatsu, N., Shiba, T., & Ito, M. (2008). A W-linked DM-domain gene, DM-W, participates in primary ovary development in *Xenopus laevis*. *Proceedings of the National Academy of Sciences of the United States of America*, *105*(7), 2469–2474. https://doi.org/10.1073/pnas.0712244105

Zhang, L., Bao, Z., Wang, S., Huang, X., & Hu, J. (2007). Chromosome rearrangements in Pectinidae (Bivalvia: Pteriomorphia) implied based on chromosomal localization of histone H3 gene in four scallops. *Genetica*, *130*(2), 193–198. https://doi.org/10.1007/s10709-006-9006-8

Zhang, Y., Chen, Q., Xie, J. Y., Yeung, Y. H., Xiao, B., Liao, B., Xu, J., & Qiu, J. W. (2019). Development of a transcriptomic database for 14 species of scleractinian corals. *BMC Genomics*, *20*(1), 1–9. https://doi.org/10.1186/S12864-019-5744-8/FIGURES/3

Zhou, Y., Wu, J., Wang, Z., Li, G., Mei, J., Zhou, L., & Gui, J. (2019). Identification of sex-specific markers and heterogametic XX/XY sex determination system by 2b-RAD sequencing in redtail catfish (*Mystus wyckioides*). *Aquaculture Research*, *50*(8), 2251–2266. https://doi.org/10.1111/ARE.14106

Appendix

Supplementary Table S1. Multiple comparison analysis (Tukey's test, alpha=0.05) of size differences between homologs of each chromosome pairs. Initial ANOVA analysis (alpha=0.05) is significant (df=13, F=6.4141, p<1.467e-10).

contrast	estimate	SE	df	t.ratio	p.value
1vs2	9.45E-02	0.0226	266	4.179	0.0031
1vs3	1.53E-01	0.0226	266	6.79	<.0001
1vs4	1.32E-01	0.0226	266	5.846	<.0001
1vs5	1.36E-01	0.0226	266	6.035	<.0001
1vs6	1.46E-01	0.0226	266	6.47	<.0001
1vs7	1.41E-01	0.0226	266	6.216	<.0001
1vs8	1.49E-01	0.0226	266	6.598	<.0001
1vs9	1.57E-01	0.0226	266	6.967	<.0001
1vs10	1.46E-01	0.0226	266	6.467	<.0001
1vs11	1.49E-01	0.0226	266	6.591	<.0001
1vs12	1.36E-01	0.0226	266	6.033	<.0001
1vs13	1.14E-01	0.0226	266	5.063	0.0001
1vs14	1.12E-01	0.0226	266	4.936	0.0001
2vs3	5.90E-02	0.0226	266	2.611	0.3386
2vs4	3.77E-02	0.0226	266	1.667	0.9256
2vs5	4.20E-02	0.0226	266	1.856	0.8479
2vs6	5.18E-02	0.0226	266	2.291	0.5633
2vs7	4.60E-02	0.0226	266	2.037	0.7428
2vs8	5.47E-02	0.0226	266	2.419	0.4692
2vs9	6.30E-02	0.0226	266	2.788	0.2371
2vs10	5.17E-02	0.0226	266	2.288	0.5653
2vs11	5.45E-02	0.0226	266	2.412	0.4746
2vs12	4.19E-02	0.0226	266	1.854	0.8488
2vs13	2.00E-02	0.0226	266	0.884	0.9998
2vs14	1.71E-02	0.0226	266	0.757	1
3vs4	-2.13E-02	0.0226	266	-0.944	0.9996
3vs5	-1.71E-02	0.0226	266	-0.755	1
3vs6	-7.24E-03	0.0226	266	-0.32	1
3vs7	-1.30E-02	0.0226	266	-0.574	1
3vs8	-4.33E-03	0.0226	266	-0.192	1
3vs9	4.00E-03	0.0226	266	0.177	1
3vs10	-7.30E-03	0.0226	266	-0.323	1
3vs11	-4.50E-03	0.0226	266	-0.199	1
3vs12	-1.71E-02	0.0226	266	-0.757	1
3vs13	-3.90E-02	0.0226	266	-1.727	0.9045
3vs14	-4.19E-02	0.0226	266	-1.854	0.849
4vs5	4.28E-03	0.0226	266	0.189	1
4vs6	1.41E-02	0.0226	266	0.624	1
4vs7	8.37E-03	0.0226	266	0.37	1

4vs8	1.70E-02	0.0226	266	0.752	1
4vs9	2.53E-02	0.0226	266	1.121	0.9977
4vs10	1.40E-02	0.0226	266	0.621	1
4vs11	1.68E-02	0.0226	266	0.745	1
4vs12	4.24E-03	0.0226	266	0.187	1
4vs13	-1.77E-02	0.0226	266	-0.783	1
4vs14	-2.06E-02	0.0226	266	-0.91	0.9997
5vs6	9.83E-03	0.0226	266	0.435	1
5vs7	4.09E-03	0.0226	266	0.181	1
5vs8	1.27E-02	0.0226	266	0.563	1
5vs9	2.11E-02	0.0226	266	0.932	0.9997
5vs10	9.77E-03	0.0226	266	0.432	1
5vs11	1.26E-02	0.0226	266	0.556	1
5vs12	-4.29E-05	0.0226	266	-0.002	1
5vs13	-2.20E-02	0.0226	266	-0.972	0.9995
5vs14	-2.48E-02	0.0226	266	-1.099	0.9981
6vs7	-5.73E-03	0.0226	266	-0.254	1
6vs8	2.90E-03	0.0226	266	0.128	1
6vs9	1.12E-02	0.0226	266	0.497	1
6vs10	-5.97E-05	0.0226	266	-0.003	1
6vs11	2.73E-03	0.0226	266	0.121	1
6vs12	-9.87E-03	0.0226	266	-0.437	1
6vs13	-3.18E-02	0.0226	266	-1.407	0.9805
6vs14	-3.47E-02	0.0226	266	-1.534	0.9603
7vs8	8.64E-03	0.0226	266	0.382	1
7vs9	1.70E-02	0.0226	266	0.751	1
7vs10	5.67E-03	0.0226	266	0.251	1
7vs11	8.47E-03	0.0226	266	0.375	1
7vs12	-4.14E-03	0.0226	266	-0.183	1
7vs13	-2.61E-02	0.0226	266	-1.153	0.9969
7vs14	-2.89E-02	0.0226	266	-1.28	0.9916
8vs9	8.34E-03	0.0226	266	0.369	1
8vs10	-2.96E-03	0.0226	266	-0.131	1
8vs11	-1.71E-04	0.0226	266	-0.008	1
8vs12	-1.28E-02	0.0226	266	-0.565	1
8vs13	-3.47E-02	0.0226	266	-1.536	0.9599
8vs14	-3.76E-02	0.0226	266	-1.662	0.9271
9vs10	-1.13E-02	0.0226	266	-0.5	1
9vs11	-8.51E-03	0.0226	266	-0.376	1
9vs12	-2.11E-02	0.0226	266	-0.934	0.9997
9vs13	-4.30E-02	0.0226	266	-1.904	0.8225
9vs14	-4.59E-02	0.0226	266	-2.031	0.7469
10vs11	2.79E-03	0.0226	266	0.124	1
10vs12	-9.81E-03	0.0226	266	-0.434	1
10vs13	-3.17E-02	0.0226	266	-1.404	0.9808
10vs14	-3.46E-02	0.0226	266	-1.531	0.9608

11vs12	-1.26E-02	0.0226	266	-0.558	1
11vs13	-3.45E-02	0.0226	266	-1.528	0.9614
11vs14	-3.74E-02	0.0226	266	-1.654	0.9294
12vs13	-2.19E-02	0.0226	266	-0.97	0.9995
12vs14	-2.48E-02	0.0226	266	-1.097	0.9981
13vs14	-2.86E-03	0.0226	266	-0.126	1

Supplementary Table S2. Blast result of each identified regions of At-p5S probe sequence against the whole genome of *Acropora digitifera* (GenBank: GCA_014634065.1). Highlighted in yellow is the probe array 5S-ITS1-U2-ITS2-U1-ITS3-5S which aligned on pos 1203043-1626684.

SW score	perc div	perc del	perc ins	scaffold	pos begin	pos end	query (left)	direction	query sequence	query pos begin	query pos end	repeat (left)	ID
273	14.6	0	2.1	BLFC01000310.1	304835	304883	-3915764	+	5S-5prime	1	48	-3	192
255	14.6	0	2.1	BLFC01000310.1	863950	863998	-3356649	+	5S-5prime	1	48	-3	193
6259	3.1	0.6	2.6	BLFC01000310.1	1202141	1202974	-3017673	+	ITS3	47	864	0	194
389	5.4	0	0	BLFC01000310.1	1202975	1203030	-3017617	+	5S-3prime	1	56	0	195
408	2	0	0	BLFC01000310.1	1203043	1203093	-3017554	+	5S-5prime	1	51	0	196
2107	0.8	0	1.6	BLFC01000310.1	1203094	1203351	-3017296	+	ITS1	1	254	0	197
1680	0	0	0	BLFC01000310.1	1203352	1203543	-3017104	+	U2	1	192	0	198
1637	0.5	0	0	BLFC01000310.1	1203544	1203734	-3016913	+	ITS2	1	191	0	199
1423	0	0	0	BLFC01000310.1	1203735	1203898	-3016749	+	U1	1	164	0	200
6547	3.1	0.6	3.4	BLFC01000310.1	1203902	1204789	-3015858	+	ITS3	1	864	0	201
389	5.4	0	0	BLFC01000310.1	1204790	1204845	-3015802	+	5S-3prime	1	56	0	202
408	2	0	0	BLFC01000310.1	1204858	1204908	-3015739	+	5S-5prime	1	51	0	203
2155	0.8	0	0	BLFC01000310.1	1204909	1205162	-3015485	+	ITS1	1	254	0	204
1680	0	0	0	BLFC01000310.1	1205163	1205354	-3015293	+	U2	1	192	0	205
1637	0.5	0	0	BLFC01000310.1	1205355	1205545	-3015102	+	ITS2	1	191	0	206
1423	0	0	0	BLFC01000310.1	1205546	1205709	-3014938	+	U1	1	164	0	207
6547	3.1	0.6	3.4	BLFC01000310.1	1205713	1206600	-3014047	+	ITS3	1	864	0	208
389	5.4	0	0	BLFC01000310.1	1206601	1206656	-3013991	+	5S-3prime	1	56	0	209
408	2	0	0	BLFC01000310.1	1206669	1206719	-3013928	+	5S-5prime	1	51	0	210
2107	0.8	0	1.6	BLFC01000310.1	1206720	1206977	-3013670	+	ITS1	1	254	0	211
1680	0	0	0	BLFC01000310.1	1206978	1207169	-3013478	+	U2	1	192	0	212
1637	0.5	0	0	BLFC01000310.1	1207170	1207360	-3013287	+	ITS2	1	191	0	213
1423	0	0	0	BLFC01000310.1	1207361	1207524	-3013123	+	U1	1	164	0	214
6605	3	0.6	3	BLFC01000310.1	1207528	1208412	-3012235	+	ITS3	1	864	0	215
389	5.4	0	0	BLFC01000310.1	1208414	1208469	-3012178	+	5S-3prime	1	56	0	216
408	2	0	0	BLFC01000310.1	1208482	1208532	-3012115	+	5S-5prime	1	51	0	217
2155	0.8	0	0	BLFC01000310.1	1208533	1208786	-3011861	+	ITS1	1	254	0	218
1680	0	0	0	BLFC01000310.1	1208787	1208978	-3011669	+	U2	1	192	0	219
1659	0	0	0	BLFC01000310.1	1208979	1209169	-3011478	+	ITS2	1	191	0	220
1423	0	0	0	BLFC01000310.1	1209170	1209333	-3011314	+	U1	1	164	0	221
6579	3.1	0.6	3.2	BLFC01000310.1	1209337	1210223	-3010424	+	ITS3	1	864	0	222
389	5.4	0	0	BLFC01000310.1	1210224	1210279	-3010368	+	5S-3prime	1	56	0	223
408	2	0	0	BLFC01000310.1	1210292	1210342	-3010305	+	5S-5prime	1	51	0	224
2129	0.4	0	1.6	BLFC01000310.1	1210343	1210600	-3010047	+	ITS1	1	254	0	225
1680	0	0	0	BLFC01000310.1	1210601	1210792	-3009855	+	U2	1	192	0	226
1659	0	0	0	BLFC01000310.1	1210793	1210983	-3009664	+	ITS2	1	191	0	227
1423	0	0	0	BLFC01000310.1	1210984	1211147	-3009500	+	U1	1	164	0	228
6603	3.1	0.6	2.8	BLFC01000310.1	1211151	1212033	-3008614	+	ITS3	1	864	0	229
389	5.4	0	0	BLFC01000310.1	1212034	1212089	-3008558	+	5S-3prime	1	56	0	230
408	2	0	0	BLFC01000310.1	1212102	1212152	-3008495	+	5S-5prime	1	51	0	231
2135	0.4	0	1.2	BLFC01000310.1	1212153	1212409	-3008238	+	ITS1	1	254	0	232
1680	0	0	0	BLFC01000310.1	1212410	1212601	-3008046	+	U2	1	192	0	233
1578	0	0.5	1.6	BLFC01000310.1	1212602	1212794	-3007853	+	ITS2	1	191	0	234
1423	0	0	0	BLFC01000310.1	1212795	1212958	-3007689	+	U1	1	164	0	235
6567	3.1	0.6	3.5	BLFC01000310.1	1212962	1213850	-3006797	+	ITS3	1	864	0	236
389	5.4	0	0	BLFC01000310.1	1213851	1213906	-3006741	+	5S-3prime	1	56	0	237
408	2	0	0	BLFC01000310.1	1213919	1213969	-3006678	+	5S-5prime	1	51	0	238
2177	0.4	0	0	BLFC01000310.1	1213970	1214223	-3006424	+	ITS1	1	254	0	239
1680	0	0	0	BLFC01000310.1	1214224	1214415	-3006232	+	U2	1	192	0	240
1698	0	0	0	BLFC01000310.1	1214416	1214606	-3006041	+	ITS2	1	191	0	241
1461	0	0	0	BLFC01000310.1	1214607	1214770	-3005877	+	U1	1	164	0	242
6714	3.5	0.5	2.7	BLFC01000310.1	1214774	1215656	-3004991	+	ITS3	1	864	0	243
407	5.4	0	0	BLFC01000310.1	1215657	1215712	-3004935	+	5S-3prime	1	56	0	244
419	2	0	0	BLFC01000310.1	1215725	1215775	-3004872	+	5S-5prime	1	51	0	245
2230	0.4	0	0	BLFC01000310.1	1215776	1216029	-3004618	+	ITS1	1	254	0	246
1715	0	0	0	BLFC01000310.1	1216030	1216221	-3004426	+	U2	1	192	0	247
1698	0	0	0	BLFC01000310.1	1216222	1216412	-3004235	+	ITS2	1	191	0	248
1461	0	0	0	BLFC01000310.1	1216413	1216576	-3004071	+	U1	1	164	0	249
6708	3.5	0.5	2.8	BLFC01000310.1	1216580	1217463	-3003184	+	ITS3	1	864	0	250
407	5.4	0	0	BLFC01000310.1	1217464	1217519	-3003128	+	5S-3prime	1	56	0	251
419	2	0	0	BLFC01000310.1	1217532	1217582	-3003065	+	5S-5prime	1	51	0	252
2230	0.4	0	0	BLFC01000310.1	1217583	1217836	-3002811	+	ITS1	1	254	0	253
1715	0	0	0	BLFC01000310.1	1217837	1218028	-3002619	+	U2	1	192	0	254
1698	0	0	0	BLFC01000310.1	1218029	1218219	-3002428	+	ITS2	1	191	0	255
1461	0	0	0	BLFC01000310.1	1218220	1218383	-3002264	+	U1	1	164	0	256
6690	3.5	0.5	3.1	BLFC01000310.1	1218387	1219273	-3001374	+	ITS3	1	864	0	257
407	5.4	0	0	BLFC01000310.1	1219274	1219329	-3001318	+	5S-3prime	1	56	0	258
419	2	0	0	BLFC01000310.1	1219342	1219392	-3001255	+	5S-5prime	1	51	0	259
2230	0.4	0	0	BLFC01000310.1	1219393	1219646	-3001001	+	ITS1	1	254	0	260

1715	0	0	0	BLFC01000310.1	1219647	1219838	-3000809	+	U2	1	192	0	261
1698	0	0	0	BLFC01000310.1	1219839	1220029	-3000618	+	ITS2	1	191	0	262
1461	0	0	0	BLFC01000310.1	1220030	1220193	-3000454	+	U1	1	164	0	263
6690	3.5	0.5	3.1	BLFC01000310.1	1220197	1221083	-2999564	+	ITS3	1	864	0	264
407	5.4	0	0	BLFC01000310.1	1221084	1221139	-2999508	+	5S-3prime	1	56	0	265
419	2	0	0	BLFC01000310.1	1221152	1221202	-2999445	+	5S-5prime	1	51	0	266
2230	0.4	0	0	BLFC01000310.1	1221203	1221456	-2999191	+	ITS1	1	254	0	267
1715	0	0	0	BLFC01000310.1	1221457	1221648	-2998999	+	U2	1	192	0	268
1698	0	0	0	BLFC01000310.1	1221649	1221839	-2998808	+	ITS2	1	191	0	269
1461	0	0	0	BLFC01000310.1	1221840	1222003	-2998644	+	U1	1	164	0	270
6690	3.5	0.5	3.1	BLFC01000310.1	1222007	1222893	-2997754	+	ITS3	1	864	0	271
407	5.4	0	0	BLFC01000310.1	1222894	1222949	-2997698	+	5S-3prime	1	56	0	272
419	2	0	0	BLFC01000310.1	1222962	1223012	-2997635	+	5S-5prime	1	51	0	273
2230	0.4	0	0	BLFC01000310.1	1223013	1223266	-2997381	+	ITS1	1	254	0	274
1715	0	0	0	BLFC01000310.1	1223267	1223458	-2997189	+	U2	1	192	0	275
1698	0	0	0	BLFC01000310.1	1223459	1223649	-2996998	+	ITS2	1	191	0	276
1441	0	0	0	BLFC01000310.1	1229453	1229614	-2991033	+	U1	3	164	0	277
6613	3.5	0.7	3.1	BLFC01000310.1	1229618	1230502	-2990145	+	ITS3	1	864	0	278
402	5.5	0	0	BLFC01000310.1	1230503	1230557	-2990090	+	5S-3prime	1	55	-1	279
419	2	0	0	BLFC01000310.1	1230570	1230620	-2990027	+	5S-5prime	1	51	0	280
2193	0.4	0.4	0	BLFC01000310.1	1230621	1230873	-2989774	+	ITS1	1	254	0	281
241	0	0	0	BLFC01000310.1	1230874	1230901	-2989746	+	U2	1	28	-164	282
1355	0	0	0.7	BLFC01000310.1	1236222	1236377	-2984270	+	U2	38	192	0	283
1698	0	0	0	BLFC01000310.1	1236378	1236568	-2984079	+	ITS2	1	191	0	284
1441	0	0	0	BLFC01000310.1	1242380	1242541	-2978106	+	U1	3	164	0	285
6405	3.8	0.2	4.2	BLFC01000310.1	1242545	1243442	-2977205	+	ITS3	1	864	0	286
407	5.4	0	0	BLFC01000310.1	1243443	1243498	-2977149	+	5S-3prime	1	56	0	287
354	2.2	0	2.2	BLFC01000310.1	1243512	1243558	-2977089	+	5S-5prime	3	48	-3	288
2170	0.4	0	0.8	BLFC01000310.1	1243563	1243818	-2976829	+	ITS1	1	254	0	289
1595	0.5	0	2.1	BLFC01000310.1	1243819	1244013	-2976634	+	U2	1	191	-1	290
1629	0	0	0.5	BLFC01000310.1	1244014	1244201	-2976446	+	ITS2	1	187	-4	291
1394	0	0.6	0.6	BLFC01000310.1	1244208	1244371	-2976276	+	U1	1	164	0	292
6181	3.3	1	3.6	BLFC01000310.1	1244393	1245269	-2975378	+	ITS3	10	864	0	293
372	5.5	0	1.8	BLFC01000310.1	1245270	1245325	-2975322	+	5S-3prime	1	55	-1	294
389	2	0	2	BLFC01000310.1	1245338	1245389	-2975258	+	5S-5prime	1	51	0	295
2140	0.4	0	1.2	BLFC01000310.1	1245390	1245646	-2975001	+	ITS1	1	254	0	296
1655	0	0	1	BLFC01000310.1	1245647	1245840	-2974807	+	U2	1	192	0	297
1570	0	0.5	1.6	BLFC01000310.1	1245841	1246033	-2974614	+	ITS2	1	191	0	298
1441	0	0	0	BLFC01000310.1	1250518	1250679	-2969968	+	U1	3	164	0	299
6690	3.5	0.5	3.1	BLFC01000310.1	1250683	1251569	-2969078	+	ITS3	1	864	0	300
407	5.4	0	0	BLFC01000310.1	1251570	1251625	-2969022	+	5S-3prime	1	56	0	301
419	2	0	0	BLFC01000310.1	1251638	1251688	-2968959	+	5S-5prime	1	51	0	302
2230	0.4	0	0	BLFC01000310.1	1251689	1251942	-2968705	+	ITS1	1	254	0	303
1715	0	0	0	BLFC01000310.1	1251943	1252134	-2968513	+	U2	1	192	0	304
1698	0	0	0	BLFC01000310.1	1252135	1252325	-2968322	+	ITS2	1	191	0	305
1404	0	0.6	0	BLFC01000310.1	1258135	1258295	-2962352	+	U1	3	164	0	306
6460	3.5	0.7	3.7	BLFC01000310.1	1258299	1259188	-2961459	+	ITS3	1	864	0	307
402	5.5	0	0	BLFC01000310.1	1259189	1259243	-2961404	+	5S-3prime	1	55	-1	308
389	2	0	2	BLFC01000310.1	1259256	1259307	-2961340	+	5S-5prime	1	51	0	309
2230	0.4	0	0	BLFC01000310.1	1259308	1259561	-2961086	+	ITS1	1	254	0	310
1715	0	0	0	BLFC01000310.1	1259562	1259753	-2960894	+	U2	1	192	0	311
1668	0	0	0.5	BLFC01000310.1	1259754	1259945	-2960702	+	ITS2	1	191	0	312
1441	0	0	0	BLFC01000310.1	1265754	1265915	-2954732	+	U1	3	164	0	313
6620	3.5	0.6	3.2	BLFC01000310.1	1265919	1266805	-2953842	+	ITS3	1	864	0	314
407	5.4	0	0	BLFC01000310.1	1266806	1266861	-2953786	+	5S-3prime	1	56	0	315
419	2	0	0	BLFC01000310.1	1266874	1266924	-2953723	+	5S-5prime	1	51	0	316
2230	0.4	0	0	BLFC01000310.1	1266925	1267178	-2953469	+	ITS1	1	254	0	317
1715	0	0	0	BLFC01000310.1	1267179	1267370	-2953277	+	U2	1	192	0	318
1668	0	0	0.5	BLFC01000310.1	1267371	1267562	-2953085	+	ITS2	1	191	0	319
1461	0	0	0	BLFC01000310.1	1267563	1267726	-2952921	+	U1	1	164	0	320
6495	3.8	0.6	3.7	BLFC01000310.1	1267730	1268620	-2952027	+	ITS3	1	864	0	321
407	5.4	0	0	BLFC01000310.1	1268621	1268676	-2951971	+	5S-3prime	1	56	0	322
378	5.9	0	0	BLFC01000310.1	1268689	1268739	-2951908	+	5S-5prime	1	51	0	323
1987	0	1.2	2	BLFC01000310.1	1268740	1268995	-2951652	+	ITS1	1	254	0	324
1445	0.5	2.1	1.6	BLFC01000310.1	1268996	1269186	-2951461	+	U2	1	192	0	325
1698	0	0	0	BLFC01000310.1	1269187	1269377	-2951270	+	ITS2	1	191	0	326
1487	0.6	0	0	BLFC01000310.1	1275306	1275467	-2945180	+	U1	3	164	0	327
6483	3.9	1.5	2.4	BLFC01000310.1	1275469	1276337	-2944310	+	ITS3	4	864	0	328
425	5.4	0	0	BLFC01000310.1	1276338	1276393	-2944254	+	5S-3prime	1	56	0	329
366	0	0	0	BLFC01000310.1	1281946	1281985	-2938662	+	5S-5prime	12	51	0	330

2343	0.4	0	0	BLFC01000310.1	1281986	1282239	-2938408	+	ITS1	1	254	0	331
1764	0	0.5	0	BLFC01000310.1	1282240	1282430	-2938217	+	U2	1	192	0	332
1754	0	0	0.5	BLFC01000310.1	1282431	1282622	-2938025	+	ITS2	1	191	0	333
1534	0	0	0	BLFC01000310.1	1282623	1282786	-2937861	+	U1	1	164	0	334
6925	2.9	0.9	3.1	BLFC01000310.1	1282790	1283672	-2936975	+	ITS3	1	864	0	335
425	5.4	0	0	BLFC01000310.1	1283673	1283728	-2936919	+	5S-3prime	1	56	0	336
440	2	0	0	BLFC01000310.1	1283741	1283791	-2936856	+	5S-5prime	1	51	0	337
2343	0.4	0	0	BLFC01000310.1	1283792	1284045	-2936602	+	ITS1	1	254	0	338
1405	1.9	0	0	BLFC01000310.1	1288719	1288873	-2931774	+	U2	38	192	0	339
1649	1.1	0	6.3	BLFC01000310.1	1288874	1289076	-2931571	+	ITS2	1	191	0	340
1513	0	0	0	BLFC01000310.1	1292937	1293098	-2927549	+	U1	3	164	0	341
6540	3.4	0.9	4.5	BLFC01000310.1	1293102	1293996	-2926651	+	ITS3	1	864	0	342
384	5.6	1.9	0	BLFC01000310.1	1293998	1294051	-2926596	+	5S-3prime	1	55	-1	343
320	4.1	4	2	BLFC01000310.1	1294064	1294113	-2926534	+	5S-5prime	1	51	0	344
2083	2	0.8	2.4	BLFC01000310.1	1294114	1294371	-2926276	+	ITS1	1	254	0	345
1456	0	0	0	BLFC01000310.1	1299533	1299687	-2920960	+	U2	38	192	0	346
1784	0	0	0	BLFC01000310.1	1299688	1299878	-2920769	+	ITS2	1	191	0	347
1483	0	0	0.6	BLFC01000310.1	1301189	1301351	-2919296	+	U1	3	164	0	348
6978	3	0.7	3.8	BLFC01000310.1	1301355	1302245	-2918402	+	ITS3	1	864	0	349
425	5.4	0	0	BLFC01000310.1	1302246	1302301	-2918346	+	5S-3prime	1	56	0	350
440	2	0	0	BLFC01000310.1	1311825	1311875	-2908772	+	5S-5prime	1	51	0	351
2343	0.4	0	0	BLFC01000310.1	1311876	1312129	-2908518	+	ITS1	1	254	0	352
1456	0	0	0	BLFC01000310.1	1317185	1317339	-2903308	+	U2	38	192	0	353
1784	0	0	0	BLFC01000310.1	1317340	1317530	-2903117	+	ITS2	1	191	0	354
1503	0.6	0	0	BLFC01000310.1	1323842	1324003	-2896644	+	U1	3	164	0	355
7072	2.9	0.6	3.2	BLFC01000310.1	1324007	1324893	-2895754	+	ITS3	1	864	0	356
425	5.4	0	0	BLFC01000310.1	1324894	1324949	-2895698	+	5S-3prime	1	56	0	357
366	0	0	0	BLFC01000310.1	1330151	1330190	-2890457	+	5S-5prime	12	51	0	358
2343	0.4	0	0	BLFC01000310.1	1330191	1330444	-2890203	+	ITS1	1	254	0	359
1456	0	0	0	BLFC01000310.1	1334107	1334261	-2886386	+	U2	38	192	0	360
1762	0.5	0	0	BLFC01000310.1	1334262	1334452	-2886195	+	ITS2	1	191	0	361
1375	0	1.2	1.2	BLFC01000310.1	1337088	1337249	-2883398	+	U1	3	164	0	362
6779	3	0.8	4.5	BLFC01000310.1	1337253	1338148	-2882499	+	ITS3	1	864	0	363
425	5.4	0	0	BLFC01000310.1	1338149	1338204	-2882443	+	5S-3prime	1	56	0	364
366	0	0	0	BLFC01000310.1	1341888	1341927	-2878720	+	5S-5prime	12	51	0	365
2333	0.8	0	0	BLFC01000310.1	1341928	1342181	-2878466	+	ITS1	1	254	0	366
1384	1.3	0.7	0	BLFC01000310.1	1347419	1347572	-2873075	+	U2	38	192	0	367
1355	3.8	1	4.3	BLFC01000310.1	1347578	1347770	-2872877	+	ITS2	5	191	0	368
1513	0	0	0	BLFC01000310.1	1353698	1353859	-2866788	+	U1	3	164	0	369
7114	3	0.7	1.9	BLFC01000310.1	1353863	1354736	-2865911	+	ITS3	1	864	0	370
379	5.6	1.9	0	BLFC01000310.1	1354737	1354790	-2865857	+	5S-3prime	1	55	-1	371
361	2	4.1	0	BLFC01000310.1	1354803	1354851	-2865796	+	5S-5prime	1	51	0	372
2302	0.4	0.4	0	BLFC01000310.1	1354852	1355104	-2865543	+	ITS1	1	254	0	373
1444	0.7	0	0	BLFC01000310.1	1360038	1360192	-2860455	+	U2	38	192	0	374
1664	0	0	2.1	BLFC01000310.1	1360193	1360387	-2860260	+	ITS2	1	191	0	375
1398	0	1.2	1.2	BLFC01000310.1	1360388	1360551	-2860096	+	U1	1	164	0	376
6619	3	1.2	3.4	BLFC01000310.1	1360555	1361436	-2859211	+	ITS3	1	864	0	377
340	5.6	3.7	0	BLFC01000310.1	1361437	1361490	-2859157	+	5S-3prime	1	56	0	378
410	2	0	2	BLFC01000310.1	1361502	1361553	-2859094	+	5S-5prime	1	51	0	379
2303	0.8	0	0.4	BLFC01000310.1	1361554	1361808	-2858839	+	ITS1	1	254	0	380
1417	1.3	0	0	BLFC01000310.1	1366640	1366794	-2853853	+	U2	38	192	0	381
1784	0	0	0	BLFC01000310.1	1366795	1366985	-2853662	+	ITS2	1	191	0	382
1405	0.6	0	2.4	BLFC01000310.1	1366986	1367153	-2853494	+	U1	1	164	0	383
6975	3.1	0.7	2.9	BLFC01000310.1	1367157	1368039	-2852608	+	ITS3	1	864	0	384
425	5.4	0	0	BLFC01000310.1	1368040	1368095	-2852552	+	5S-3prime	1	56	0	385
423	3.9	0	0	BLFC01000310.1	1368108	1368158	-2852489	+	5S-5prime	1	51	0	386
2343	0.4	0	0	BLFC01000310.1	1368159	1368412	-2852235	+	ITS1	1	254	0	387
1456	0	0	0	BLFC01000310.1	1373504	1373658	-2846989	+	U2	38	192	0	388
1664	1.6	0.5	0.5	BLFC01000310.1	1373659	1373849	-2846798	+	ITS2	1	191	0	389
1534	0	0	0	BLFC01000310.1	1373850	1374013	-2846634	+	U1	1	164	0	390
7052	3.3	0.7	2.2	BLFC01000310.1	1374017	1374893	-2845754	+	ITS3	1	864	0	391
420	5.5	0	0	BLFC01000310.1	1374894	1374948	-2845699	+	5S-3prime	1	55	-1	392
440	2	0	0	BLFC01000310.1	1374961	1375011	-2845636	+	5S-5prime	1	51	0	393
1946	3.4	6.7	0	BLFC01000310.1	1375012	1375249	-2845398	+	ITS1	1	254	0	394
1456	0	0	0	BLFC01000310.1	1376688	1376842	-2843805	+	U2	38	192	0	395
1653	1.6	0	6.3	BLFC01000310.1	1376843	1377045	-2843602	+	ITS2	1	191	0	396
1457	1.9	0	0	BLFC01000310.1	1382963	1383124	-2837523	+	U1	3	164	0	397
7319	3.1	0.1	0.9	BLFC01000310.1	1383128	1383998	-2836649	+	ITS3	1	864	0	398
425	5.4	0	0	BLFC01000310.1	1383999	1384054	-2836593	+	5S-3prime	1	56	0	399
363	0	0	0	BLFC01000310.1	1393925	1393964	-2826683	+	5S-5prime	12	51	0	400

1938	2.9	6.7	0	BLFC01000310.1	1393965	1394202	-2826445	+	ITS1	1	254	0	401
1264	1.3	0	12.9	BLFC01000310.1	1409653	1409827	-2810820	+	U2	38	192	0	402
1628	1.6	0	6.3	BLFC01000310.1	1409828	1410030	-2810617	+	ITS2	1	191	0	403
1406	0.7	0	0	BLFC01000310.1	1410031	1410184	-2810463	+	U1	1	154	-10	404
3278	4.8	1.7	0.9	BLFC01000310.1	1410184	1410603	-2810044	+	ITS3	351	773	-91	405
1480	1.2	0	0	BLFC01000310.1	1410776	1410937	-2809710	+	U1	3	164	0	406
6921	3.4	0.6	2.9	BLFC01000310.1	1415289	1416149	-2804498	+	ITS3	23	864	0	407
395	7.1	0	0	BLFC01000310.1	1416150	1416205	-2804442	+	5S-3prime	1	56	0	408
437	2	0	0	BLFC01000310.1	1416218	1416268	-2804379	+	5S-5prime	1	51	0	409
1828	3.8	6.6	1.6	BLFC01000310.1	1416269	1416510	-2804137	+	ITS1	1	254	0	410
349	4.3	2.2	0	BLFC01000310.1	1421420	1421465	-2799182	+	U2	38	84	-108	411
1449	0	0	0	BLFC01000310.1	1426189	1426343	-2794304	+	U2	38	192	0	412
1599	1.6	0	6.3	BLFC01000310.1	1426344	1426546	-2794101	+	ITS2	1	191	0	413
1500	0	0	0	BLFC01000310.1	1432184	1432345	-2788302	+	U1	3	164	0	414
7169	3.4	0.7	1.4	BLFC01000310.1	1432349	1433218	-2787429	+	ITS3	1	864	0	415
370	7.3	1.8	0	BLFC01000310.1	1433219	1433273	-2787374	+	5S-3prime	1	56	0	416
363	0	0	0	BLFC01000310.1	1449487	1449526	-2771121	+	5S-5prime	12	51	0	417
1784	4.6	6.6	1.6	BLFC01000310.1	1449527	1449768	-2770879	+	ITS1	1	254	0	418
1313	0	1.3	0.7	BLFC01000310.1	1454932	1455082	-2765565	+	U2	41	192	0	419
1751	0.5	0	0	BLFC01000310.1	1455083	1455273	-2765374	+	ITS2	1	191	0	420
1462	0	0	1.2	BLFC01000310.1	1455274	1455439	-2765208	+	U1	1	164	0	421
6527	3.3	0.6	5	BLFC01000310.1	1455443	1456344	-2764303	+	ITS3	1	864	0	422
418	5.4	0	0	BLFC01000310.1	1456345	1456400	-2764247	+	5S-3prime	1	56	0	423
360	2	1.9	3.9	BLFC01000310.1	1456413	1456464	-2764183	+	5S-5prime	1	51	0	424
2227	0.8	0	2	BLFC01000310.1	1456465	1456723	-2763924	+	ITS1	1	254	0	425
1795	0	0	0	BLFC01000310.1	1456724	1456915	-2763732	+	U2	1	192	0	426
1721	0.5	0	0.5	BLFC01000310.1	1456916	1457107	-2763540	+	ITS2	1	191	0	427
1522	0	0	0	BLFC01000310.1	1457108	1457271	-2763376	+	U1	1	164	0	428
7003	3.1	0.7	3	BLFC01000310.1	1457275	1458158	-2762489	+	ITS3	1	864	0	429
418	5.4	0	0	BLFC01000310.1	1458159	1458214	-2762433	+	5S-3prime	1	56	0	430
437	2	0	0	BLFC01000310.1	1458227	1458277	-2762370	+	5S-5prime	1	51	0	431
2257	0.8	0	1.6	BLFC01000310.1	1458278	1458535	-2762112	+	ITS1	1	254	0	432
1765	0	0	0.5	BLFC01000310.1	1458536	1458728	-2761919	+	U2	1	192	0	433
1751	0.5	0	0	BLFC01000310.1	1458729	1458919	-2761728	+	ITS2	1	191	0	434
1522	0	0	0	BLFC01000310.1	1458920	1459083	-2761564	+	U1	1	164	0	435
7045	3.1	0.6	3	BLFC01000310.1	1459087	1459971	-2760676	+	ITS3	1	864	0	436
418	5.4	0	0	BLFC01000310.1	1459972	1460027	-2760620	+	5S-3prime	1	56	0	437
437	2	0	0	BLFC01000310.1	1460040	1460090	-2760557	+	5S-5prime	1	51	0	438
2257	0.8	0	1.6	BLFC01000310.1	1460091	1460348	-2760299	+	ITS1	1	254	0	439
1449	0	0	0	BLFC01000310.1	1465500	1465654	-2754993	+	U2	38	192	0	440
1751	0.5	0	0	BLFC01000310.1	1465655	1465845	-2754802	+	ITS2	1	191	0	441
1522	0	0	0	BLFC01000310.1	1465846	1466009	-2754638	+	U1	1	164	0	442
6950	3	0.9	3.1	BLFC01000310.1	1466013	1466895	-2753752	+	ITS3	1	864	0	443
413	5.5	0	0	BLFC01000310.1	1466896	1466950	-2753697	+	5S-3prime	1	55	-1	444
437	2	0	0	BLFC01000310.1	1466963	1467013	-2753634	+	5S-5prime	1	51	0	445
2257	0.8	0	1.6	BLFC01000310.1	1467014	1467271	-2753376	+	ITS1	1	254	0	446
1795	0	0	0	BLFC01000310.1	1467272	1467463	-2753184	+	U2	1	192	0	447
1751	0.5	0	0	BLFC01000310.1	1467464	1467654	-2752993	+	ITS2	1	191	0	448
1522	0	0	0	BLFC01000310.1	1467655	1467818	-2752829	+	U1	1	164	0	449
7014	3.1	0.7	2.9	BLFC01000310.1	1467822	1468704	-2751943	+	ITS3	1	864	0	450
418	5.4	0	0	BLFC01000310.1	1468705	1468760	-2751887	+	5S-3prime	1	56	0	451
437	2	0	0	BLFC01000310.1	1468773	1468823	-2751824	+	5S-5prime	1	51	0	452
2257	0.8	0	1.6	BLFC01000310.1	1468824	1469081	-2751566	+	ITS1	1	254	0	453
1795	0	0	0	BLFC01000310.1	1469082	1469273	-2751374	+	U2	1	192	0	454
1751	0.5	0	0	BLFC01000310.1	1469274	1469464	-2751183	+	ITS2	1	191	0	455
1522	0	0	0	BLFC01000310.1	1469465	1469628	-2751019	+	U1	1	164	0	456
7042	3	0.6	3	BLFC01000310.1	1469632	1470516	-2750131	+	ITS3	1	864	0	457
418	5.4	0	0	BLFC01000310.1	1470517	1470572	-2750075	+	5S-3prime	1	56	0	458
437	2	0	0	BLFC01000310.1	1470585	1470635	-2750012	+	5S-5prime	1	51	0	459
2257	0.8	0	1.6	BLFC01000310.1	1470636	1470893	-2749754	+	ITS1	1	254	0	460
252	0	0	0	BLFC01000310.1	1470894	1470921	-2749726	+	U2	1	28	-164	461
1449	0	0	0	BLFC01000310.1	1476242	1476396	-2744251	+	U2	38	192	0	462
1751	0.5	0	0	BLFC01000310.1	1476397	1476587	-2744060	+	ITS2	1	191	0	463
1522	0	0	0	BLFC01000310.1	1476588	1476751	-2743896	+	U1	1	164	0	464
7051	3.1	0.6	2.9	BLFC01000310.1	1476755	1477638	-2743009	+	ITS3	1	864	0	465
418	5.4	0	0	BLFC01000310.1	1477639	1477694	-2742953	+	5S-3prime	1	56	0	466
437	2	0	0	BLFC01000310.1	1477707	1477757	-2742890	+	5S-5prime	1	51	0	467
2257	0.8	0	1.6	BLFC01000310.1	1477758	1478015	-2742632	+	ITS1	1	254	0	468
1795	0	0	0	BLFC01000310.1	1478016	1478207	-2742440	+	U2	1	192	0	469
1751	0.5	0	0	BLFC01000310.1	1478208	1478398	-2742249	+	ITS2	1	191	0	470

1484	0	0.6	0	BLFC01000310.1	1478399	1478561	-2742086	+	U1	1	164	0	471
6765	2.9	1.1	3.5	BLFC01000310.1	1478565	1479448	-2741199	+	ITS3	1	864	0	472
413	5.5	0	0	BLFC01000310.1	1479449	1479503	-2741144	+	5S-3prime	1	55	-1	473
407	2	0	2	BLFC01000310.1	1479516	1479567	-2741080	+	5S-5prime	1	51	0	474
2163	1.2	0.8	0.8	BLFC01000310.1	1479568	1479821	-2740826	+	ITS1	1	254	0	475
252	0	0	0	BLFC01000310.1	1479822	1479849	-2740798	+	U2	1	28	-164	476
1449	0	0	0	BLFC01000310.1	1485159	1485313	-2735334	+	U2	38	192	0	477
1774	0	0	0	BLFC01000310.1	1485314	1485504	-2735143	+	ITS2	1	191	0	478
1522	0	0	0	BLFC01000310.1	1485505	1485668	-2734979	+	U1	1	164	0	479
7062	3.1	0.6	3.2	BLFC01000310.1	1485672	1486558	-2734089	+	ITS3	1	864	0	480
418	5.4	0	0	BLFC01000310.1	1486559	1486614	-2734033	+	5S-3prime	1	56	0	481
437	2	0	0	BLFC01000310.1	1486627	1486677	-2733970	+	5S-5prime	1	51	0	482
2329	0.4	0	0	BLFC01000310.1	1486678	1486931	-2733716	+	ITS1	1	254	0	483
1795	0	0	0	BLFC01000310.1	1486932	1487123	-2733524	+	U2	1	192	0	484
1774	0	0	0	BLFC01000310.1	1487124	1487314	-2733333	+	ITS2	1	191	0	485
1522	0	0	0	BLFC01000310.1	1487315	1487478	-2733169	+	U1	1	164	0	486
7062	3.1	0.6	3.2	BLFC01000310.1	1487482	1488368	-2732279	+	ITS3	1	864	0	487
418	5.4	0	0	BLFC01000310.1	1488369	1488424	-2732223	+	5S-3prime	1	56	0	488
437	2	0	0	BLFC01000310.1	1488437	1488487	-2732160	+	5S-5prime	1	51	0	489
2329	0.4	0	0	BLFC01000310.1	1488488	1488741	-2731906	+	ITS1	1	254	0	490
1419	0	0	0.7	BLFC01000310.1	1493782	1493937	-2726710	+	U2	38	192	0	491
1774	0	0	0	BLFC01000310.1	1493938	1494128	-2726519	+	ITS2	1	191	0	492
1522	0	0	0	BLFC01000310.1	1494129	1494292	-2726355	+	U1	1	164	0	493
6821	3.1	0.9	2.9	BLFC01000310.1	1494314	1495185	-2725462	+	ITS3	10	864	0	494
418	5.4	0	0	BLFC01000310.1	1495186	1495241	-2725406	+	5S-3prime	1	56	0	495
437	2	0	0	BLFC01000310.1	1495254	1495304	-2725343	+	5S-5prime	1	51	0	496
2329	0.4	0	0	BLFC01000310.1	1495305	1495558	-2725089	+	ITS1	1	254	0	497
252	0	0	0	BLFC01000310.1	1495559	1495586	-2725061	+	U2	1	28	-164	498
1458	0	0.6	0	BLFC01000310.1	1498037	1498195	-2722452	+	U2	33	192	0	499
1665	0	1.1	0.5	BLFC01000310.1	1498196	1498385	-2722262	+	ITS2	1	191	0	500
1484	0	0.6	0	BLFC01000310.1	1498386	1498548	-2722099	+	U1	1	164	0	501
6813	4	0.7	3.5	BLFC01000310.1	1498552	1499439	-2721208	+	ITS3	1	864	0	502
387	3.9	2	0	BLFC01000310.1	1499440	1499490	-2721157	+	5S-3prime	1	52	-4	503
437	2	0	0	BLFC01000310.1	1499505	1499555	-2721092	+	5S-5prime	1	51	0	504
2262	0.4	0.4	0.4	BLFC01000310.1	1499556	1499809	-2720838	+	ITS1	1	254	0	505
1795	0	0	0	BLFC01000310.1	1499810	1500001	-2720646	+	U2	1	192	0	506
1774	0	0	0	BLFC01000310.1	1500002	1500192	-2720455	+	ITS2	1	191	0	507
1522	0	0	0	BLFC01000310.1	1500193	1500356	-2720291	+	U1	1	164	0	508
7019	3	0.7	3.1	BLFC01000310.1	1500360	1501244	-2719403	+	ITS3	1	864	0	509
418	5.4	0	0	BLFC01000310.1	1501244	1501299	-2719348	+	5S-3prime	1	56	0	510
437	2	0	0	BLFC01000310.1	1501312	1501362	-2719285	+	5S-5prime	1	51	0	511
2181	0.4	1.2	0.8	BLFC01000310.1	1501363	1501615	-2719032	+	ITS1	1	254	0	512
252	0	0	0	BLFC01000310.1	1501616	1501643	-2719004	+	U2	1	28	-164	513
1366	0	0	1.9	BLFC01000310.1	1506963	1507120	-2713527	+	U2	38	192	0	514
1784	0	0	0	BLFC01000310.1	1507121	1507311	-2713336	+	ITS2	1	191	0	515
1466	0	0.6	0.6	BLFC01000310.1	1507312	1507475	-2713172	+	U1	1	164	0	516
6726	3.5	0.7	4.4	BLFC01000310.1	1507479	1508374	-2712273	+	ITS3	1	864	0	517
425	5.4	0	0	BLFC01000310.1	1508375	1508430	-2712217	+	5S-3prime	1	56	0	518
403	2	2	0	BLFC01000310.1	1508443	1508492	-2712155	+	5S-5prime	1	51	0	519
2343	0.4	0	0	BLFC01000310.1	1508493	1508746	-2711901	+	ITS1	1	254	0	520
253	0	0	0	BLFC01000310.1	1508747	1508774	-2711873	+	U2	1	28	-164	521
1420	0	0	1.3	BLFC01000310.1	1514118	1514274	-2706373	+	U2	38	192	0	522
1754	0	0	0.5	BLFC01000310.1	1514275	1514466	-2706181	+	ITS2	1	191	0	523
1504	0	0	0.6	BLFC01000310.1	1514467	1514631	-2706016	+	U1	1	164	0	524
6990	3.1	0.8	3.1	BLFC01000310.1	1514635	1515518	-2705129	+	ITS3	1	864	0	525
405	7.1	0	0	BLFC01000310.1	1515519	1515574	-2705073	+	5S-3prime	1	56	0	526
440	2	0	0	BLFC01000310.1	1515587	1515637	-2705010	+	5S-5prime	1	51	0	527
2241	2	0.4	0	BLFC01000310.1	1515638	1515890	-2704757	+	ITS1	1	254	0	528
292	5.6	0	0	BLFC01000310.1	1515891	1515926	-2704721	+	U2	1	36	-156	529
1456	0	0	0	BLFC01000310.1	1518910	1519064	-2701583	+	U2	38	192	0	530
1784	0	0	0	BLFC01000310.1	1519065	1519255	-2701392	+	ITS2	1	191	0	531
1493	0.6	0	0	BLFC01000310.1	1519256	1519417	-2701230	+	U1	1	162	-2	532
3298	1.6	0	3.1	BLFC01000310.1	1519420	1519816	-2700831	+	ITS3	4	388	-476	533
1513	0	0	0	BLFC01000310.1	1521206	1521367	-2699280	+	U1	3	164	0	534
6935	3.3	0.7	3.8	BLFC01000310.1	1521371	1522261	-2698386	+	ITS3	1	864	0	535
425	5.4	0	0	BLFC01000310.1	1522262	1522317	-2698330	+	5S-3prime	1	56	0	536
440	2	0	0	BLFC01000310.1	1522330	1522380	-2698267	+	5S-5prime	1	51	0	537
2205	0.4	0.8	0.8	BLFC01000310.1	1522381	1522634	-2698013	+	ITS1	1	254	0	538
1625	0	1.6	1	BLFC01000310.1	1522635	1522825	-2697822	+	U2	1	192	0	539
1745	0	0.5	0	BLFC01000310.1	1522826	1523015	-2697632	+	ITS2	1	191	0	540

1534	0	0	0	BLFC01000310.1	1523016	1523179	-2697468	+	U1	1	164	0	541
6878	3.1	0.6	6	BLFC01000310.1	1523183	1524093	-2696554	+	ITS3	1	864	0	542
425	5.4	0	0	BLFC01000310.1	1524094	1524149	-2696498	+	5S-3prime	1	56	0	543
440	2	0	0	BLFC01000310.1	1524162	1524212	-2696435	+	5S-5prime	1	51	0	544
2343	0.4	0	0	BLFC01000310.1	1524213	1524466	-2696181	+	ITS1	1	254	0	545
1456	0	0	0	BLFC01000310.1	1529651	1529805	-2690842	+	U2	38	192	0	546
1784	0	0	0	BLFC01000310.1	1529806	1529996	-2690651	+	ITS2	1	191	0	547
1513	0	0	0	BLFC01000310.1	1531421	1531582	-2689065	+	U1	3	164	0	548
6805	3.3	0.8	5.4	BLFC01000310.1	1531586	1532489	-2688158	+	ITS3	1	864	0	549
425	5.4	0	0	BLFC01000310.1	1532490	1532545	-2688102	+	5S-3prime	1	56	0	550
421	2	0	0	BLFC01000310.1	1532559	1532607	-2688040	+	5S-5prime	3	51	0	551
2343	0.4	0	0	BLFC01000310.1	1532608	1532861	-2687786	+	ITS1	1	254	0	552
1415	0	0.7	0	BLFC01000310.1	1537790	1537943	-2682704	+	U2	38	192	0	553
1784	0	0	0	BLFC01000310.1	1537944	1538134	-2682513	+	ITS2	1	191	0	554
1513	0	0	0	BLFC01000310.1	1539400	1539561	-2681086	+	U1	3	164	0	555
6559	3.3	1	6.4	BLFC01000310.1	1539565	1540474	-2680173	+	ITS3	1	864	0	556
395	5.4	0	1.8	BLFC01000310.1	1540475	1540531	-2680116	+	5S-3prime	1	56	0	557
440	2	0	0	BLFC01000310.1	1540544	1540594	-2680053	+	5S-5prime	1	51	0	558
2343	0.4	0	0	BLFC01000310.1	1540595	1540848	-2679799	+	ITS1	1	254	0	559
1456	0	0	0	BLFC01000310.1	1542273	1542427	-2678220	+	U2	38	192	0	560
1784	0	0	0	BLFC01000310.1	1542428	1542618	-2678029	+	ITS2	1	191	0	561
1513	0	0	0	BLFC01000310.1	1548633	1548794	-2671853	+	U1	3	164	0	562
6889	3.3	0.6	5.8	BLFC01000310.1	1548798	1549706	-2670941	+	ITS3	1	864	0	563
425	5.4	0	0	BLFC01000310.1	1549707	1549762	-2670885	+	5S-3prime	1	56	0	564
366	0	0	0	BLFC01000310.1	1552103	1552142	-2668505	+	5S-5prime	12	51	0	565
2333	0.8	0	0	BLFC01000310.1	1552143	1552396	-2668251	+	ITS1	1	254	0	566
246	5.9	0	0	BLFC01000310.1	1552397	1552430	-2668217	+	U2	1	34	-158	567
1456	0	0	0	BLFC01000310.1	1557686	1557840	-2662807	+	U2	38	192	0	568
1784	0	0	0	BLFC01000310.1	1557841	1558031	-2662616	+	ITS2	1	191	0	569
1513	0	0	0	BLFC01000310.1	1559288	1559449	-2661198	+	U1	3	164	0	570
6989	3.4	0.3	3.9	BLFC01000310.1	1559453	1560347	-2660300	+	ITS3	1	864	0	571
384	5.5	1.8	0	BLFC01000310.1	1560347	1560401	-2660246	+	5S-3prime	1	56	0	572
366	0	0	0	BLFC01000310.1	1562725	1562764	-2657883	+	5S-5prime	12	51	0	573
1977	2.5	6.7	0	BLFC01000310.1	1562765	1563002	-2657645	+	ITS1	1	254	0	574
1456	0	0	0	BLFC01000310.1	1567200	1567354	-2653293	+	U2	38	192	0	575
1664	1.1	0	6.3	BLFC01000310.1	1567355	1567557	-2653090	+	ITS2	1	191	0	576
1513	0	0	0	BLFC01000310.1	1573929	1574090	-2646557	+	U1	3	164	0	577
6939	3.7	0.3	4.2	BLFC01000310.1	1574094	1574990	-2645657	+	ITS3	1	864	0	578
425	5.4	0	0	BLFC01000310.1	1574991	1575046	-2645601	+	5S-3prime	1	56	0	579
366	0	0	0	BLFC01000310.1	1580332	1580371	-2640276	+	5S-5prime	12	51	0	580
1848	3.8	6.6	1.6	BLFC01000310.1	1580372	1580613	-2640034	+	ITS1	1	254	0	581
1803	0	0	0	BLFC01000310.1	1580614	1580805	-2639842	+	U2	1	192	0	582
1641	1.1	0	6.3	BLFC01000310.1	1580806	1581008	-2639639	+	ITS2	1	191	0	583
1534	0	0	0	BLFC01000310.1	1581009	1581172	-2639475	+	U1	1	164	0	584
7050	3.6	1.1	0.7	BLFC01000310.1	1581176	1582036	-2638611	+	ITS3	1	864	0	585
425	5.4	0	0	BLFC01000310.1	1582037	1582092	-2638555	+	5S-3prime	1	56	0	586
439	3.9	0	0	BLFC01000310.1	1582105	1582155	-2638492	+	5S-5prime	1	51	0	587
1898	4.2	6.7	0	BLFC01000310.1	1582156	1582393	-2638254	+	ITS1	1	254	0	588
1431	1.3	0	0	BLFC01000310.1	1587316	1587470	-2633177	+	U2	38	192	0	589
1034	0	0	10	BLFC01000310.1	1587471	1587602	-2633045	+	ITS2	1	120	-71	590
273	3.3	0	0	BLFC01000310.1	1587603	1587632	-2633015	+	ITS2	162	191	0	591
1534	0	0	0	BLFC01000310.1	1587633	1587796	-2632851	+	U1	1	164	0	592
7155	3	0.8	1.2	BLFC01000310.1	1587800	1588666	-2631981	+	ITS3	1	864	0	593
425	5.4	0	0	BLFC01000310.1	1588667	1588722	-2631925	+	5S-3prime	1	56	0	594
440	2	0	0	BLFC01000310.1	1588735	1588785	-2631862	+	5S-5prime	1	51	0	595
1877	3	6.7	1.6	BLFC01000310.1	1588786	1589025	-2631622	+	ITS1	1	252	-2	596
1211	1.4	8.4	0	BLFC01000310.1	1590529	1590671	-2629976	+	U2	38	192	0	597
1453	0.6	0	7.2	BLFC01000310.1	1590672	1590850	-2629797	+	ITS2	1	167	-24	598
2881	3.8	1.4	0.3	BLFC01000310.1	1595338	1595682	-2624965	+	ITS3	516	864	0	599
421	7.1	0	0	BLFC01000310.1	1595683	1595738	-2624909	+	5S-3prime	1	56	0	600
440	2	0	0	BLFC01000310.1	1595751	1595801	-2624846	+	5S-5prime	1	51	0	601
1887	2.9	6.5	3.1	BLFC01000310.1	1595802	1596047	-2624600	+	ITS1	1	254	0	602
1456	0	0	0	BLFC01000310.1	1600967	1601121	-2619526	+	U2	38	192	0	603
1761	1.1	0	0	BLFC01000310.1	1601122	1601312	-2619335	+	ITS2	1	191	0	604
1488	0.6	0	0	BLFC01000310.1	1607137	1607298	-2613349	+	U1	3	164	0	605
7070	2.9	0.5	2	BLFC01000310.1	1607302	1608178	-2612469	+	ITS3	1	864	0	606
425	5.4	0	0	BLFC01000310.1	1608179	1608234	-2612413	+	5S-3prime	1	56	0	607
376	4.1	0	4.1	BLFC01000310.1	1613712	1613762	-2606885	+	5S-5prime	3	51	0	608
1922	2.9	6.6	1.6	BLFC01000310.1	1613763	1614004	-2606643	+	ITS1	1	254	0	609
1396	1.9	0.6	0	BLFC01000310.1	1619040	1619197	-2601450	+	U2	34	192	0	610

1642	1.1	0	6.3	BLFC01000310.1	1619198	1619400	-2601247	+	ITS2	1	191	0	611
1500	0	0	0	BLFC01000310.1	1625647	1625808	-2594839	+	U1	3	164	0	612
7346	2.5	0.6	1.5	BLFC01000310.1	1625812	1626683	-2593964	+	ITS3	1	864	0	613
418	5.4	0	0	BLFC01000310.1	1626684	1626739	-2593908	+	5S-3prime	1	56	0	614
363	0	0	0	BLFC01000310.1	1629038	1629077	-2591570	+	5S-5prime	12	51	0	615
1968	1.3	6.6	1.6	BLFC01000310.1	1629078	1629319	-2591328	+	ITS1	1	254	0	616
363	0	0	0	BLFC01000310.1	1640900	1640939	-2579708	+	5S-5prime	12	51	0	617
2136	4.3	0	0	BLFC01000310.1	1640940	1641193	-2579454	+	ITS1	1	254	0	618
550	4.4	0	0	BLFC01000310.1	1645139	1645206	-2575441	+	U2	38	105	-87	619
363	0	0	0	BLFC01000310.1	1670954	1670993	-2549654	+	5S-5prime	12	51	0	620
2078	4.3	0	1.6	BLFC01000310.1	1670994	1671251	-2549396	+	ITS1	1	254	0	621
1364	2.6	0	0	BLFC01000310.1	1686480	1686634	-2534013	+	U2	38	192	0	622
1463	2.9	0	2.3	BLFC01000310.1	1686635	1686810	-2533837	+	ITS2	1	172	-19	623
857	1.7	27.5	0	BLFC01000310.1	1695177	1695296	-2525351	+	U2	38	190	-2	624
1555	4.7	0	2.1	BLFC01000310.1	1695299	1695493	-2525154	+	ITS2	1	191	0	625
2123	3.9	0	0	BLFC01000310.1	1699013	1699266	-2521381	C	ITS1	0	254	1	626
363	0	0	0	BLFC01000310.1	1699267	1699306	-2521341	C	5S-5prime	0	51	12	627
746	6.5	0	0	BLFC01000310.1	1713696	1713787	-2506860	+	U2	101	192	0	628
1591	1.6	0.5	4.2	BLFC01000310.1	1713788	1713985	-2506662	+	ITS2	1	191	0	629
1478	0.6	0	0	BLFC01000310.1	1715296	1715457	-2505190	+	U1	3	164	0	630
686	11.4	1.8	0	BLFC01000310.1	1715442	1715555	-2505092	+	ITS3	8	123	-741	631
325	7.5	0	0	BLFC01000310.1	1717996	1718035	-2502612	+	5S-5prime	12	51	0	632
2101	6.3	0	0	BLFC01000310.1	1718036	1718289	-2502358	+	ITS1	1	254	0	633
6486	3.9	1.2	1.7	BLFC01000310.1	1721272	1722099	-2498548	+	ITS3	41	864	0	634
413	5.5	0	0	BLFC01000310.1	1722100	1722154	-2498493	+	5S-3prime	1	55	-1	635
414	3.9	0	0	BLFC01000310.1	1722167	1722217	-2498430	+	5S-5prime	1	51	0	636
2299	0.4	0	0.4	BLFC01000310.1	1722218	1722472	-2498175	+	ITS1	1	254	0	637
1364	1.9	0.7	0	BLFC01000310.1	1726219	1726372	-2494275	+	U2	38	192	0	638
1660	1.6	0	4.2	BLFC01000310.1	1726373	1726571	-2494076	+	ITS2	1	191	0	639
1382	3.7	0	0	BLFC01000310.1	1731562	1731722	-2488925	+	U1	4	164	0	640
5320	6	0	1	BLFC01000310.1	1731724	1732401	-2488246	+	ITS3	4	674	-190	641
375	7.3	0	0	BLFC01000310.1	1732400	1732454	-2488193	+	5S-3prime	2	56	0	642
341	8.7	0	0	BLFC01000310.1	1732472	1732517	-2488130	+	5S-5prime	6	51	0	643
1871	5	5.4	0	BLFC01000310.1	1732518	1732756	-2487891	+	ITS1	1	252	-2	644
1406	2.6	0	0	BLFC01000310.1	1736562	1736716	-2483931	+	U2	38	192	0	645
1715	2.1	0	0	BLFC01000310.1	1736717	1736907	-2483740	+	ITS2	1	191	0	646
1439	2.5	0	0	BLFC01000310.1	1741754	1741914	-2478733	+	U1	3	163	-1	647
6535	4.2	0.9	4.9	BLFC01000310.1	1741917	1742811	-2477836	+	ITS3	4	864	0	648
395	5.4	0	1.8	BLFC01000310.1	1742813	1742869	-2477778	+	5S-3prime	1	56	0	649
440	2	0	0	BLFC01000310.1	1742882	1742932	-2477715	+	5S-5prime	1	51	0	650
1899	2.5	6.5	3.1	BLFC01000310.1	1742933	1743178	-2477469	+	ITS1	1	254	0	651
1456	0	0	0	BLFC01000310.1	1744603	1744757	-2475890	+	U2	38	192	0	652
1664	1.1	0	6.3	BLFC01000310.1	1744758	1744960	-2475687	+	ITS2	1	191	0	653
1457	0.6	0	0.6	BLFC01000310.1	1750713	1750875	-2469772	+	U1	3	164	0	654
3256	5.4	8.2	0	BLFC01000310.1	1750879	1751307	-2469340	+	ITS3	1	464	-400	655
1788	6.9	3.4	0	BLFC01000310.1	1751885	1752117	-2468530	+	ITS1	12	252	-2	656
992	0.9	0	0	BLFC01000310.1	1756946	1757053	-2463594	+	U2	38	145	-47	657
989	3.5	0	0	BLFC01000310.1	1757057	1757172	-2463475	+	ITS2	76	191	0	658
1292	5.2	0	0	BLFC01000310.1	1761296	1761450	-2459197	+	U2	38	192	0	659
1651	2.6	0	4.2	BLFC01000310.1	1761451	1761649	-2458998	+	ITS2	1	191	0	660
1363	0	5.2	0	BLFC01000310.1	1763098	1763251	-2457396	+	U1	3	164	0	661
2627	5.9	8.7	0	BLFC01000310.1	1763253	1763608	-2457039	+	ITS3	4	390	-474	662
308	7.9	0	0	BLFC01000310.1	1763610	1763647	-2457000	+	5S-5prime	14	51	0	663
1808	4.3	8.6	0	BLFC01000310.1	1763648	1763879	-2456768	+	ITS1	1	252	-2	664
1398	1.9	0	0	BLFC01000310.1	1768096	1768250	-2452397	+	U2	38	192	0	665
784	7.3	3.6	0.9	BLFC01000310.1	1768251	1768360	-2452287	+	ITS2	1	113	-78	666
300	7.7	0	0	BLFC01000310.1	1768349	1768387	-2452260	+	ITS2	153	191	0	667
966	1.8	0	0	BLFC01000310.1	1769102	1769210	-2451437	+	U1	3	111	-53	668
471	3.4	0	1.7	BLFC01000310.1	1776242	1776301	-2444346	+	U1	106	164	0	669
6651	5.5	1.3	1.7	BLFC01000310.1	1776303	1777167	-2443480	+	ITS3	4	864	0	670
425	5.4	0	0	BLFC01000310.1	1777168	1777223	-2443424	+	5S-3prime	1	56	0	671
417	3.9	0	0	BLFC01000310.1	1777236	1777286	-2443361	+	5S-5prime	1	51	0	672
1847	7	4.1	0	BLFC01000310.1	1777287	1777528	-2443119	+	ITS1	1	252	-2	673
1251	2.8	0	0	BLFC01000310.1	1785423	1785563	-2435084	+	U2	38	178	-14	674
1541	4.7	0	4.2	BLFC01000310.1	1785557	1785755	-2434892	+	ITS2	1	191	0	675
1512	1.2	0	0	BLFC01000310.1	1785756	1785919	-2434728	+	U1	1	164	0	676
703	3.5	0	0	BLFC01000310.1	1785921	1786007	-2434640	+	ITS3	4	90	-774	677
1653	3.1	0	0	BLFC01000310.1	1786020	1786210	-2434437	+	ITS2	1	191	0	678
1452	1.2	0	0	BLFC01000310.1	1791718	1791878	-2428769	+	U1	4	164	0	679
6800	5.3	1.4	0.8	BLFC01000310.1	1791880	1792735	-2427912	+	ITS3	4	864	0	680

401	8.9	0	0	BLFC01000310.1	1792736	1792791	-2427856	+	5S-3prime	1	56	0	681
439	2	0	0	BLFC01000310.1	1792804	1792854	-2427793	+	5S-5prime	1	51	0	682
1740	5.2	9.6	0	BLFC01000310.1	1792855	1793084	-2427563	+	ITS1	1	252	-2	683
1458	0	0	1.9	BLFC01000310.1	1802281	1802445	-2418202	+	U1	3	164	0	684
6749	4.7	1.6	0.9	BLFC01000310.1	1802447	1803301	-2417346	+	ITS3	4	864	0	685
400	7.1	0	0	BLFC01000310.1	1803302	1803357	-2417290	+	5S-3prime	1	56	0	686
272	7.7	0	2.6	BLFC01000310.1	1803370	1803409	-2417238	+	5S-5prime	1	39	-12	687
2060	5.5	0	0.4	BLFC01000310.1	1803417	1803671	-2416976	+	ITS1	1	254	0	688
1349	1.3	1.3	0	BLFC01000310.1	1808573	1808725	-2411922	+	U2	38	192	0	689
1642	2.1	0	4.2	BLFC01000310.1	1808726	1808924	-2411723	+	ITS2	1	191	0	690
1416	1.9	0	0	BLFC01000310.1	1810140	1810297	-2410350	+	U1	7	164	0	691
593	5.3	13.7	0	BLFC01000310.1	1810299	1810393	-2410254	+	ITS3	4	111	-753	692
1399	3.7	0.6	0	BLFC01000310.1	1811405	1811565	-2409082	+	U1	3	164	0	693
6043	3.6	8.2	1.1	BLFC01000310.1	1811567	1812370	-2408277	+	ITS3	4	864	0	694
344	10.9	1.8	0	BLFC01000310.1	1812371	1812425	-2408222	+	5S-3prime	1	56	0	695
450	2	0	0	BLFC01000310.1	1812438	1812488	-2408159	+	5S-5prime	1	51	0	696
1950	4.9	3.3	0	BLFC01000310.1	1812489	1812732	-2407915	+	ITS1	1	252	-2	697
1361	3.9	0	0	BLFC01000310.1	1818723	1818877	-2401770	+	U2	38	192	0	698
1658	3.7	0	0	BLFC01000310.1	1818878	1819068	-2401579	+	ITS2	1	191	0	699
1434	1.9	0	0.6	BLFC01000310.1	1834718	1834880	-2385767	+	U1	3	164	0	700
6406	4.6	4	3	BLFC01000310.1	1834882	1835734	-2384913	+	ITS3	4	864	0	701
398	7.1	0	0	BLFC01000310.1	1835735	1835790	-2384857	+	5S-3prime	1	56	0	702
408	7.8	0	0	BLFC01000310.1	1835803	1835853	-2384794	+	5S-5prime	1	51	0	703
1571	4.6	16.5	0	BLFC01000310.1	1835854	1836071	-2384576	+	ITS1	1	254	0	704
628	0.9	46.2	0	BLFC01000310.1	1845148	1845253	-2375394	+	U2	38	192	0	705
1373	3.4	7	4.2	BLFC01000310.1	1845254	1845439	-2375208	+	ITS2	1	191	0	706
1282	3.1	0	11	BLFC01000310.1	1845440	1845621	-2375026	+	U1	1	164	0	707
478	11.6	0	3.9	BLFC01000310.1	1845623	1845703	-2374944	+	ITS3	4	81	-783	708
5504	4.3	0.9	1.2	BLFC01000310.1	1845703	1846379	-2374268	+	ITS3	190	864	0	709
401	8.9	0	0	BLFC01000310.1	1846380	1846435	-2374212	+	5S-3prime	1	56	0	710
363	0	0	0	BLFC01000310.1	1848705	1848744	-2371903	+	5S-5prime	12	51	0	711
1718	4.7	9.5	0	BLFC01000310.1	1848745	1848976	-2371671	+	ITS1	1	254	0	712
1399	0.7	0.7	0	BLFC01000310.1	1853569	1853722	-2366925	+	U2	38	192	0	713
1499	3.2	0.5	8.4	BLFC01000310.1	1853723	1853928	-2366719	+	ITS2	1	191	0	714
583	4.3	0	0	BLFC01000310.1	1893360	1893429	-2327218	+	ITS2	122	191	0	715
1367	3.7	0	0	BLFC01000310.1	1908024	1908185	-2312462	+	U1	3	164	0	716
6718	4.9	2.1	2.3	BLFC01000310.1	1908187	1909049	-2311598	+	ITS3	4	864	0	717
407	3.6	0	1.8	BLFC01000310.1	1909050	1909105	-2311542	+	5S-3prime	1	55	-1	718
413	5.9	0	0	BLFC01000310.1	1909118	1909168	-2311479	+	5S-5prime	1	51	0	719
2132	4.3	0	0	BLFC01000310.1	1909169	1909422	-2311225	+	ITS1	1	254	0	720
471	1.9	0	0	BLFC01000310.1	1914165	1914216	-2306431	+	U1	111	162	-2	721
6511	5	2.4	0.2	BLFC01000310.1	1914237	1915073	-2305574	+	ITS3	10	864	0	722
378	8.9	0	0	BLFC01000310.1	1915074	1915129	-2305518	+	5S-3prime	1	56	0	723
437	2	0	0	BLFC01000310.1	1915142	1915192	-2305455	+	5S-5prime	1	51	0	724
1874	4.2	6.7	0	BLFC01000310.1	1915193	1915430	-2305217	+	ITS1	1	254	0	725
379	0	0	0	BLFC01000310.1	1915431	1915471	-2305176	+	U2	1	41	-151	726
302	5.3	0	0	BLFC01000310.1	1929102	1929139	-2291508	+	ITS1	217	254	0	727
244	3.2	0	3.2	BLFC01000310.1	1929140	1929171	-2291476	+	U2	1	31	-161	728
1108	0	15.7	0	BLFC01000310.1	1934528	1934661	-2285986	+	U2	38	192	0	729
1527	4.2	0	6.3	BLFC01000310.1	1934662	1934864	-2285783	+	ITS2	1	191	0	730
1241	3.9	5.9	0	BLFC01000310.1	1957211	1957363	-2263284	+	U1	3	164	0	731
834	13.7	0	2.6	BLFC01000310.1	1957353	1957509	-2263138	+	ITS3	17	169	-695	732
1334	8.7	2.2	0	BLFC01000310.1	1957504	1957687	-2262960	+	ITS3	677	864	0	733
409	8.9	0	0	BLFC01000310.1	1957688	1957743	-2262904	+	5S-3prime	1	56	0	734
429	3.9	0	0	BLFC01000310.1	1957756	1957806	-2262841	+	5S-5prime	1	51	0	735
1904	7.3	1.6	0	BLFC01000310.1	1957807	1958054	-2262593	+	ITS1	1	252	-2	736
4043	9	5	0	BLFC01000310.1	1958564	1959149	-2261498	+	ITS3	28	642	-222	737
702	8.3	3.7	0	BLFC01000310.1	1959154	1959261	-2261386	+	ITS3	753	864	0	738
389	7.7	0	0	BLFC01000310.1	1959266	1959317	-2261330	+	5S-3prime	5	56	0	739
390	6	0	0	BLFC01000310.1	1959330	1959379	-2261268	+	5S-5prime	1	50	-1	740
1848	8.9	0	0.8	BLFC01000310.1	1959377	1959626	-2261021	+	ITS1	5	252	-2	741
414	12.5	0	0	BLFC01000310.1	1965308	1965371	-2255276	+	U2	35	98	-94	742
1288	11.2	1.6	2.1	BLFC01000310.1	1971780	1971971	-2248676	C	ITS2	0	191	1	743
1126	11	0	0	BLFC01000310.1	1971972	1972126	-2248521	C	U2	0	192	38	744
1641	16	18.9	0	BLFC01000310.1	1992354	1992777	-2227870	+	ITS3	361	864	0	745
307	14	0	0	BLFC01000310.1	1992778	1992827	-2227820	+	5S-3prime	1	50	-6	746
306	15.7	0	0	BLFC01000310.1	1992846	1992896	-2227751	+	5S-5prime	1	51	0	747
1890	9.5	0	0	BLFC01000310.1	1992897	1993148	-2227499	+	ITS1	1	252	-2	748
253	16.7	0	2.1	BLFC01000310.1	2748700	2748748	-1471899	C	5S-5prime	-3	48	1	749

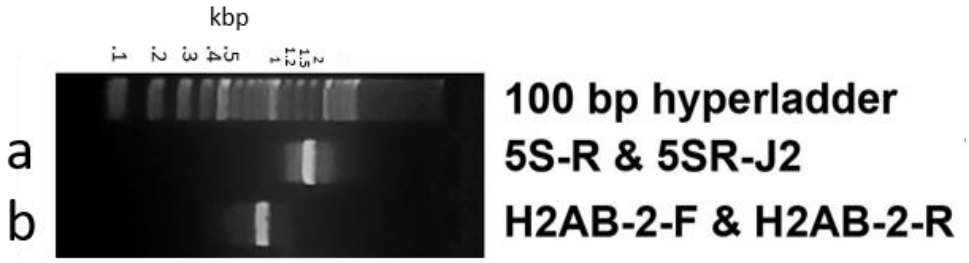

Supplementary Figure S1. Gel electrophoresis image of PCR-amplified repetitive 5S-U1-U2 snRNA (a) and core histone gene (b).